

Bayesian spatiotemporal modelling of political violence and conflict events using discrete-time Hawkes processes

Raiha Browning^{1,2,3}, Hamish Patten⁴, Judith Rousseau^{5,6}, Kerrie Mengersen^{2,3}

¹Department of Statistics, University of Warwick, United Kingdom

²School of Mathematical Sciences, Queensland University of Technology, Australia

³Centre for Data Science, Queensland University of Technology, Australia

⁴Information Management, International Federation of the Red Cross Red Crescent Societies (IFRC)

⁵Ceremade, CNRS, UMR 7534, Université Paris-Dauphine, PSL University, France

⁶Department of Statistics, University of Oxford, United Kingdom

Abstract

The monitoring of conflict risk in the humanitarian sector is largely based on simple historic averages. To advance our understanding, we propose Hawkes processes, a self-exciting stochastic process used to describe phenomena whereby past events increase the probability of future events occurring. The overarching goal of this work is to assess the potential for using a more statistically rigorous approach to monitor the risk of political violence and conflict events in practice, and characterise their temporal and spatial patterns.

The region of South Asia was selected as an exemplar of how our model can be applied globally. We individually analyse the various types of conflict events for the countries in this region. In particular, a Bayesian, spatiotemporal variant of the Hawkes process is fitted to data gathered by the Armed Conflict Location and Event Data (ACLED) project to obtain sub-national estimates of conflict risk over time and space. We find that our model can effectively estimate the risk level of these events within a statistically sound framework, with a more precise understanding of the uncertainty around these estimates than was previously possible. The model also provides insights into differences in behaviours between countries and conflict types. This enables a better understanding of the temporal and spatial patterns inherent in the data which can help to inform preventative measures.

We demonstrate the advantages of the Bayesian framework by comparing our results to a less computationally intensive approach using maximum likelihood estimation. We find that while the maximum likelihood approach gives reasonable point estimates, the Bayesian approach is preferred when possible. Practical examples are presented to demonstrate how the proposed model can be used to monitor conflict risk. Comparing to current practices that rely on historical averages, we also show that our model is more stable and robust to outliers. In showcasing these promising results, we aim to support actors in the humanitarian and political sciences sectors in making data-informed decisions, such as the allocation of resources in conflict-prone regions.

1 Introduction

A key indicator of disorder in society is the occurrence of political violence and conflict events, such as protests and riots. To promote sustainable development and prevent future violence and displacement, the underlying causes of conflict must first be understood and addressed. From a humanitarian perspective, understanding both the real-time and longer term trends of these events is crucial as it allows organisations to protect civilians, provide aid, and foster peace among communities. This knowledge is also important for other key parties such as governments, journalists and researchers, especially during times of instability and unrest. A recent report by the United Nations Office for the Coordination of Humanitarian Affairs (Caldwell, 2022) also highlighted this fact, emphasising the need to focus on understanding the risk of conflict events, in favour of other activities such as forecasting and event classification, to drive anticipatory action.

The Armed Conflict Location and Event Data (ACLED) project (Raleigh et al., 2010) provides a comprehensive, geo-referenced database containing details of political violence and protests worldwide. Currently, ACLED uses a combination of historical averages and machine learning models to assess and predict conflict risk respectively, and these results are generally aggregated to the national level. A key use case for these data is in determining appropriate measures to take in anticipation of a future hazard to reduce the humanitarian impact of the event before it fully unfolds, referred to as anticipatory action by the United Nations Office for the Coordination of Humanitarian Affairs. In this article, we introduce a new statistical approach to conflict monitoring, that is more sophisticated than historical averages, but remains easily interpretable with an enhanced understanding of model uncertainty compared to traditional machine learning approaches.

Hawkes processes (Hawkes, 1971) are self-exciting stochastic processes whereby previous events in the process increase the probability of future events occurring. They have previously been used to study phenomena such as earthquakes (Ogata, 1988), crime and terrorism (White et al., 2013; Mohler et al., 2011), and social media interactions (Chen and Tan, 2018; Dutta et al., 2020). In this article, we extend the standard temporal model to include a spatial kernel that quantifies the spatial impact of events to the intensity of the process. A discrete-time variant of the spatiotemporal Hawkes process is fit to the ACLED data at a fine spatial scale to obtain sub-national estimates of conflict risk. This approach aids in characterising the temporal and spatial patterns that emerge from these types of conflicts, and provides an estimate of risk over space and time that can be used both for real-time monitoring and for making short-term predictions. We use data from the region of South Asia to showcase our approach; however, the methodology can easily be extended to other countries. For the purposes of this example, the four countries considered are Bangladesh, Sri Lanka, Nepal and Pakistan. In addition to modelling each of the countries separately, the various types of conflict events in each country are also modelled individually. By doing so, we can compare the spatial and temporal dynamics of events between both countries and conflict types.

The overarching goal of this article is to determine whether spatiotemporal discrete-time Hawkes processes can provide new spatial and temporal insights that can help practitioners and key actors in the humanitarian sector to better understand conflict events. Specifically, we address three main questions throughout the article: (i) are spatiotemporal discrete-time Hawkes processes useful for explaining conflict events, (ii) what can we learn from them, that we cannot learn from other approaches, and (iii) how can these models be used in practice.

1.1 Discrete-time Hawkes processes

Hawkes processes (HPs) (Hawkes, 1971) were introduced to model phenomena that exhibit self-exciting behaviour whereby events occur in groups or clusters. HPs were originally introduced as a continuous-time process. However, since the data collected by the ACLED project is in the form of daily counts we adopt a discrete-time version of the HP (Linderman and Adams, 2015; Browning et al., 2021; Mohler, 2013), referred to in this article as the discrete-time Hawkes process (DTHP).

For a given DTHP we assume that the number of events that occur at a particular time is distributed according to a Poisson distribution. This distribution can be characterised by its conditional intensity function which governs the rate at which events occur. The intensity function is comprised of two components: the baseline process and the self-exciting process. The baseline process describes the arrival rate of events that occur independently, and not as a result of other events. The self-exciting component on the other hand, describes the clustering behaviours of the process. The aspect of the self-exciting component that describes the impact that past events have on the current intensity of the process is referred to as the triggering kernel, and is a function of the time that has elapsed since an event occurred.

To state this formally, consider a linear DTHP N , where $N(t)$ represents the number of events up to the t -th time interval. $N(t)$ is dependent on the set of events to occur up to but not including time t , denoted by $\mathcal{H}_{t-1} = \{y_s : s \leq t - 1\}$, where y_s represents the observed number of events during a given time interval s . We denote the conditional intensity function as $\lambda(t)$. This quantity represents the number of events expected to occur in the counting process $N(t)$ during time interval t , conditionally on the past. Furthermore, the random variable $Y(t) = N(t) - N(t - 1)$ represents the number of event occurrences in time interval $(t - 1, t]$, and thus,

$$\begin{aligned} \lambda(t) &= \mathbb{E}\{N(t) - N(t - 1) | \mathcal{H}_{t-1}\} \\ &= \mu + \alpha \sum_{i:t_i < t} y_{t_i} g(t - t_i) \end{aligned} \tag{1}$$

where μ represents the baseline mean of the process and the second term represents the self-exciting component of the HP. In particular, α is a magnitude parameter that describes the expected number of events that a single event is expected to produce. The triggering kernel $g(t - t_i)$ is a probability

mass function that describes the influence of these past events on the intensity of the process, given the time elapsed since time t_i , where $t > t_i$.

The number of events observed during time interval t , namely y_t , is distributed according to the random variable, $Y(t)$, which has conditional mean $\mathbb{E}\{Y(t|\mathcal{H}_{t-1})\} = \lambda(t)$ as defined in (1). In this analysis, $Y(t)$ is assumed to be Poisson distributed such that $Y(t|\mathcal{H}_{t-1}) \sim \text{Pois}(\lambda(t))$. Thus, for the proposed DTHP model, the probability that time interval t has y_t events is,

$$P(Y(t) = y_t | \mu, \alpha, g) = \frac{(\mu + \alpha \sum_{i:t_i < t} y_{t_i} g(t - t_i))^{y_t} \exp(-\mu - \alpha \sum_{i:t_i < t} y_{t_i} g(t - t_i))}{y_t!}.$$

The corresponding likelihood function is then,

$$L(t) \propto \prod_{t=1}^T \left(\mu + \alpha \sum_{i:t_i < t} y_{t_i} g(t - t_i) \right)^{y_t} \exp \left(- \left(\mu + \alpha \sum_{i:t_i < t} y_{t_i} g(t - t_i) \right) \right). \quad (2)$$

1.2 Related work and contributions

ACLED provides two main tools for tracking conflict risk. The first tool is the ACLED Trendfinder Dashboard, that monitors previous and current trends and identifies periods in which an unusually high level of activity occurred. These thresholds are based on historical moving averages. The second tool is the Conflict Alert System (CAST), a forecasting tool used to predict future conflict activity for battles, explosions/remote violence, and violence against civilians. CAST is trained using a series of machine learning models. These two tools are intended to be used in conjunction with one another. While the approach taken in this article could also be extended to provide forecasts, we focus instead on gaining a better understanding of conflict risk as discussed in Caldwell (2022).

Several authors have proposed HPs as a method for modelling conflict events using the ACLED project data. Zhu et al. (2021) models the temporal triggering kernel for the HP through a mixture of neural networks that encode a latent function to capture underlying dynamics of community states and apply this model to the ACLED data. Campedelli and D’Orsogna (2021) use HPs to cluster events and explain the temporal behaviour patterns of disorder events during the COVID-19 pandemic. To account for spatial dependency among events, the authors used K-means clustering to group spatial locations with similar characteristics. None of these approaches directly incorporate a spatial triggering kernel into the Hawkes model. By doing so in this article, we are able to better understand the extent of spatial correlation inherent within the process.

Hengel and Franses (2020) does model an explicit spatial triggering kernel within the context of a marked variant of the Hawkes process known as the Epidemic Type Aftershock Sequence (ETAS),

which assumes a specific form for the kernel. Okawa et al. (2022) introduce the convolutional Hawkes process, incorporating spatial heterogeneity through a convolutional neural network that takes images as an input. To our knowledge, there have been no Bayesian approaches to modelling the ACLED data with spatiotemporal Hawkes processes.

Other classes of spatiotemporal models have also been fitted to the ACLED data. Xie et al. (2023) and Weidmann and Ward (2010) use boosted regression trees and autoregressive regression techniques respectively. Recent work by Egbon et al. (2024) introduces an autoregressive model with spatial effects modelled through a stochastic partial differential equation. Estimation was carried out using the Integrated Nested Laplace Approximation (INLA). There are also other examples of Bayesian spatiotemporal models used to model other conflict datasets (Zammit-Mangion et al., 2012; Tench, 2018; Python et al., 2019) that employ, respectively, log-Gaussian Cox processes, Dirichlet process mixture models and stochastic partial differential equations.

While the focus of this paper is on the ACLED database, other geo-referenced conflict databases also exist. The Global Terrorism Database (GTD) (START (National Consortium for the Study of Terrorism and Responses to Terrorism), 2021) contains records of terrorist activity that occurred worldwide since 1970. Naturally, the GTD has a smaller range of conflict types compared to ACLED, since events in the former database must be outside the context of legitimate warfare activities. Several authors have proposed Hawkes processes to model these data (White et al., 2013; Porter and White, 2012); however, these are limited to studying the temporal dimension of the data. The model proposed by Jun and Cook (2024) considers the spatial dimension through a flexible representation of the spatiotemporal triggering kernel. For parameter inference, these authors rely on maximum likelihood estimation, whereas our analysis is focused on utilising the Bayesian framework analysing conflict to reap the benefits discussed in Section 2.3. Clark and Dixon (2018) use a spatiotemporal Hawkes process within the Bayesian framework, however using a simplified construction of the temporal and spatial components where the temporal component is represented as a point mass and there is no explicit spatial kernel.

The Uppsala Conflict Data Program (UCDP) (Strandow et al., 2011) is another rich source of data for events involving armed conflict. While the ACLED data has a larger scope of conflict types recorded, the UCDP records have a longer history, in some cases going back to 1946. Using these data, Mueller and Rauh (2022) propose a framework to generate predictions of conflict using a combination of unsupervised and supervised machine learning techniques. This work differs substantially from ours as it is prediction-focused, with the authors integrating a web-scraping machine learning algorithm to characterise conflict risk. Spatiotemporal models considered for these data include spatiotemporal regression techniques (Racek et al., 2024) and spatial Poisson processes (Schutte, 2017).

To our knowledge, we propose the first Bayesian, spatiotemporal Hawkes model applied to the ACLED data. We study countries in South Asia as an exemplar of how this model can be applied

to these types of data worldwide. The models are fitted on a univariate level, so given sufficient computational resources the number of countries included in the study can be extended to include a much larger sample. Different types of conflict events are also considered individually, allowing us to compare the patterns of excitation for different conflict types. The proposed model enables a data-driven approach to monitoring and understanding the current risk of conflict events throughout time and space. Combined with input and expertise from key actors in the humanitarian and political sciences sectors, such as ACLED, this work can have important implications for the understanding and management of these events.

1.3 Outline

Section 2 introduces the data, the spatiotemporal model, and the inference methods used in this article. Section 3 follows by presenting the results of our analysis. We first present our Bayesian, spatiotemporal model, assess the model fit and interpret the outputs. Next, we present an alternative, less computationally intensive approach using maximum likelihood estimation. In Section 4, we demonstrate how our models can be used to assess conflict risk in practice and benchmark against the types of risk models used by organisations, such as ACLED, that rely on historical averages. Finally, Section 5 concludes with a discussion of the outcomes of this analysis, limitations of the model and avenues for future work.

2 Materials and methods

2.1 Data

The ACLED project (Raleigh et al., 2010) provides a comprehensive geo-referenced database containing details of political violence and protests worldwide and has recorded in total more than one million individual events. In addition to the date and location of events, the database also records the number of fatalities, type of violence and the actors involved, which allows the user to further analyse and understand conflict events. Summaries and reports on the ACLED website are often segmented by conflict type, indicating that this type of segmentation is of interest to key stakeholders in the humanitarian sector. The types of conflicts recorded in the ACLED database and their respective definitions (ACLED, 2019) are,

- Battles: violent interactions between two organised armed groups;
- Explosions/Remote violence: one-sided violence events in which the tool for engaging in conflict creates asymmetry by taking away the ability of the target to respond;
- Violence against civilians: violent events where an organised armed group deliberately inflicts violence upon unarmed non-combatants;

- Protests: a public demonstration against a political entity, government institution, policy or group in which the participants are not violent;
- Riots: violent events where demonstrators or mobs engage in disruptive acts or disorganised acts of violence against property or people;
- Strategic development: accounts for often non-violent activity by conflict and other agents within the context of the war/dispute. Recruitment, looting and arrests are included.

As mentioned in Section 1, for the purposes of illustrating our approach, we focus on South Asia as an exemplar region. We consider monthly counts of conflict events in South Asia over a 5 year period from 2010–2014. During the selected 5 year period, there were four countries with conflict data recorded in the ACLED database, namely Bangladesh, Sri Lanka, Nepal and Pakistan. Several other countries comprise the South Asian region, but did not have data available during the observation window for this study. Data from South and Southeast Asia start from 2010 in the ACLED dataset, and the 5 year period was chosen to reduce computational expense and because it avoids the period in 2016 when ACLED significantly increased capacity and updated their reporting methodology.

We are also interested in modelling spatial dynamics in these data to understand how conflict intensity is influenced by events in neighbouring regions. The inclusion of spatial information also enables the comparison of spatial dynamics between countries and conflict types. Despite having an additional parameter, we find that estimating a spatial kernel does not generally deteriorate the model fit based on the Bayesian Information Criterion (BIC). Further details are available in the supplementary materials.

To determine the spatial aggregation we discretised according to administrative boundaries, which define the borders of a geographic area under a given political or social structure, rather than considering the individual location of each event. These boundaries were obtained from the Database of Global Administrative Areas (GADM) (Global Administrative Areas, 2012) and the Level 2 county level administrative boundaries were used in this analysis. The coordinates for each administrative boundary was then defined as the centroid of each region.

The data were aggregated to the monthly level, and broken down by each of the countries and conflict types present in our analyses. A daily temporal aggregation was considered initially; however, this was found to be unsuitable due to substantial zero-inflation present in the data at finer this discretisation, particularly when breaking down further into spatial regions. For completeness, this preliminary analysis is summarised in the supplementary materials.

2.2 Spatiotemporal discrete-time Hawkes process

The temporal DTHP defined in Section 1.1 can be extended to a spatiotemporal variation that incorporates a spatial triggering kernel. This means the level of excitation is then governed by both the time since an event elapsed and distance from the location where the event occurred. Incorporating spatial dependence into the existing model gives the following rate parameter $\lambda(t, x, y)$ for a particular time t and location with coordinates (x, y) ,

$$\lambda(t, x, y) = \mu + \alpha \sum_{(t_i, x_i, y_i): t_i < t} y_{(t_i, x_i, y_i)} g(t - t_i) h(x - x_i, y - y_i) \quad (3)$$

where $y_{(t, x, y)}$ denotes the number of events at time t in location (x, y) and $h(\cdot)$ is the spatial triggering kernel that determines how the distance between events affects the intensity of the process.

Similar to the the temporal case, the number of events observed during time interval t and location (x, y) , $Y(t, x, y)$ is assumed to be Poisson distributed such that $Y(t, x, y | \mathcal{H}_{t-1}) \sim \text{Pois}(\lambda(t, x, y))$. If the set of centroids for all spatial regions is $\mathcal{S} \subset \mathbb{R}^2$, the probability that time period t and location with coordinates (x, y) has $y_{(t, x, y)}$ events is,

$$\begin{aligned} L(t, x, y) &\propto \prod_{t=1}^T \prod_{(x, y) \in (\mathcal{X}, \mathcal{Y})} \left(\mu + \alpha \sum_{(t_i, x_i, y_i): t_i < t} y_{(t_i, x_i, y_i)} g(t - t_i) h(x - x_i, y - y_i) \right)^{y_{(t, x, y)}} \\ &\times \exp \left(- \left(\mu + \alpha \sum_{(t_i, x_i, y_i): t_i < t} y_{(t_i, x_i, y_i)} g(t - t_i) h(x - x_i, y - y_i) \right) \right). \end{aligned} \quad (4)$$

The model parameters could be allowed to vary by spatial region. Moreover, we did consider a simple model for which μ and α varied based on a coarsely discretised population indicator. However, this simple approach had very little impact on the results, and further research is necessary to better understand the relationship between population size and the intensity of conflict events. Further details are available in the supplementary materials; however, in this article we will only consider the case where the model parameters are constant for all locations. Furthermore, allowing spatially-varying model parameters, in addition to issues with computational resources, could also result in poor model fit for regions with low event counts.

An important distinction between temporal and spatiotemporal DTHPs is in the interpretation of α . The mass of excitation coming from another region (x_i, y_i) is given by $\alpha h(x - x_i, y - y_i)$. Thus the global mass of excitation received from a previous time period t_i is α multiplied by a sum over all locations of events that occurred at time t_i .

As it is presented in (3), the temporal triggering kernel $g(\cdot)$ is defined on \mathbb{Z}^+ . However, in many contexts its reasonable to assume that the maximum length of excitation is not infinite, and the

impact of past events will eventually dissipate. Thus, the triggering kernel could be truncated to some finite value t_{\max} with little impact when there is negligible mass at higher time intervals. Truncating the triggering kernel also reduces computational expense since the summations involved in (4) comprise less terms. In this study, we therefore specify the temporal triggering kernel in the form of a truncated, re-normalised geometric distribution such that

$$g(s) = \frac{\beta(1 - \beta)^{s-1}}{\sum_{j=1}^{t_{\max}} \beta(1 - \beta)^{j-1}}.$$

where $\beta \in [0, 1]$ represents the success probability for the geometric distribution.

Furthermore, we represent the spatial triggering kernel $h(\cdot)$ by a radial basis function (RBF) kernel. Incorporating a spatial dimension into these models increases the computational cost, thus the RBF kernel was selected as it is simple and cheap to evaluate, and it is the most common spatial triggering kernel used for these models. For vectors of coordinates $z = (x, y)$ and $z_i = (x_i, y_i)$, the RBF spatial decay kernel h is,

$$h(z, z_i) = \exp\left(-\frac{d(z, z_i)}{2\sigma^2}\right) \quad (5)$$

where d is assumed to be the Euclidean distance function with bandwidth σ such that,

$$d(z, z_i) = \sqrt{(x - x_i)^2 + (y - y_i)^2}. \quad (6)$$

We note that distance in the latitude-longitude coordinate space can be poorly defined, as the latitude coordinate grid is equally spaced but the longitude has a strong dependence on the associated latitude value. This distorts the comparison of distances, thus if countries further away from the equator were being considered, then an alternative distance such as the Haversine distance should be used.

2.3 Inference

Several inferential approaches, namely Bayesian methods and maximum likelihood estimation (MLE), are used in this work. In the first instance, we adopt the Bayesian framework, due to its advantages such as the ability to directly quantify uncertainty and introduce prior knowledge from experts or previous studies directly in the inference. This model was fitted using the probabilistic programming language **Stan** (Stan Development Team, 2022), which implements MCMC sampling through the No U-Turn Sampler (NUTS). Prior sensitivity analysis found that the algorithm did not converge when placing uniform priors on the model parameters. Thus, weakly informative priors were placed on all model parameters such that,

- $\mu \sim \text{Gamma}(2, 2)$,

- $\alpha \sim \text{Gamma}(2, 2)$,
- $\beta \sim \mathcal{U}(0, 1)$,
- $\sigma \sim \mathcal{IG}(5, 5)$,

whereby ‘Gamma’ is the Gamma distribution, ‘ \mathcal{U} ’ the uniform distribution and ‘ \mathcal{IG} ’ the inverse Gamma distribution. While the Bayesian approach has many advantages, this comes at the expense of computational time. As such, we also consider a maximum likelihood approach where the optimisation was performed in R using the `optim()` function. In addition to being a less computationally intensive alternative, the MLE can also be used as a starting point for the Bayesian method.

3 Results

We first present the results obtained from fitting the Bayesian spatiotemporal model described in Sections 2.2 and 2.3 to the monthly counts of conflict events from the 2010 – 2014 ACLED data for each country and conflict type combination detailed in Section 2.1. We also propose an alternative inference scheme based on maximum likelihood estimation, and compare the modelled estimates obtained through both approaches.

In this study, the maximum excitation time t_{\max} was assumed to be 3 months. The impact of this assumption in our modelling is that past events cannot affect the intensity of the process after 3 months have elapsed. As such, the model was trained on data starting from the fourth month of 2010 to mitigate edge effects and ensure that the model is not biased due to past events not being included in the intensity function calculations. To determine the timescale of temporal correlation in the data, exploratory data analysis was performed and the ARIMA model (Hyndman and Athanasopoulos, 2018) was fitted to the data in R using the `auto.arima()` function from the `forecast` package. The best model found for each country and conflict type combination indicated that all maximum lags were less than 3 months. The full analysis can be found in the supplementary materials.

3.1 Bayesian Spatiotemporal DTHP

In this section, we first describe the fitting and then compare the observed event counts with the expected number of events estimated from our model. The posterior triggering kernels are also visualised and we present maps of the posterior median event counts. Lastly, out-of-sample posterior predictive checks are shown.

The Bayesian spatiotemporal DTHP with intensity function given by (3) was fitted to the data described in Section 2.1. As discussed in Section 2.3, the fitting was performed in `Stan`. The $\hat{\mathcal{R}}$ diagnostic (Vehtari et al., 2021) suggested that all models successfully converged. This was further

validated by inspecting convergence diagnostic plots including autocorrelation functions and trace plots, and confirming that there were no divergent transitions that would indicate `Stan` could not find algorithm settings that allowed the posterior to be explored, while not failing. These diagnostics can be found in the supplementary materials. Furthermore, implementation code is available at <https://github.com/RaihaTuiTaura/st-hawkes-thesis>.

To learn about short term trends, Figure 1 shows the expected number of events for each month, estimated by the intensity function $\lambda(t, x, y)$, and compares these to the observed event counts. As a result of using the Bayesian methodology, we obtained 95% posterior intervals to represent the uncertainty around these estimated values. For each month, the event counts at each location were summed to obtain the total monthly event count. The estimated mean number of events in each month is in line with the observed data and the model is able to react quickly to recent events. Furthermore, updated estimates of conflict risk can be calculated as new data arrives by simply re-evaluating the intensity function using the estimated model parameters.

The posterior median excitation kernels estimated from the Bayesian model for each country are presented in Figure 2. For several conflict types Nepal has a quickly decaying temporal triggering kernel, suggesting that the level of self-excitation is highest in the first month following an event and subsides quickly thereafter. While for the remaining scenarios, the temporal kernels generally have a longer memory, meaning the influence of past events can persist as time elapses.

Furthermore for most conflict types, spatial clustering of conflict events is more localised in Bangladesh and Pakistan with quickly decaying spatial triggering kernels. On the other hand, Nepal and Sri Lanka have more slowly decaying kernels for all conflict types excluding Protests and Riots, suggesting that the influence to the intensity function for events occurring in nearby locations and those further away are more similar compared to other conflict types.

Figure 3 presents a map of the median conflict risk over the 5 year observation window considered in this study. The maps show that most activity occurs in or near the capital cities for Bangladesh, Nepal and Pakistan. Pakistan also has a high concentration of protests on the southeastern border. Areas of the maps that are missing correspond to locations where no events were recorded over the 5 year period. These missing areas are particularly pronounced in Sri Lanka, which experienced a much lower volume of events over the observation window. Maps of the absolute value of the corresponding residuals for each country can be found in the supplementary materials. The residuals are generally quite low, with larger residuals corresponding to areas with a higher volume of events.

To assess the predictive ability of the Bayesian model, Figures 4 and 5 show the results from out-of-sample posterior predictive checks. Using 100 posterior samples, we simulated three months of data following on from the end of the 5 year observation window, which corresponds to predicting the first three months of 2015. The results were then aggregated, over both location and time, for each country and conflict type pair. Overall, the 95% interval for the predicted number of events usually encapsulates the observed number of events. However there are some larger than

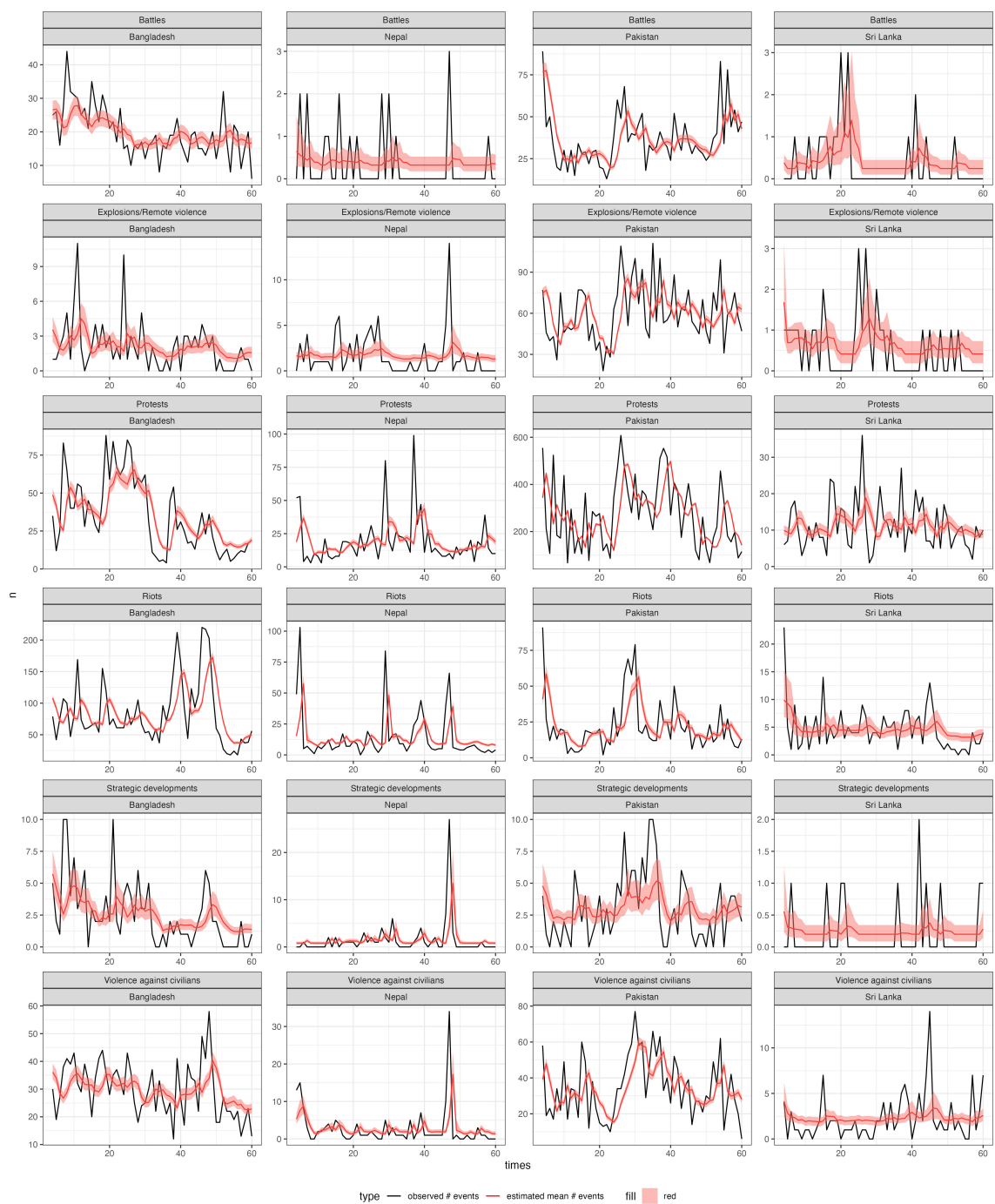
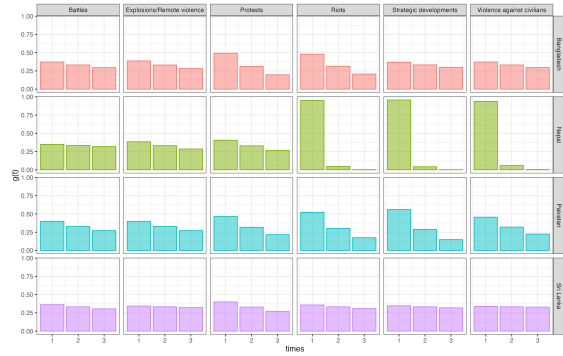
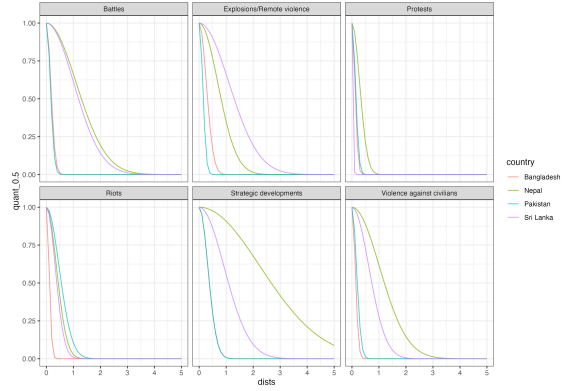


Figure 1: Observed data on month t (black line) versus estimated $\lambda(t)$ (red line) and 95% posterior interval (red ribbon). Bayesian model estimated via Stan.



(a) Estimated temporal excitation kernels.



(b) Estimated spatial excitation kernels. Units for horizontal axis are distance between two sets of coordinates, measured by Euclidean distance.

Figure 2: Posterior median estimated excitation kernels for all countries.

expected event counts that are not captured in our prediction intervals. This is likely because there is no mechanism in our model to allow for more extreme event counts, such as an over-dispersion parameter.

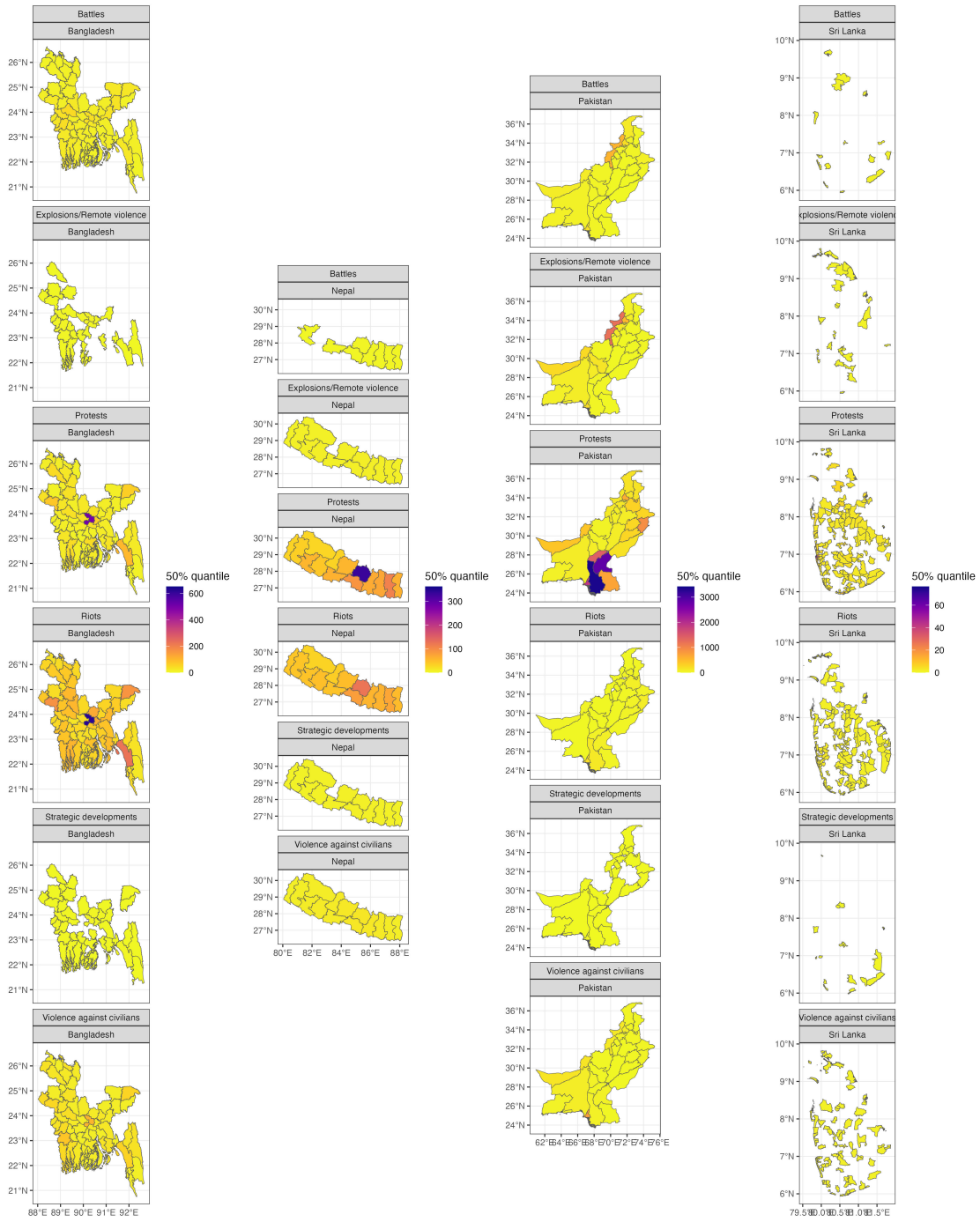


Figure 3: Posterior median number of events over 5 year observation window

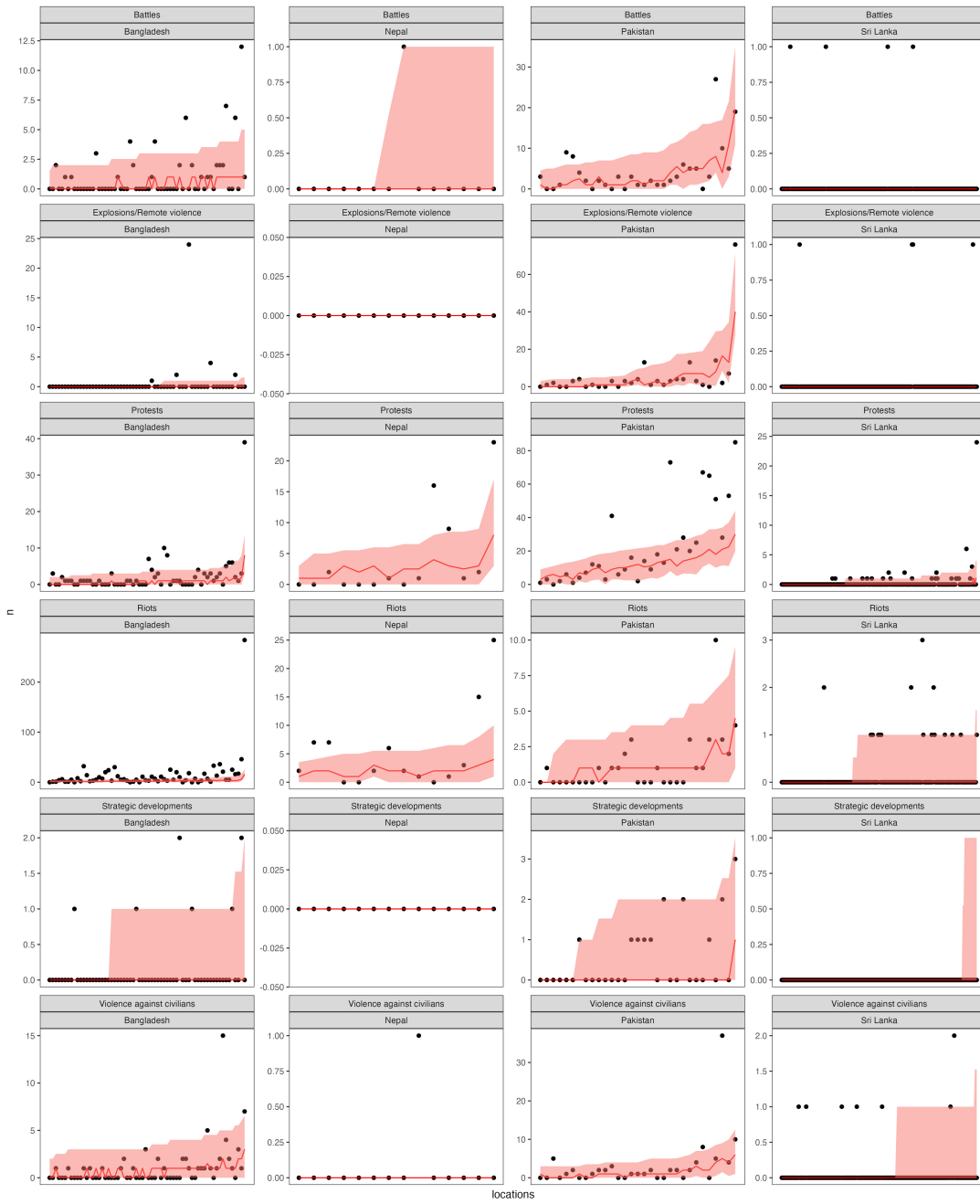


Figure 4: Out of sample predictive checks, aggregated over 3 month prediction interval for each location and conflict type. The black dots show the observed number of events. The red bars show the 95% interval of simulated events using parameter values from 100 posterior samples.

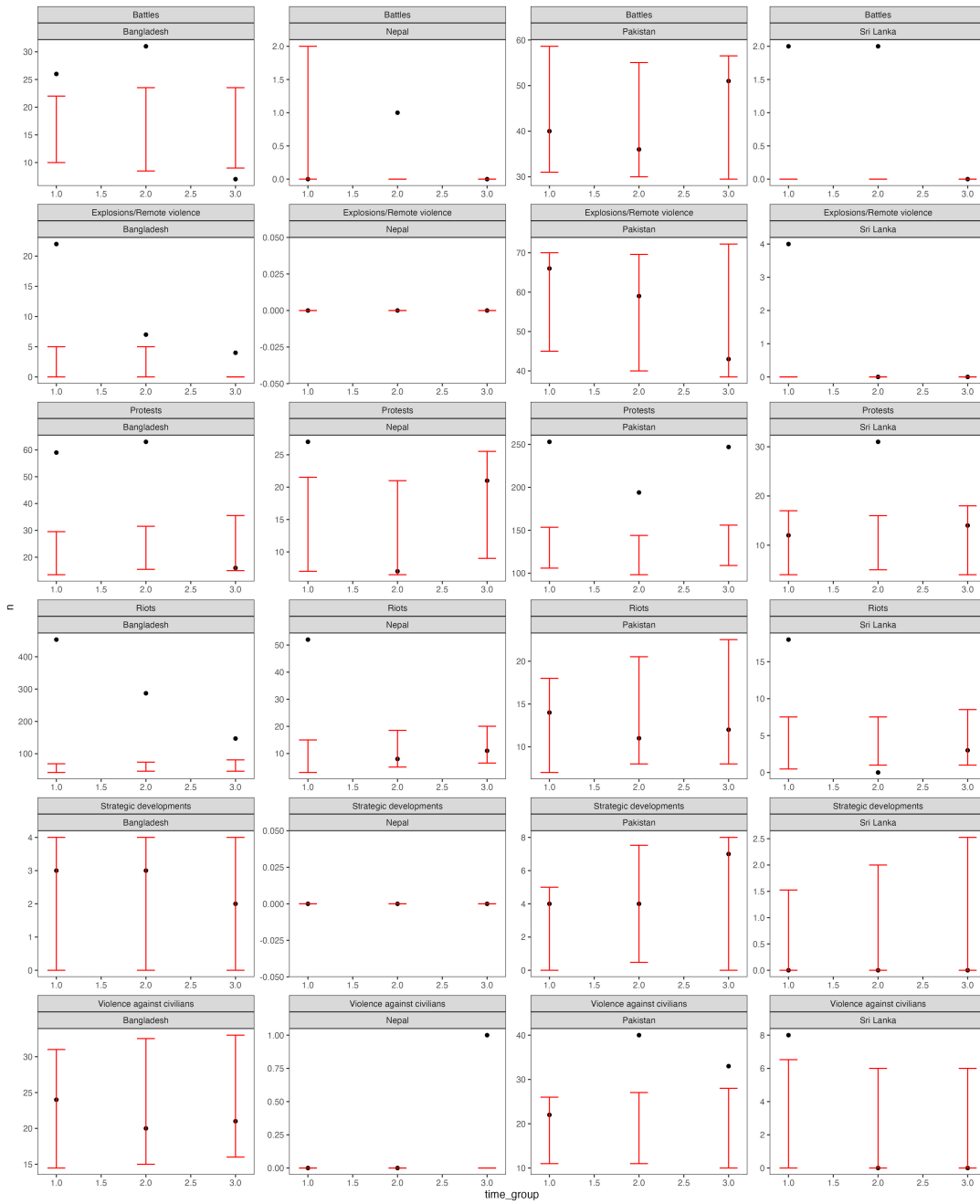


Figure 5: Out of sample predictive checks, aggregated over all locations for each month and conflict type. The red bars show the 95% interval of simulated events using parameter values from 100 posterior samples.

3.2 Maximum likelihood approach

While the Bayesian approach presented in Section 3.1 has many advantages, as discussed in Section 2.3, maximum likelihood estimation is a less computationally expensive approach. Therefore, here we present this alternative inference method and compare the estimated model with the Bayesian approach. The point estimates obtained via maximum likelihood estimation for all countries and conflict types and the corresponding estimates from the Bayesian approach are presented in Figure 6. In most cases the maximum likelihood estimates (MLEs) lie within or are close to their respective 95% posterior credible intervals. The intensity functions estimated also align closely with the observed data, as in the Bayesian approach. The MLEs obtained and plots of the estimated intensity functions are available in the supplementary materials.

The magnitude parameter α indicates the level of self-excitation present in the data. For all countries, strategic developments have the lowest level of self-excitation with the lowest α parameters, while, protests have the highest level out of all conflict types. In Sri Lanka, protests are the only conflict type that exhibits a reasonably high level of self-excitation, since α is very low for all other types. Overall, Pakistan displays the highest tendency for self-exciting behaviour out of all countries, with a consistently higher or comparable α for all conflict types. The inverse mean of the geometric temporal triggering kernel β is generally low, with the exception of several conflict types in Nepal. This indicates that the influence of past events on the future intensity is more sustained throughout the 3 month excitation time. The background rate μ is generally higher for protests and riots, indicating that, compared to other conflict types, more protests and riots arise independently as opposed to arising due to other events in the process. The spatial influence of these conflict types also tends to be more localised, as indicated by a small σ , the bandwidth for the spatial triggering kernel.

Figure 7 presents a comparison of the estimated model parameters and corresponding uncertainty quantification obtained using both inference approaches considered throughout this article for a single example scenario, namely Battles in Bangladesh. To calculate the standard errors of the MLEs, we assume asymptotic normality and subsequently take the square root of the negative inverse Hessian matrix. In the Bayesian setting, standard 95% posterior credible intervals are used. It is apparent that the Bayesian approach gives much more precise estimates of parameter uncertainty. Additionally, we found in some scenarios that the Hessian matrix was singular. Thus, while the MLE approach can give reasonable point estimates, it should be used with caution when being used for uncertainty quantification. Overall, the Bayesian approach is preferable when possible, but MLEs can be a reasonable alternative when computational resources are limited provided the results are carefully scrutinised, and if the user is mainly concerned with point estimates.

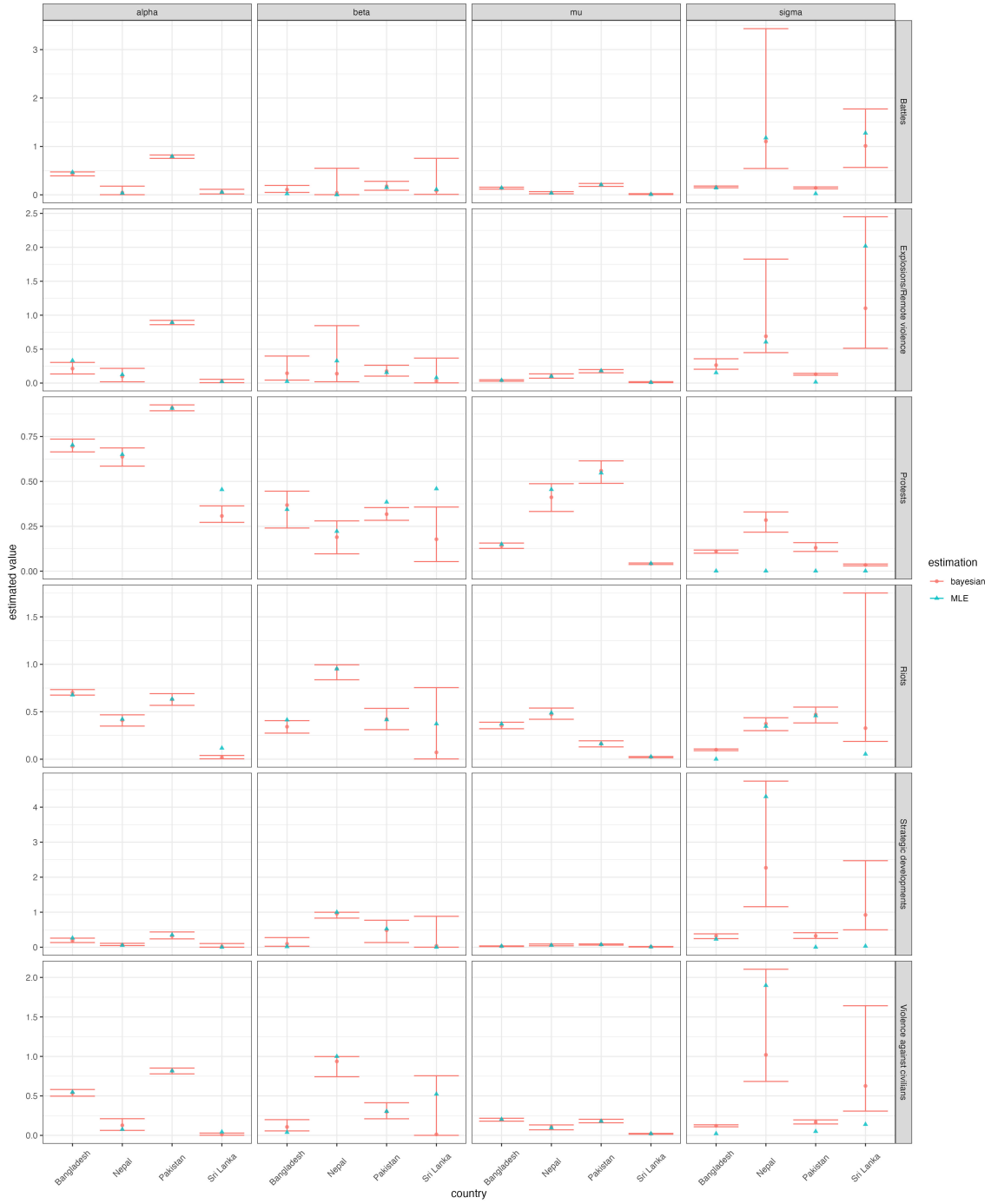


Figure 6: Comparison of estimated parameters for all conflict types and countries. MLE point estimates (blue) and posterior median and 95% interval (red).

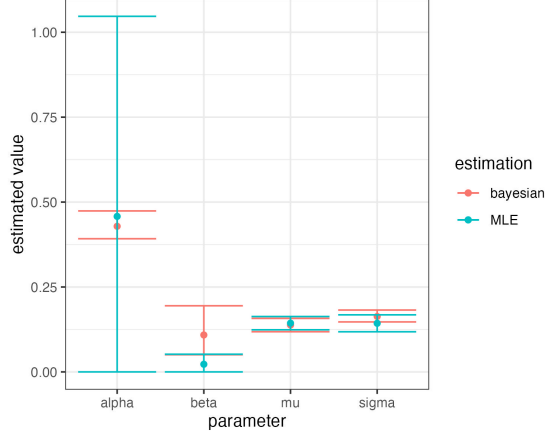


Figure 7: Battles in Bangladesh. 95% confidence intervals based on MLE approach versus 95% credible intervals based on Bayesian approach.

4 Assessing conflict risk in practice

Compared to relying on historical moving averages, a key advantage of using our model is the ability to mitigate the impact of noisy data and obtain stable estimates of risk. Our approach is also more interpretable than other statistical methods based on machine learning techniques, and our Bayesian approach provides a more precise understanding of uncertainty. By incorporating the time elapsed since past events and considering the influence of spatial distance between events in a sophisticated, yet interpretable way, we can provide a more robust foundation for monitoring risk and developing early warning tools, thus informing the allocation of resources for anticipatory actions.

In this section, we demonstrate through practical examples how our statistical model provides valuable insights that enable stakeholders to make more informed decisions about how to address conflict risks. In particular, we illustrate three types of insights from our modelling approach that may be useful for decision makers: an early warning tool for monitoring current trends, visualisations of the spatial risk profile of conflict events, and short term predictions about the future risk of conflict events.

Early warning tools are essential for funding bodies to be able to make decisions on how to allocate resources. While defining the thresholds for these early warnings is beyond the scope of this work, we aim to provide a more nuanced perspective by statistically modelling the trend of events, rather than using simple historical averages. To capture longer-term trends of increasing threat, we adopt a methodology closely based on that used by ACLED in their Trendfinder dashboard,

with the necessary modifications made to the time scale and spatial units to directly compare our model.

The Trendfinder dashboard calculates a rolling 12-month historical average of event counts, and flags time periods where the event count is more than two standard deviations above the rolling average. To benchmark this approach against our model, we instead used the quantile function of a Poisson distribution with mean given by the estimated intensity function from our model to determine time periods with unusually high activity. In particular, the estimated intensity function was calculated using 100 posterior samples of the model parameters. Then, for each posterior estimate of the intensity function, we obtained the median number of events and corresponding 95% interval of event counts at each month using the quantile function. Rolling 12-month averages were then taken of the median of these quantiles at each month. Time periods were then flagged if the observed number of events exceeded the rolling average of the 97.5% quantile.

Figures 8 and 9 present examples of early warning tools respectively based on our modelled risk estimates, and a naive approach using simple historical moving averages over the same time period, inspired by the ACLED Trendfinder dashboard. The naive approach has very over-confident and volatile uncertainty bounds, whereas our approach provides wider and more stable bounds. As a result, the naive approach is highly sensitive and flags many more months as having unusually high activity. Many of the event counts in months flagged using the naive approach are within the reasonable range of values expected from our model based on the estimated intensity function. Furthermore, in Sri Lanka a single event from either the battles or explosions/remote violence categories is flagged using the naive approach. Our approach is also more robust to outliers, since these events do not directly contribute to the calculation of the rolling average. The 97.5% trigger threshold was chosen arbitrarily in this example, but this threshold percentage can also be adapted to suit the risk appetite of the user.

The visualisation of the spatial risk profile for conflict events is also an important aspect of conflict risk monitoring. As an example, Figure 10 presents the median number of events expected during December 2014, the last month of the observation window considered in these analyses. Our modelling operates at a finer spatial scale than current methods employed by organisations such as ACLED. This granularity takes into account the unique attributes of each administrative region. Furthermore, the estimates can easily be aggregated up to obtain more accurate estimates of a coarser spatial resolution, with corresponding estimates of uncertainty.

Another notable advantage of adopting a statistical model for analysing conflict risk is the ability to generate short-term predictions of future events. In addition to estimating the level of future risk, our Bayesian approach also produces estimates of uncertainty surrounding the predicted number of events. In Section 3.1, we used 100 posterior samples to predict the expected number of events in the first 3 months of 2015, namely 3 months from the end of our modelling observation window. Figures 11 to 13 present the 2.5%, 50% and 97.5% percentiles of the cumulative number of



Figure 8: Hawkes model. **Grey bars:** no flag. **Blue bars:** flagged months (observed counts greater than 97.5% rolling 12-month average). **Red line and ribbon:** 12-month rolling average of the median 50%, 2.5% and 97.5% quantiles from the Poisson distribution, calculated from 100 posterior samples of the estimated intensity function.



Figure 9: Historical averages (based on ACLED Trendfinder dashboard). **Grey bars:** no flag. **Blue bars:** flagged months (observed counts more than two standard deviations above the rolling 12-month historical average). **Red line and ribbon:** 12-month rolling historical average plus or minus two standard deviations.

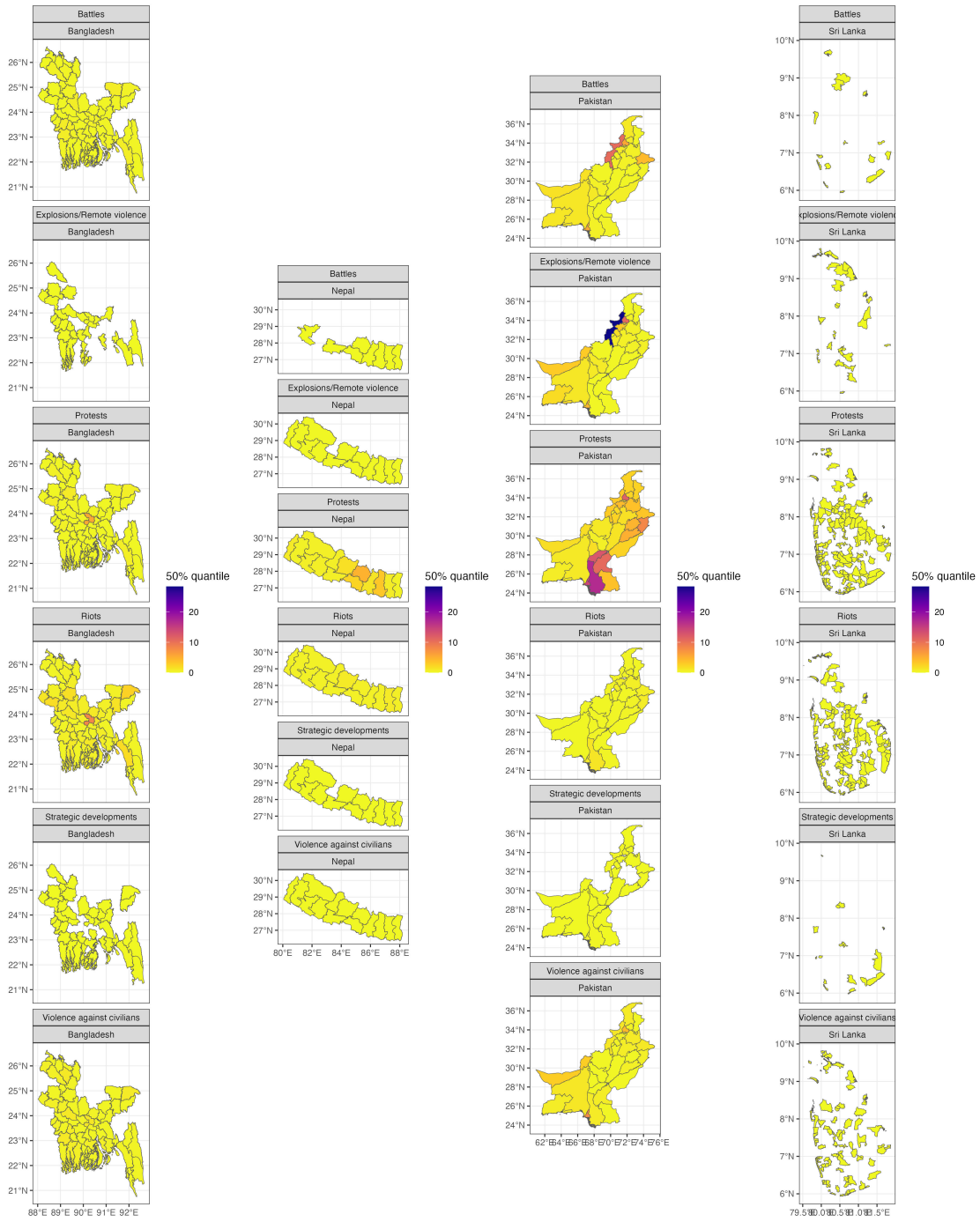


Figure 10: Risk of conflict events at December 2014 (i.e. the end of the observation window)

events predicted over these 3 months. Across most regions, the projected risk level for these three months is relatively low. However, there are numerous hotspots, particularly in Pakistan, where even the predictions for the lowest percentile suggest a substantial number of events. These spatial predictions, along with their uncertainty intervals, provide valuable insights into the distribution and intensity of anticipated conflict events, enabling policymakers and stakeholders to prioritise resources and interventions accordingly.

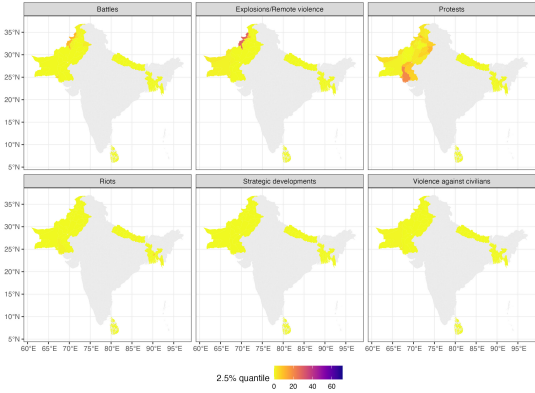


Figure 11: Out-of-sample 3-month-ahead predictions. 2.5% percentile of predicted events.

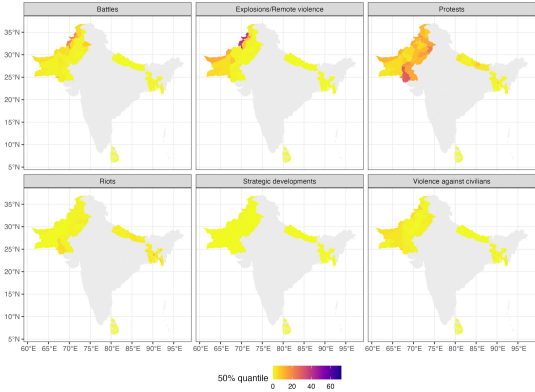


Figure 12: Out-of-sample 3-month-ahead predictions. 50% percentile of predicted events.

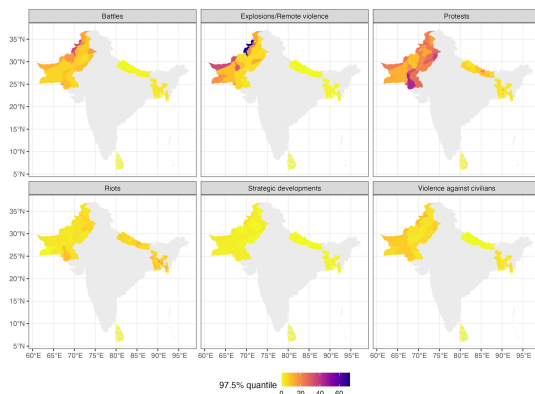


Figure 13: Out-of-sample 3-month-ahead predictions. 97.5% percentile of predicted events.

5 Discussion

This work addressed three main questions about spatiotemporal DTHPs: (i) are they useful for modelling conflict risk, (ii) what can we learn about conflict events using these models, and (iii) how can these models be used to improve current practices for conflict monitoring. Our main contributions and the results, and how they relate to these questions, are first summarised. This is followed by a discussion of the limitations and future work, and finally concluding remarks.

5.1 Summary

In this analysis we presented a unified framework using spatiotemporal DTHPs to analyse both the short and long term trends of conflict risk. Through the Bayesian framework, we can gain a more precise understanding of the uncertainty inherent in our estimates of conflict risk, compared to other approaches based on machine learning techniques and optimisation methods such as maximum likelihood estimation. To our knowledge this is the first analysis of its kind applied to the ACLED database, and the first to compare the various conflict types between each other and also among neighbouring countries. We also demonstrated from the practitioners' perspective the advantages of our approach and examples of how to interact with our model to gain valuable insights.

In response to our first research question, we find that spatiotemporal DTHPs are indeed a useful tool for policy makers to model and monitor conflict events. Our model was fitted to each of the individual countries within South Asia, and broken down further by the conflict type. The resulting models performed well and reacted quickly to recent events to capture and understand the self-exciting nature of conflict in the short term. A less computationally intensive approach based on maximum likelihood estimation was also presented, and we determined that while this approach gives reasonable point estimates, the Bayesian model is preferred due to more reliable uncertainty

quantification. We also performed out-of-sample predictive checks, which showed that our model was generally capable of producing a reasonable range of estimates for the predicted number of events over a 3 month period, with the exception of some extreme observations.

There are several key learnings from using spatiotemporal DTHPs for modelling conflict events that address our second question. While other modelling approaches can also provide a measure of conflict risk, interpretation of the parameters in our model offers unique insights. The level of independent events and those that are caused by past events can be directly quantified through the baseline and magnitude parameters respectively. This can help to inform preventative measures, for example where the baseline rate of events is high, there should be a focus on preventing new events from occurring. Whereas, if the magnitude parameter is high, there should be focus on monitoring ongoing events. We also quantified the effect that time and distance have on the risk of future conflict events by explicitly parameterising the temporal and spatial patterns of the process through their respective triggering kernels. We then used these kernels to compare the self-exciting characteristics of the various conflict types and countries to further deepen our understanding of these processes.

To address our final research question, we provided specific examples of how to use and adopt our models in practice and benchmark against current practices. We demonstrated how an early warning tool, used to monitor longer-term trends in the data and thus inform anticipatory actions, can be developed based on our statistical model. Specifically, this tool identifies when the observed level of events exceeds a threshold percentile determined by the posterior distribution, and we showed that our model is more stable and robust than the alternative based on historical averages. Visualisations for the current level of conflict risk estimated from our model were also presented. Our modelling was performed at a finer spatial resolution compared to similar analyses, allowing for more accurate estimates of conflict risk, even when aggregating into coarser spatial regions. Lastly, our statistical modelling approach allows us to make short-term predictions, and calculate the corresponding uncertainty in these estimates.

Our model provides a more sophisticated outlook on conflict risk compared to relying on historical averages, while remaining interpretable. Compared to ACLED's new prediction tool for conflict activity, CAST, the outputs of our models can be easily interpreted to quantify specific characteristics of conflict. Currently ACLED uses a combination of techniques to understand conflict, namely historical moving averages to analyse both short and long term trends and machine learning models for prediction. However, our model can fulfil both roles in one cohesive framework, meaning it could be a useful addition to the toolkit for conflict monitoring.

5.2 Limitations and future work

A major direction for future work is connecting the modelling of conflict risk with the human impact of conflict. To achieve this, covariates for the number of fatalities or other economic or demographic variables could be included in the model to inform and refine parameter estimates. An alternative approach is to jointly model the number of events and the number of people impacted by each of these events. The financial impact of conflict events, and how this corresponds with the type of anticipatory actions taken could also be explored.

Given sufficient computational resources or a more computationally efficient inference method, a global, multivariate model for conflict events could be estimated to characterise the interactions between countries and regions. Alternatively, if interactions were less important, and instead similarities between regions were of interest, univariate studies could be conducted in parallel and the estimated parameters grouped via a clustering algorithm to determine countries or regions with similar risk profiles. Furthermore, a multivariate model between conflict types could be fitted, to capture and quantify dependencies between each of the conflict types. The level of risk identified in our analysis could also be compared to other trends, for example economic or demographic time series to determine any interactions.

The estimation of the spatial kernel enables the characterisation of spatial risk profiles between countries and conflict types. However, its inclusion does not greatly improve predictive accuracy as shown in the supplementary materials. While prediction is not a key focus of this article, further work could be undertaken to explore alternative modelling approaches to improve predictive performance.

One phenomenon observed throughout this analysis was that the proposed model struggles to capture more extreme event counts. The mean intensity, represented by $\lambda(t)$, will rarely reach these peaks since they are in the tails of the posterior distribution. However, some modifications could be made to the model to better represent this range in values. For example, one could incorporate an over-dispersion term by adopting a negative binomial likelihood as opposed to the Poisson likelihood. Another approach could use a hurdle model (Porter and White, 2012), that models a binary response for whether there will be a non-zero number of events, and the magnitude of events given a non-zero count. Further extensions could be considered to accommodate excess counts under this framework, such as a hidden Markov model or a simple mixture model.

The level of discretisation, both spatial and temporal, is also an important consideration in the modelling. The inference is more stable given a coarser discretisation as it avoids the issue of zero-inflated event counts. A coarser aggregation level also reduces the computational expense of the inference. However, there is an approximation error introduced in the discrete-time model that assumes events that occur in the same interval are independent, and thus cannot have been produced by one another. Therefore, if the discretisation is too coarse, there is the potential to artificially inflate the baseline rate. The discretisation error is explored for temporal Hawkes processes in

Kirchner (2016). Further work could be undertaken to explore the impact of this approximation error, and to determine the optimal discretisation level for a given dataset. The same arguments also apply to the spatial aggregation, however in this case study we believe the administrative boundaries used are sensible given the implicit modelling assumption of homogeneity between all events that occur in the same region. Siviero et al. (2024) also investigate this discretisation error for spatiotemporal Hawkes processes.

5.3 Conclusion

Overall, a better statistical model of both shorter and longer term trends in the risk of conflict can lead to more accurate predictions, more effective policy interventions and enhanced early warning systems. These benefits can ultimately help to prevent conflicts and minimise their impact on individuals and communities. To our knowledge, we propose the first spatiotemporal Hawkes model for conflict data in the Bayesian setting, with full characterisation of the spatial and temporal triggering kernels. While this article explores its use among countries in South Asia, the methodology could easily be extended to other countries or continents to provide an estimate of the spatiotemporal risk of conflict events worldwide. We propose South Asia as an intrinsically meritorious study and as an important exemplar of how these models can be used.

Our proposed model provides a means for up to date estimates of the risk of conflict events. Our model can provide reasonable estimates of both short and long term trends in the occurrence of conflict events and also provide short-term predictions, determined using the posterior predictive distribution. This is also the first study we are aware of that captures and compares the characteristics of conflict events across different countries and types of events, and that demonstrates the advantage of using a statistical model to monitor conflict risk, compared to relying on historical averages. These features make this work a useful tool for actors in the humanitarian and social sciences sectors to better understand these risks and make more informed decisions.

This work paves the way for new explorations in spatiotemporal modelling for conflict events. Our desire is that this work advances the current state of conflict risk modelling by providing a nuanced foundation for which anticipatory action and financing decisions can be based. We hope that it enables further discussions with key stakeholders to enable more sophisticated and data driven risk estimates of conflict events worldwide.

References

- ACLED. Armed Conflict Location and Event Data Project (ACLED) Codebook. https://www.acleddata.com/wp-content/uploads/dlm_uploads/2019/04/General-User-Guide_FINAL.pdf, 2019. Accessed: 04 April 2022.
- Raiha Browning, Deborah Sulem, Kerrie Mengersen, Vincent Rivoirard, and Judith Rousseau. Simple discrete-time self-exciting models can describe complex dynamic processes: A case study of COVID-19. *PLoS one*, 16(4):e0250015, 2021. doi: 10.1371/journal.pone.0250015.
- Raiha Browning, Judith Rousseau, and Kerrie Mengersen. A flexible, random histogram kernel for discrete-time Hawkes processes. *arXiv*, 2022. doi: 10.48550/arxiv.2208.02921.
- Seth Caldwell. Assessing the technical feasibility of conflict prediction for anticipatory action. Technical report, United Nations Office for the Coordination of Humanitarian Affairs (OCHA) Centre for Humanitarian Data, 2022.
- Gian Maria Campedelli and Maria R. D’Orsogna. Temporal clustering of disorder events during the COVID-19 pandemic. *PLoS ONE*, 16(4):e0250433, 2021. doi: 10.1371/journal.pone.0250433.
- Feng Chen and Wai Hong Tan. Marked self-exciting point process modelling of information diffusion on Twitter. *Annals of Applied Statistics*, 12:2175 – 2196, 12 2018. doi: 10.1214/18-aos1148. URL <https://projecteuclid.org/euclid.aos/1542078041>.
- Nicholas J. Clark and Philip M. Dixon. Modeling and estimation for self-exciting spatio-temporal models of terrorist activity. *The Annals of Applied Statistics*, 12(1):633–653, 2018. ISSN 1932-6157. doi: 10.1214/17-aos1112.
- Hridoy Sankar Dutta, Vishal Raj Dutta, Aditya Adhikary, and Tanmoy Chakraborty. HawkesEye: Detecting Fake Retweeters Using Hawkes Process and Topic Modeling. *IEEE Transactions on Information Forensics and Security*, 15:2667–2678, 2020. ISSN 1556-6013. doi: 10.1109/tifs.2020.2970601.
- Osafu Augustine Egbon, Asrat Mekonnen Belachew, Mariella Ananias Bogoni, Bayowa Teniola Babalola, and Francisco Louzada. Bayesian spatio-temporal statistical modeling of violent-related fatality in western and central Africa. *Spatial Statistics*, 60:100828, 2024. ISSN 2211-6753. doi: 10.1016/j.spasta.2024.100828.
- Global Administrative Areas. GADM database of Global Administrative Areas, version 2.0. www.gadm.org., 2012. Accessed: 14 July 2022.
- Alan G Hawkes. Spectra of some self-exciting and mutually exciting point processes. *Biometrika*, 58(1):83 – 90, 04 1971. doi: 10.2307/2334319. URL <https://www.jstor.org/stable/2334319>.

- Gilian van den Hengel and Philip Hans Franses. Forecasting Social Conflicts in Africa Using an Epidemic Type Aftershock Sequence Model. *Forecasting*, 2(3):284–308, 2020. doi: 10.3390/forecast2030016.
- Robin John Hyndman and George Athanasopoulos. *Forecasting: Principles and Practice*. OTexts, Australia, 2nd edition, 2018.
- Mikyoung Jun and Scott Cook. Flexible multivariate spatiotemporal Hawkes process models of terrorism. *The Annals of Applied Statistics*, 18(2), 2024. ISSN 1932-6157. doi: 10.1214/23-aoas1839.
- M Kirchner. Hawkes and INAR(infty) processes. *Stochastic Processes and their Applications*, 126(8):2494 – 2525, 08 2016. doi: 10.1016/j.spa.2016.02.008. URL <https://linkinghub.elsevier.com/retrieve/pii/S0304414916000399>.
- Scott W Linderman and Ryan P Adams. Scalable Bayesian Inference for Excitatory Point Process Networks. *arXiv*, 07 2015. URL <https://arxiv.org/abs/1507.03228>.
- G O Mohler, M B Short, P J Brantingham, F P Schoenberg, and G E Tita. Self-exciting point process modeling of crime. *Journal of the American Statistical Association*, 106(493):100 – 108, 00 2011. doi: 10.1198/jasa.2011.ap09546. URL <https://doi.org/10.1198/jasa.2011.ap09546>.
- George Mohler. Modeling and estimation of multi-source clustering in crime and security data. *Annals of Applied Statistics*, 7(3):1525 – 1539, 09 2013. ISSN 1932-6157. doi: 10.1214/13-aoas647.
- Hannes Mueller and Christopher Rauh. The Hard Problem of Prediction for Conflict Prevention. *Journal of the European Economic Association*, 20(6):2440–2467, 2022. ISSN 1542-4766. doi: 10.1093/jeea/jvac025.
- Yosihiko Ogata. Statistical models for earthquake occurrences and residual analysis for point processes. *Journal of Computational and Graphical Statistics*, 83(401):9 – 27, 03 1988. doi: 10.2307/2288914. URL <https://www.jstor.org/stable/2288914>.
- Maya Okawa, Tomoharu Iwata, Yusuke Tanaka, Takeshi Kurashima, Hiroyuki Toda, and Hisashi Kashima. Context-aware spatio-temporal event prediction via convolutional Hawkes processes. *Machine Learning*, 111(8):2929–2950, 2022. ISSN 0885-6125. doi: 10.1007/s10994-022-06136-5.
- Michael D Porter and Gentry White. Self-exciting hurdle models for terrorist activity. *The Annals of Applied Statistics*, 6:106 – 124, 03 2012. doi: 10.1214/11-aoas513. URL <https://doi.org/10.1214/11-AOAS513>.
- André Python, Janine B Illian, Charlotte M Jones Todd, and Marta Blangiardo. A Bayesian approach to modelling subnational spatial dynamics of worldwide non-state terrorism, 2010–2016.

- Journal of the Royal Statistical Society: Series A (Statistics in Society)*, 182(1):323 – 344, 01 2019. doi: 10.1111/rssa.12384. URL <https://rss.onlinelibrary.wiley.com/doi/full/10.1111/rssa.12384>.
- Daniel Racek, Paul Thurner, and Goeran Kauermann. Integrating Spatio-temporal Diffusion into Statistical Forecasting Models of Armed Conflict via Non-parametric Smoothing. OSF Preprints q59dr, Center for Open Science, March 2024. URL <https://ideas.repec.org/p/osf/osfxxx/q59dr.html>.
- Clionadh Raleigh, reu Linke, Håvard Hegre, and Joakim Karlsen. Introducing ACLED: An Armed Conflict Location and Event Dataset. *Journal of Peace Research*, 47(5):651–660, 2010. ISSN 0022-3433. doi: 10.1177/0022343310378914.
- Carl Edward Rasmussen and Christopher K I Williams. *Gaussian Processes for Machine Learning*. Mit Press. Mit Press, 01 2006. ISBN 9780262182539.
- Sebastian Schutte. Regions at Risk: Predicting Conflict Zones in African Insurgencies*. *Political Science Research and Methods*, 5(3):447–465, 2017. ISSN 2049-8470. doi: 10.1017/psrm.2015.84.
- Emilia Siviero, Guillaume Staerman, Stephan Cléménçon, and Thomas Moreau. Flexible parametric inference for space-time hawkes processes. *arXiv preprint arXiv:2406.06849*, 2024.
- Stan Development Team. Stan Modeling Language Users Guide and Reference Manual, version 2.3. <https://mc-stan.org>, 2022.
- START (National Consortium for the Study of Terrorism and Responses to Terrorism). Global Terrorism Database 1970 - 2020. <https://www.start.umd.edu/gtd/>, 2021. Accessed: 23 Feb 2021.
- D Strandow, M Findley, D Nielson, and J Powell. The ucdp and aiddata codebook on georeferencing aid. <https://urn.kb.se/resolve?urn=urn:nbn:se:uu:diva-174842>, 2011. Accessed: 23 Feb 2021.
- Ralph Sundberg and Erik Melander. Introducing the UCDP Georeferenced Event Dataset. *Journal of Peace Research*, 50(4):523–532, 2013. ISSN 0022-3433. doi: 10.1177/0022343313484347.
- S A Tench. *Space-time modelling of terrorism and counter-terrorism. Doctoral thesis (Ph.D)*. PhD thesis, Department of Security and Crime Science, 2018.
- Aki Vehtari, Andrew Gelman, Daniel Simpson, Bob Carpenter, and Paul-Christian Bürkner. Rank-Normalization, Folding, and Localization: An Improved \hat{R} for Assessing Convergence of MCMC (with Discussion). *Bayesian Analysis*, 16(2):667 – 718, 2021. doi: 10.1214/20-BA1221. URL <https://doi.org/10.1214/20-BA1221>.

- Nils B Weidmann and Michael D Ward. Predicting Conflict in Space and Time. *Journal of Conflict Resolution*, 54(6):883–901, 2010. ISSN 0022-0027. doi: 10.1177/0022002710371669.
- Gentry White, Michael D Porter, and Lorraine Mazerolle. Terrorism Risk, Resilience and Volatility: A Comparison of Terrorism Patterns in Three Southeast Asian Countries. *Journal of Quantitative Criminology*, 29(2):295 – 320, 2013. ISSN 0748-4518. doi: 10.1007/s10940-012-9181-y. URL <http://link.springer.com/10.1007/s10940-012-9181-y>.
- WorldPop. WorldPop database. www.worldpop.org, 2022. Accessed: 14 July 2022.
- Xiaolan Xie, Dong Jiang, Mengmeng Hao, and Fangyu Ding. Modeling analysis of armed conflict risk in sub-Saharan Africa, 2000–2019. *PLOS ONE*, 18(10):e0286404, 2023. doi: 10.1371/journal.pone.0286404.
- Andrew Zammit-Mangion, Michael Dewar, Visakan Kadirkamanathan, and Guido Sanguinetti. Point process modelling of the Afghan War Diary. *Proceedings of the National Academy of Sciences*, 109(31):12414–12419, 2012. ISSN 0027-8424. doi: 10.1073/pnas.1203177109.
- Feida Zhu, Beng Chin Ooi, Chunyan Miao, Maya Okawa, Tomoharu Iwata, Yusuke Tanaka, Hiroyuki Toda, Takeshi Kurashima, and Hisashi Kashima. Dynamic Hawkes Processes for Discovering Time-evolving Communities’ States behind Diffusion Processes. *arXiv*, pages 1276–1286, 2021. doi: 10.1145/3447548.3467248.

A Analysis of spatiotemporal DTHPs

Here we aim to quantify the effect of incorporating a spatial triggering kernel into the DTHP by comparing a spatiotemporal model to one with only a temporal element. First, the maximum likelihood estimate for each model for all countries and conflict types in the data was estimated. We then compared the respective root mean squared error (RMSE) and Bayesian information criterion (BIC) for the two models. The RMSE was calculated via the square of the difference between y , the observed number of events, and λ , the estimated expected number of events given by the intensity function evaluated at the MLE, averaged over all event locations and times for the duration of the 5-year observation window considered in this study. Let k be an index denoting each unique time and location pairing (t, x, y) . Then the RMSE for a particular country and conflict type has the form,

$$\text{RMSE} = \sqrt{\frac{\sum_{k=1}^n (y_k - \lambda_k)^2}{n}} \quad (7)$$

where n is equal to the product of the total number of locations and time points in the sample. This RMSE is a measure of predictive risk and represents the average residual value for each country and conflict type pair over all spatial regions and times.

To construct a DTHP that does not account for spatial dependencies, while enabling direct comparison to the spatiotemporal alternative defined by the intensity function (3), we fix the spatial kernel $h(\cdot) = 1$ and restrict events that contribute to the intensity function to those occurring in the same region. The temporal comparison model then has a conditional mean function given by,

$$\lambda(t, x, y) = \mu + \alpha \sum_{i:t_i < t} y(t_i, x, y)g(t - t_i). \quad (8)$$

Table 1 compares the respective RMSE and BIC, defined in (7), that were obtained from the temporal and spatiotemporal models.

Country	Conflict Type	RMSE		BIC	
		Temporal	Spatiotemporal	Temporal	Spatiotemporal
Bangladesh	Battles	0.71	0.71	5071.95	5068.44
	Explosions/ remote violence	0.31	0.30	827.48	827.18
	Protests	1.35	1.35	6097.99	6102.04
	Riots	2.17	2.17	11002.97	11014.16
	Strategic developments	0.28	0.28	1108.90	1102.70
	Violence against civilians	0.87	0.87	6379.67	6383.71
Sri Lanka	Battles	0.15	0.13	195.51	190.77
	Explosions/ remote violence	0.14	0.13	310.33	308.29
	Protests	0.38	0.38	3942.13	3954.76
	Riots	0.20	0.20	2307.79	2290.09
	Strategic developments	0.11	0.11	132.65	136.70
	Violence against civilians	0.17	0.17	1222.23	1224.40
Nepal	Battles	0.21	0.21	170.64	173.66
	Explosions/ remote violence	0.44	0.42	576.15	579.24
	Protests	2.69	2.69	2884.76	2889.93
	Riots	2.16	2.17	2606.76	2605.53
	Strategic developments	0.47	0.46	554.72	525.04
	Violence against civilians	0.62	0.61	870.54	845.14
Pakistan	Battles	1.84	1.84	4426.67	4430.71
	Explosions/ remote violence	2.57	2.57	4934.38	4938.43
	Protests	12.19	12.20	14655.04	14670.93
	Riots	1.47	1.47	3732.09	3723.38
	Strategic developments	0.41	0.41	1046.76	1050.82
	Violence against civilians	2.13	2.13	4092.02	4096.07

Table 1: BIC and RMSE between the observed event counts and the estimated number of events from a temporal model versus a spatiotemporal model.

B Daily temporal aggregation

We initially considered a daily temporal aggregation of the spatiotemporal DTHP in Bangladesh from the period 2010 – 2011, for which the intensity function is given by (3). In this section, to obtain the set of locations \mathcal{S} , a naive discretisation was performed whereby the spatial boundaries in the data for each country were divided evenly into a 20×20 grid. The model parameters were then estimated via maximum likelihood estimation. The parameter estimates are presented in Table 2.

Conflict type	μ	α	β	σ
Battles	0.0054	0.1862	0.092	0.1784
Protests	0.0069	0.6664	0.0513	0.0993
Riots	0.0086	0.5989	0.0583	0.0901
Violence against civilians	0.0057	0.2092	0.1108	0.1624
Strategic developments	0	0	0.2665	0
Explosions/Remote violence	0.0058	0.0344	0.989	0.0269

Table 2: MLEs for spatiotemporal DTHP with daily temporal aggregation in Bangladesh

Figure 14 presents the observed events on day t versus the estimated mean number of events on day t , grouping together events on the same day at different locations. We find that the estimated number of events on each day closely follows the trend of the observed data, but some larger residuals are observed due to excess zero counts and also larger than expected daily counts.

Figure 15 assesses the predictive capability of the proposed model using out of sample predictive checks, using the same approach as in Section 3. It is difficult to compare these predictions to the actual number of events due to an excess number of zero counts, since most locations over the three-week testing window experienced few or no events. In most cases, the 80% prediction interval spans from 0 to 1 events, whereas in reality we know that most of these locations indeed experienced no events.

A Bayesian version of this spatiotemporal model was also considered at the daily temporal aggregation level using `Stan`. A large proportion of the model runs for each of the conflict types did not converge and had divergent transitions, indicating that Stan could not find algorithm settings that allowed the posterior to be explored, while not failing. This was likely due to model misspecification. There are many regions at each time increment that experienced no events, and the likelihood function used does not account for the level of excess number of zero counts present in these data.

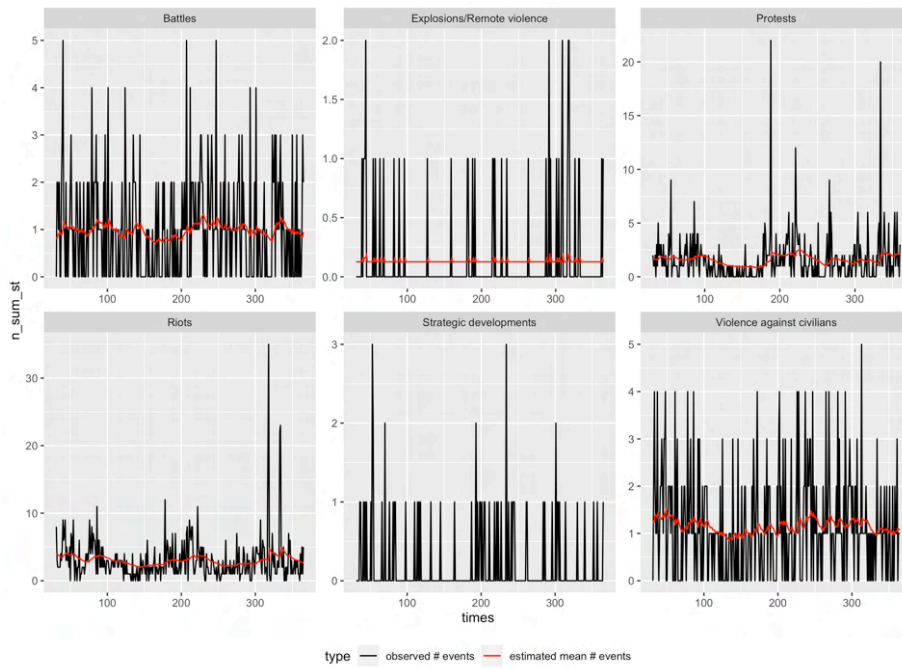
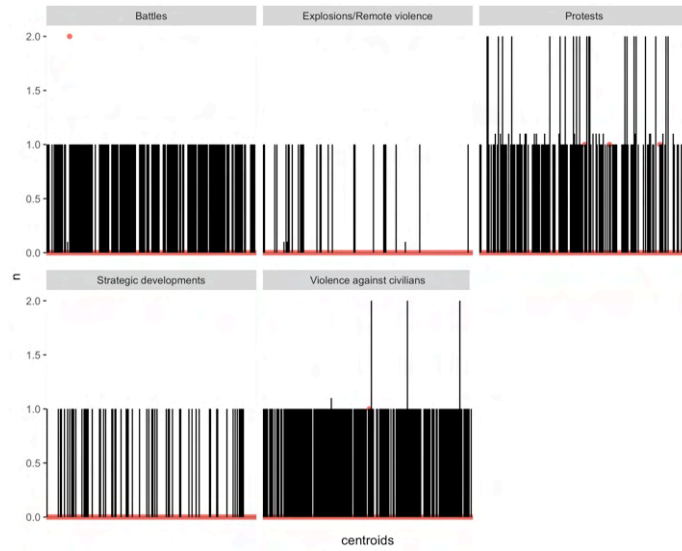
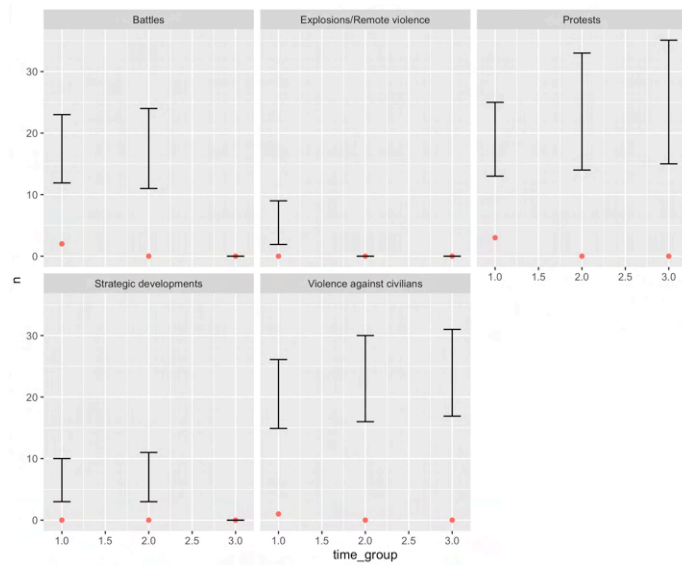


Figure 14: Spatiotemporal DTHP by conflict type for Bangladesh. Observed data on day t (black line) versus estimated $\lambda(t)$ (red line)



(a) Grouped by location and conflict type



(b) Grouped by months and conflict type

Figure 15: Out of sample predictive checks. The red dots show the observed number of events. The bars show the 80% interval of simulated events using the MLEs (from 100 simulations).

C Population model

Population data by administrative boundaries was obtained from WorldPop [2022]. We incorporated population into the model by introducing a population indicator defined by a binary variable indicating areas with “Low” and “High” population density. The population density was calculated by taking the total population in a given region relative to the area of the administrative boundary. The indicator was then determined by whether the population density for a particular region with centroid (x, y) fell below or above a given quantile of the population distribution for each country. To determine an appropriate threshold, each octile from $[0.5, 1)$ was considered. The root mean squared error (RMSE) for each of these thresholds was calculated using the approach outlined in Section A. While the difference in the various thresholds was not significant, the highest threshold of 87.5% had the lowest RMSE in the most cases. However, under this scenario there were several country and conflict type pairs that did not converge, indicating this more extreme threshold is less robust for all scenarios. Thus, the next lowest threshold of 75% was selected.

We assume that the population of a region could impact both the baseline and self-exciting components of the process, and thus we included population based parameters for the baseline rate μ and the magnitude parameter α . The model then has the following rate parameter $\lambda(t, x, y)$ for a particular time interval t and location with coordinates (x, y) ,

$$\begin{aligned} \lambda(t, x, y) = & (\mu_{\text{low}}\mathbb{I}_{\text{low}}(t, x, y) + \mu_{\text{high}}\mathbb{I}_{\text{high}}(t, x, y)) \\ & + \sum_{(t_i, x_i, y_i): t_i < t} (\alpha_{\text{low}}\mathbb{I}_{\text{low}}(t, x, y) + \alpha_{\text{high}}\mathbb{I}_{\text{high}}(t, x, y))g(t - t_i)h(x - x_i, y - y_i) \end{aligned} \quad (9)$$

where \mathbb{I}_{low} and \mathbb{I}_{high} indicate whether the location (x, y) is a region of low or high population density, respectively, at time interval t .

Here we compare the spatiotemporal models, namely the models that include and exclude population density information. For both of these models, RMSE is used to compare the observed event counts with the expected number of events, estimated via maximum likelihood estimation.

Table 3 presents the RMSE for the population and non-population models. There are several scenarios for which the model including population density information outperforms the model excluding population. However, there are also some cases for which the model excluding population performs better, and the differences in RMSE for all of these scenarios are often negligible. Moreover, in the majority of cases the RMSE is equal under both models. This suggests that for some scenarios, the particular population density threshold that was selected for classifying an area as high or low density may be useful, but a single threshold for all scenarios is inappropriate. Overall, it seems there is value in incorporating population density information into the model, however the full benefit is perhaps not being realised due to the general and coarse discretisation applied in these

analyses. Thus we leave this to future work, and excluded population density for the remainder of the analysis in this article.

Country	Conflict type	Non-population	Population
Bangladesh	Battles	0.71	0.71
	Explosions/Remote violence	0.30	0.30
	Protests	1.35	1.31
	Riots	2.17	2.15
	Strategic developments	0.28	0.28
	Violence against civilians	0.87	0.88
Sri Lanka	Battles	0.13	0.13
	Explosions/Remote violence	0.13	0.13
	Protests	0.38	0.37
	Riots	0.20	0.20
	Strategic developments	0.11	0.11
	Violence against civilians	0.17	0.17
Nepal	Battles	0.21	0.21
	Explosions/Remote violence	0.42	0.42
	Protests	2.69	2.65
	Riots	2.17	2.14
	Strategic developments	0.46	0.46
	Violence against civilians	0.61	0.61
Pakistan	Battles	1.84	1.84
	Explosions/Remote violence	2.57	2.57
	Protests	12.20	12.25
	Riots	1.47	1.46
	Strategic developments	0.41	0.41
	Violence against civilians	2.13	2.11

Table 3: RMSE between the estimated number of events using the maximum likelihood model and observed number of events for the models with and without population density

D Output from ARIMA analysis

To determine the extent of temporal autocorrelation, and thus set the maximum excitation time in our model, ARIMA models were fit for all country and conflict type combinations. The output from these analysis are below, and show that the maximum lag for any scenario is less than 3 months. The residuals were also checked for each of these models. There are some irregularities but they are generally within threshold limits.

```
[1] "Bangladesh"
[1] "Battles"
Series: tseries[[c]][[t]]
ARIMA(0,1,1) with drift

Coefficients:
          ma1      drift
      -0.8187  -0.2719
s.e.   0.0815   0.1552

sigma^2 = 37.93:  log likelihood = -190.51
AIC=387.01  AICc=387.45  BIC=393.25

Ljung-Box test

data:  Residuals from ARIMA(0,1,1) with drift
Q* = 8.2276, df = 9, p-value = 0.5114

Model df: 1.  Total lags used: 10

Saving 9.14 x 8.31 in image
[1] "Bangladesh"
[1] "Explosions/Remote violence"
Series: tseries[[c]][[t]]
ARIMA(0,1,1)

Coefficients:
          ma1
      -0.8795
s.e.   0.0671
```

sigma^2 = 5.08: log likelihood = -131.9
AIC=267.8 AICc=268.02 BIC=271.96

Ljung-Box test

data: Residuals from ARIMA(0,1,1)
Q* = 6.8066, df = 9, p-value = 0.6572

Model df: 1. Total lags used: 10

Saving 9.14 x 8.31 in image

[1] "Bangladesh"

[1] "Protests"

Series: tseries[[c]][[t]]

ARIMA(0,1,2)

Coefficients:

	ma1	ma2
	-0.2114	-0.3613
s.e.	0.1284	0.1422

sigma^2 = 263.2: log likelihood = -247.3
AIC=500.6 AICc=501.03 BIC=506.83

Ljung-Box test

data: Residuals from ARIMA(0,1,2)
Q* = 11.505, df = 8, p-value = 0.1747

Model df: 2. Total lags used: 10

Saving 9.14 x 8.31 in image

[1] "Bangladesh"

[1] "Riots"

Series: tseries[[c]][[t]]

ARIMA(1,0,0) with non-zero mean

Coefficients:

	ar1	mean
	0.6564	85.8648
s.e.	0.0961	13.5511

sigma² = 1431: log likelihood = -302.38
AIC=610.76 AICc=611.18 BIC=617.04

Ljung-Box test

data: Residuals from ARIMA(1,0,0) with non-zero mean
Q* = 12.612, df = 9, p-value = 0.181

Model df: 1. Total lags used: 10

Saving 9.14 x 8.31 in image

[1] "Bangladesh"

[1] "Strategic developments"

Series: tseries[[c]][[t]]

ARIMA(0,1,2)

Coefficients:

	ma1	ma2
	-0.547	-0.2125
s.e.	0.135	0.1391

sigma² = 6.124: log likelihood = -136.53
AIC=279.07 AICc=279.51 BIC=285.3

Ljung-Box test

data: Residuals from ARIMA(0,1,2)
Q* = 4.9268, df = 8, p-value = 0.7654

Model df: 2. Total lags used: 10

Saving 9.14 x 8.31 in image

[1] "Bangladesh"

[1] "Violence against civilians"

Series: tseries[[c]][[t]]

ARIMA(1,1,1)

Coefficients:

	ar1	ma1
	0.3387	-0.9037
s.e.	0.1531	0.0852

$\sigma^2 = 85.62$: log likelihood = -214.51

AIC=435.03 AICc=435.47 BIC=441.26

Ljung-Box test

data: Residuals from ARIMA(1,1,1)

Q* = 1.7261, df = 8, p-value = 0.9883

Model df: 2. Total lags used: 10

Saving 9.14 x 8.31 in image

[1] "Nepal"

[1] "Battles"

Series: tseries[[c]][[t]]

ARIMA(0,1,1)

Coefficients:

	ma1
	-0.8991
s.e.	0.0661

$\sigma^2 = 0.7275$: log likelihood = -74.65

AIC=153.31 AICc=153.52 BIC=157.46

Ljung-Box test

data: Residuals from ARIMA(0,1,1)
Q* = 6.0984, df = 9, p-value = 0.73

Model df: 1. Total lags used: 10

Saving 9.14 x 8.31 in image

[1] "Nepal"

[1] "Explosions/Remote violence"

Series: tseries[[c]][[t]]

ARIMA(1,0,0) with non-zero mean

Coefficients:

	ar1	mean
	0.1966	1.5415
s.e.	0.1259	0.3639

$\sigma^2 = 5.346$: log likelihood = -134.43

AIC=274.86 AICc=275.29 BIC=281.14

Ljung-Box test

data: Residuals from ARIMA(1,0,0) with non-zero mean

Q* = 2.3461, df = 9, p-value = 0.9847

Model df: 1. Total lags used: 10

Saving 9.14 x 8.31 in image

[1] "Nepal"

[1] "Protests"

Series: tseries[[c]][[t]]

ARIMA(0,0,0) with non-zero mean

Coefficients:

	mean
	18.9667
s.e.	2.2113

sigma² = 298.4: log likelihood = -255.58
AIC=515.16 AICc=515.38 BIC=519.35

Ljung-Box test

data: Residuals from ARIMA(0,0,0) with non-zero mean
Q* = 7.6303, df = 10, p-value = 0.6649

Model df: 0. Total lags used: 10

Saving 9.14 x 8.31 in image

[1] "Nepal"

[1] "Riots"

Series: tseries[[c]][[t]]

ARIMA(0,0,1) with non-zero mean

Coefficients:

	ma1	mean
	0.2892	13.7135
s.e.	0.1245	3.0635

sigma² = 353.1: log likelihood = -260.16
AIC=526.33 AICc=526.76 BIC=532.61

Ljung-Box test

data: Residuals from ARIMA(0,0,1) with non-zero mean
Q* = 3.7622, df = 9, p-value = 0.9264

Model df: 1. Total lags used: 10

Saving 9.14 x 8.31 in image

[1] "Nepal"

[1] "Strategic developments"

Series: tseries[[c]][[t]]

ARIMA(0,0,1) with non-zero mean

Coefficients:

	ma1	mean
	0.3103	1.3828
s.e.	0.1229	0.5853

sigma² = 12.48: log likelihood = -159.9
AIC=325.79 AICc=326.22 BIC=332.08

Ljung-Box test

data: Residuals from ARIMA(0,0,1) with non-zero mean
Q* = 1.552, df = 9, p-value = 0.9967

Model df: 1. Total lags used: 10

Saving 9.14 x 8.31 in image

```
[1] "Nepal"  
[1] "Violence against civilians"  
Series: tseries[[c]][[t]]  
ARIMA(1,0,0) with non-zero mean
```

Coefficients:

	ar1	mean
	0.3058	2.9415
s.e.	0.1225	0.9023

sigma² = 24.71: log likelihood = -180.38
AIC=366.76 AICc=367.19 BIC=373.05

Ljung-Box test

data: Residuals from ARIMA(1,0,0) with non-zero mean
Q* = 3.6536, df = 9, p-value = 0.9327

Model df: 1. Total lags used: 10

Saving 9.14 x 8.31 in image

```
[1] "Pakistan"
[1] "Battles"
Series: tseries[[c]][[t]]
ARIMA(1,0,2) with non-zero mean
```

Coefficients:

	ar1	ma1	ma2	mean
	0.5513	-0.1805	0.4891	39.9163
s.e.	0.1690	0.1572	0.1440	5.1788

```
sigma^2 = 213: log likelihood = -244.42
AIC=498.83 AICc=499.95 BIC=509.31
```

Ljung-Box test

```
data: Residuals from ARIMA(1,0,2) with non-zero mean
Q* = 2.4517, df = 7, p-value = 0.9307
```

Model df: 3. Total lags used: 10

Saving 9.14 x 8.31 in image

```
[1] "Pakistan"
[1] "Explosions/Remote violence"
Series: tseries[[c]][[t]]
ARIMA(2,0,2) with non-zero mean
```

Coefficients:

	ar1	ar2	ma1	ma2	mean
	-0.3002	-0.5983	0.4515	0.9662	60.8505
s.e.	0.1545	0.1528	0.0888	0.1719	3.1316

```
sigma^2 = 398.1: log likelihood = -263.47
AIC=538.94 AICc=540.52 BIC=551.51
```

Ljung-Box test

```
data: Residuals from ARIMA(2,0,2) with non-zero mean
```

Q* = 4.1697, df = 6, p-value = 0.6537

Model df: 4. Total lags used: 10

Saving 9.14 x 8.31 in image

[1] "Pakistan"

[1] "Protests"

Series: tseries[[c]][[t]]

ARIMA(1,0,0) with non-zero mean

Coefficients:

	ar1	mean
	0.3387	277.0373
s.e.	0.1217	26.3073

sigma² = 19077: log likelihood = -379.87

AIC=765.73 AICc=766.16 BIC=772.02

Ljung-Box test

data: Residuals from ARIMA(1,0,0) with non-zero mean

Q* = 4.6214, df = 9, p-value = 0.866

Model df: 1. Total lags used: 10

Saving 9.14 x 8.31 in image

[1] "Pakistan"

[1] "Riots"

Series: tseries[[c]][[t]]

ARIMA(1,0,0) with non-zero mean

Coefficients:

	ar1	mean
	0.5199	22.6802
s.e.	0.1084	4.2232

sigma² = 264.3: log likelihood = -251.58

AIC=509.17 AICc=509.6 BIC=515.45

Ljung-Box test

data: Residuals from ARIMA(1,0,0) with non-zero mean
Q* = 3.0805, df = 9, p-value = 0.961

Model df: 1. Total lags used: 10

Saving 9.14 x 8.31 in image

[1] "Pakistan"

[1] "Strategic developments"

Series: tseries[[c]][[t]]

ARIMA(1,0,0) with non-zero mean

Coefficients:

	ar1	mean
	0.4912	3.1458
s.e.	0.1106	0.5852

$\sigma^2 = 5.68$: log likelihood = -136.37

AIC=278.73 AICc=279.16 BIC=285.02

Ljung-Box test

data: Residuals from ARIMA(1,0,0) with non-zero mean
Q* = 5.161, df = 9, p-value = 0.8201

Model df: 1. Total lags used: 10

Saving 9.14 x 8.31 in image

[1] "Pakistan"

[1] "Violence against civilians"

Series: tseries[[c]][[t]]

ARIMA(1,0,0) with non-zero mean

Coefficients:

```
          ar1      mean
    0.3708  34.2850
s.e.  0.1224   3.1886
```

```
sigma^2 = 253.7:  log likelihood = -250.28
AIC=506.56  AICc=506.99  BIC=512.84
```

Ljung-Box test

```
data:  Residuals from ARIMA(1,0,0) with non-zero mean
Q* = 5.5022, df = 9, p-value = 0.7885
```

Model df: 1. Total lags used: 10

Saving 9.14 x 8.31 in image

```
[1] "Sri Lanka"
```

```
[1] "Battles"
```

```
Series: tseries[[c]][[t]]
```

```
ARIMA(2,0,0) with non-zero mean
```

Coefficients:

```
          ar1      ar2      mean
    0.1281  0.3535  0.3310
s.e.  0.1198  0.1198  0.1496
```

```
sigma^2 = 0.3999:  log likelihood = -56.26
AIC=120.52  AICc=121.24  BIC=128.89
```

Ljung-Box test

```
data:  Residuals from ARIMA(2,0,0) with non-zero mean
Q* = 2.2225, df = 8, p-value = 0.9734
```

Model df: 2. Total lags used: 10

Saving 9.14 x 8.31 in image

```
[1] "Sri Lanka"
```

```
[1] "Explosions/Remote violence"
Series: tseries[[c]][[t]]
ARIMA(0,1,1)
```

```
Coefficients:
      ma1
      -0.7071
s.e.    0.1888
```

```
sigma^2 = 1.427: log likelihood = -94.06
AIC=192.12  AICc=192.33  BIC=196.27
```

Ljung-Box test

```
data: Residuals from ARIMA(0,1,1)
Q* = 12.108, df = 9, p-value = 0.2073
```

Model df: 1. Total lags used: 10

Saving 9.14 x 8.31 in image

```
[1] "Sri Lanka"
[1] "Protests"
Series: tseries[[c]][[t]]
ARIMA(0,0,0) with non-zero mean
```

```
Coefficients:
      mean
      11.1000
s.e.    0.8621
```

```
sigma^2 = 45.35: log likelihood = -199.06
AIC=402.12  AICc=402.33  BIC=406.31
```

Ljung-Box test

```
data: Residuals from ARIMA(0,0,0) with non-zero mean
Q* = 15.33, df = 10, p-value = 0.1205
```

Model df: 0. Total lags used: 10

Saving 9.14 x 8.31 in image

[1] "Sri Lanka"

[1] "Riots"

Series: tseries[[c]][[t]]

ARIMA(2,1,0)

Coefficients:

	ar1	ar2
	-0.5520	-0.4800
s.e.	0.1187	0.1373

sigma² = 25.71: log likelihood = -178.82

AIC=363.65 AICc=364.09 BIC=369.88

Ljung-Box test

data: Residuals from ARIMA(2,1,0)

Q* = 4.6727, df = 8, p-value = 0.7919

Model df: 2. Total lags used: 10

Saving 9.14 x 8.31 in image

[1] "Sri Lanka"

[1] "Strategic developments"

Series: tseries[[c]][[t]]

ARIMA(0,0,2) with non-zero mean

Coefficients:

	ma1	ma2	mean
	0.0931	0.5736	0.3547
s.e.	0.1313	0.1162	0.1519

sigma² = 0.5342: log likelihood = -65.19

AIC=138.37 AICc=139.1 BIC=146.75

Ljung-Box test

data: Residuals from ARIMA(0,0,2) with non-zero mean
Q* = 4.9934, df = 8, p-value = 0.7583

Model df: 2. Total lags used: 10

Saving 9.14 x 8.31 in image

[1] "Sri Lanka"

[1] "Violence against civilians"

Series: tseries[[c]][[t]]

ARIMA(1,0,0) with non-zero mean

Coefficients:

	ar1	mean
	0.3122	2.8027
s.e.	0.1772	0.6369

sigma² = 11.53: log likelihood = -157.51
AIC=321.01 AICc=321.44 BIC=327.3

Ljung-Box test

data: Residuals from ARIMA(1,0,0) with non-zero mean
Q* = 4.9006, df = 9, p-value = 0.8429

Model df: 1. Total lags used: 10

Saving 9.14 x 8.31 in image

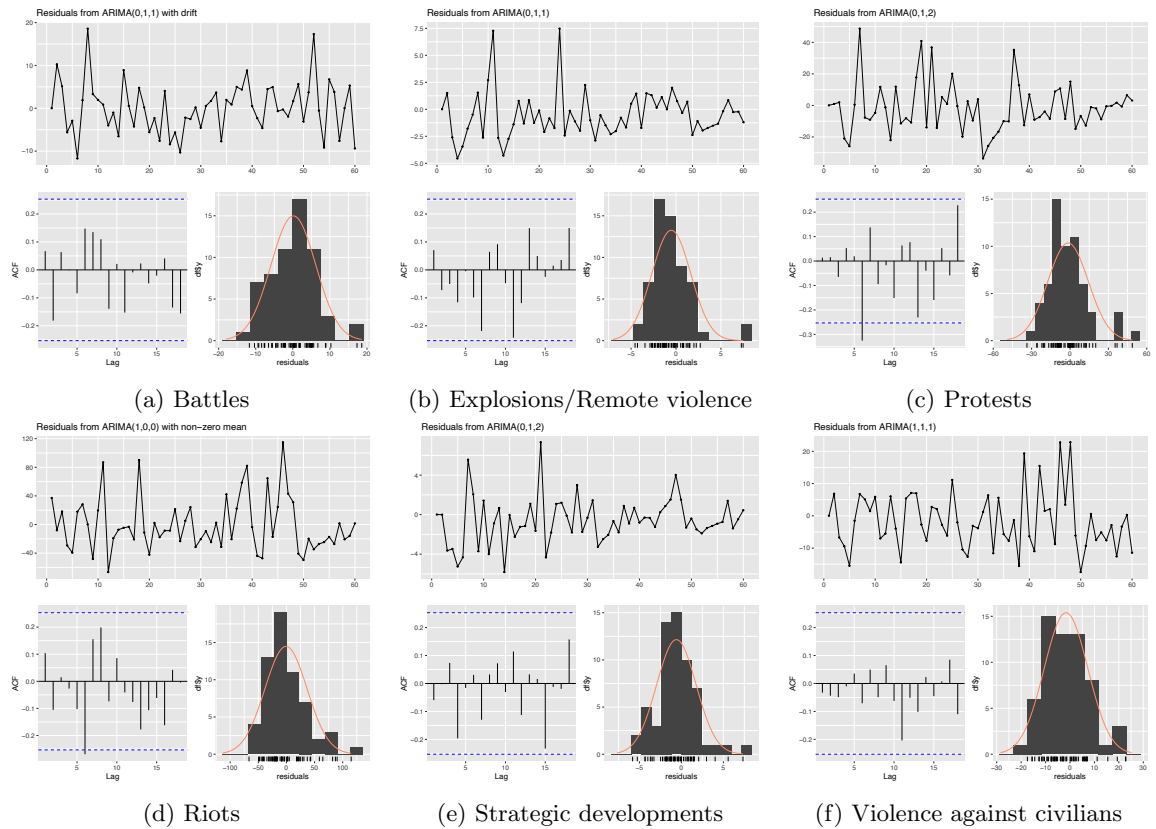


Figure 16: Bangladesh. Time plot of the residuals, the corresponding ACF, and a histogram.

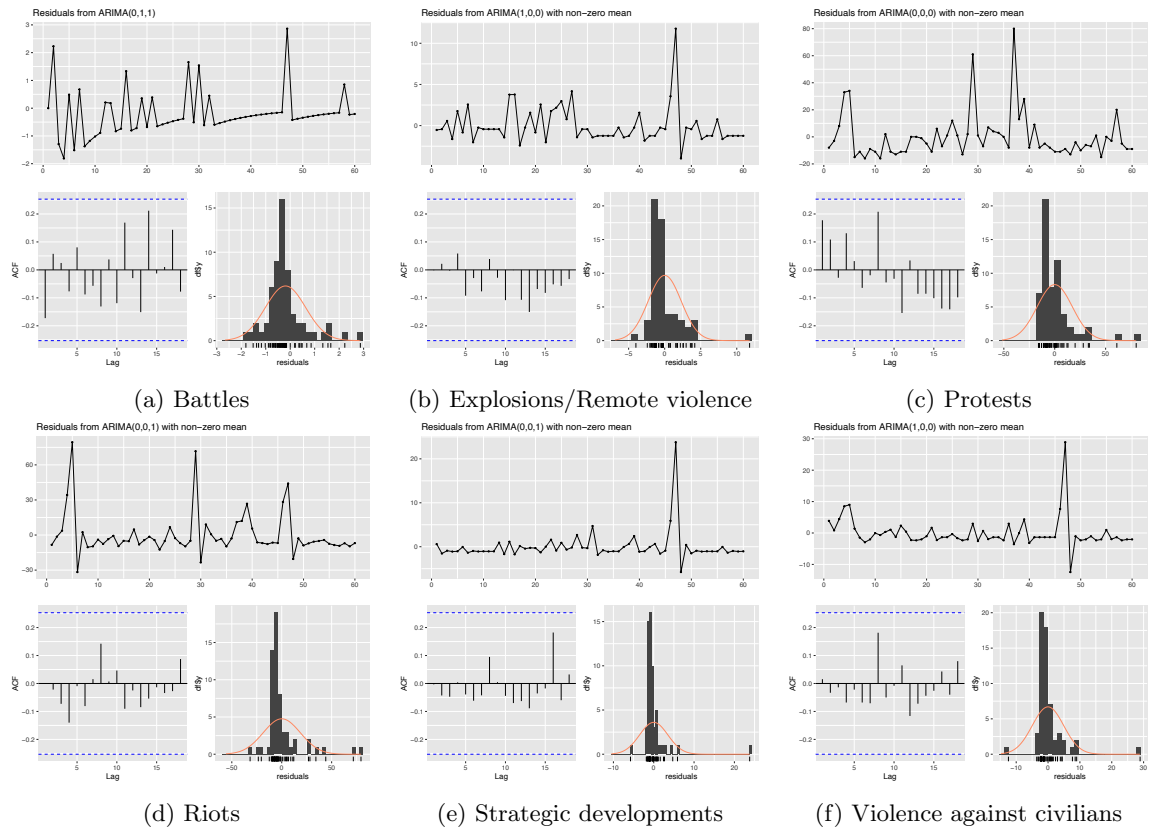


Figure 17: Nepal. Time plot of the residuals, the corresponding ACF, and a histogram.

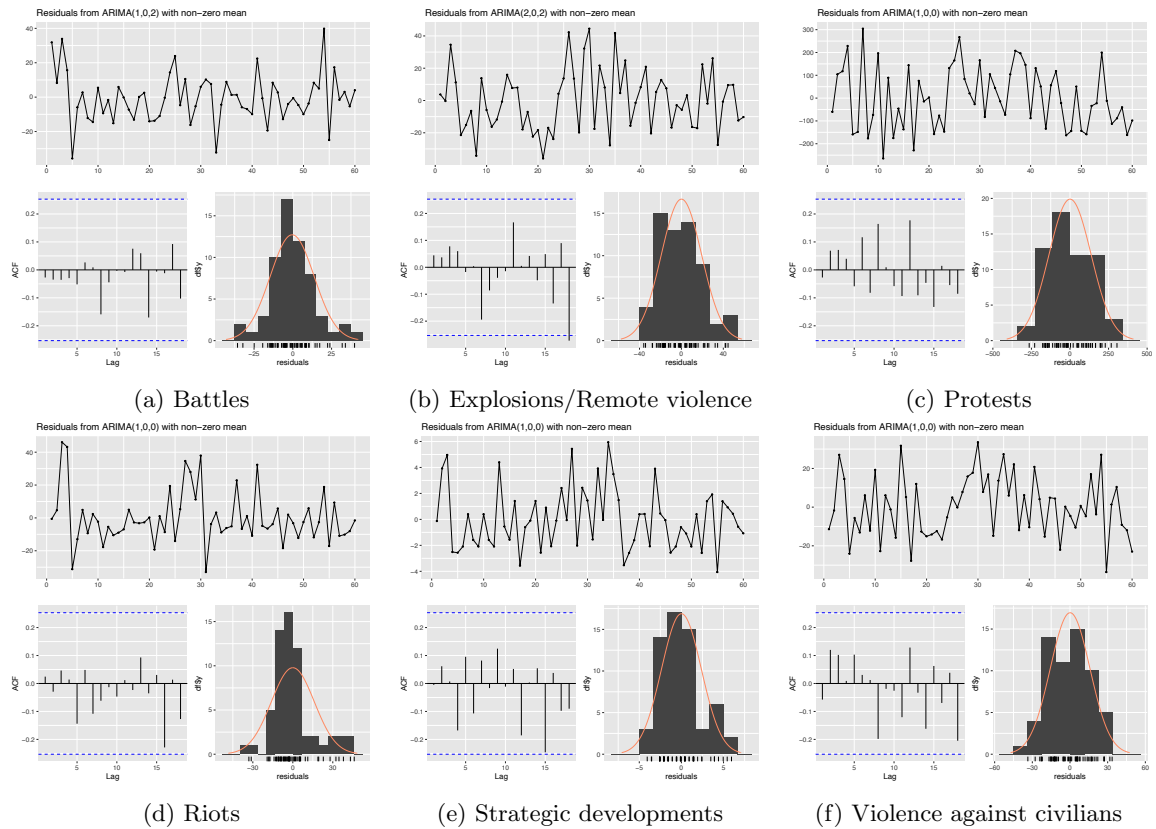


Figure 18: Pakistan. Time plot of the residuals, the corresponding ACF, and a histogram.

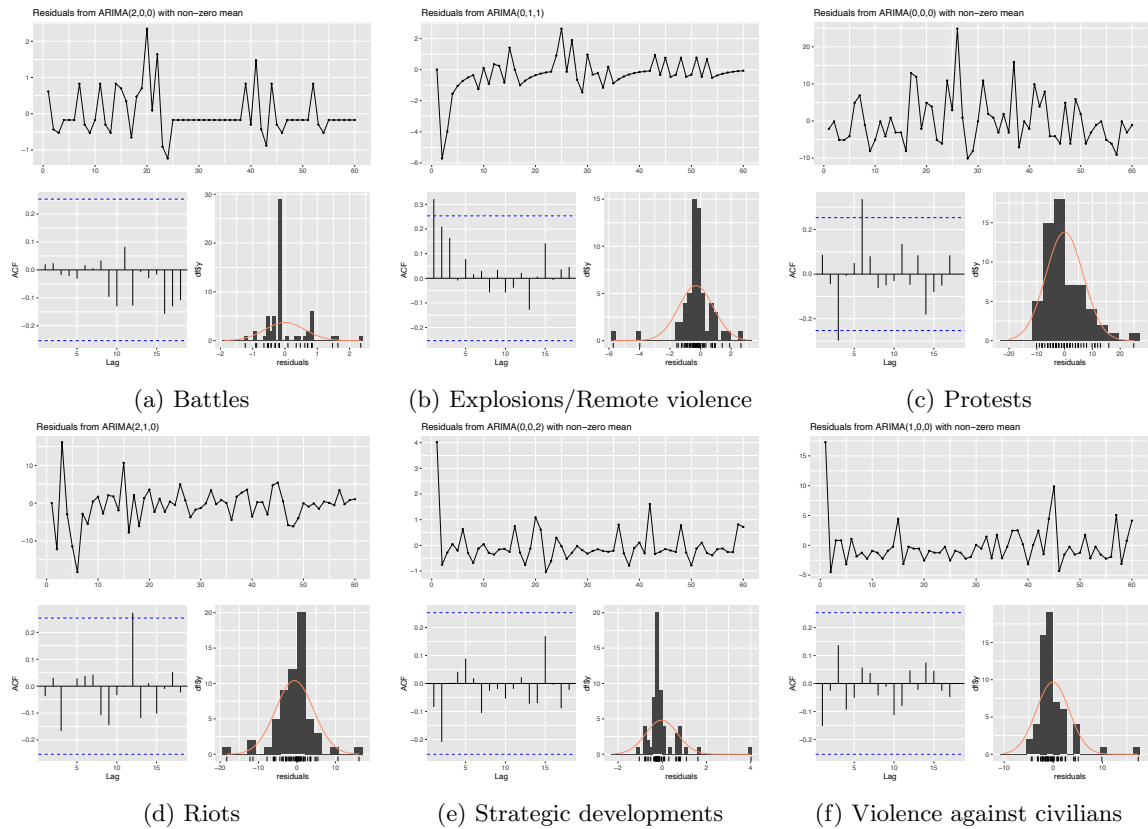


Figure 19: Sri Lanka. Time plot of the residuals, the corresponding ACF, and a histogram.

E MCMC diagnostics

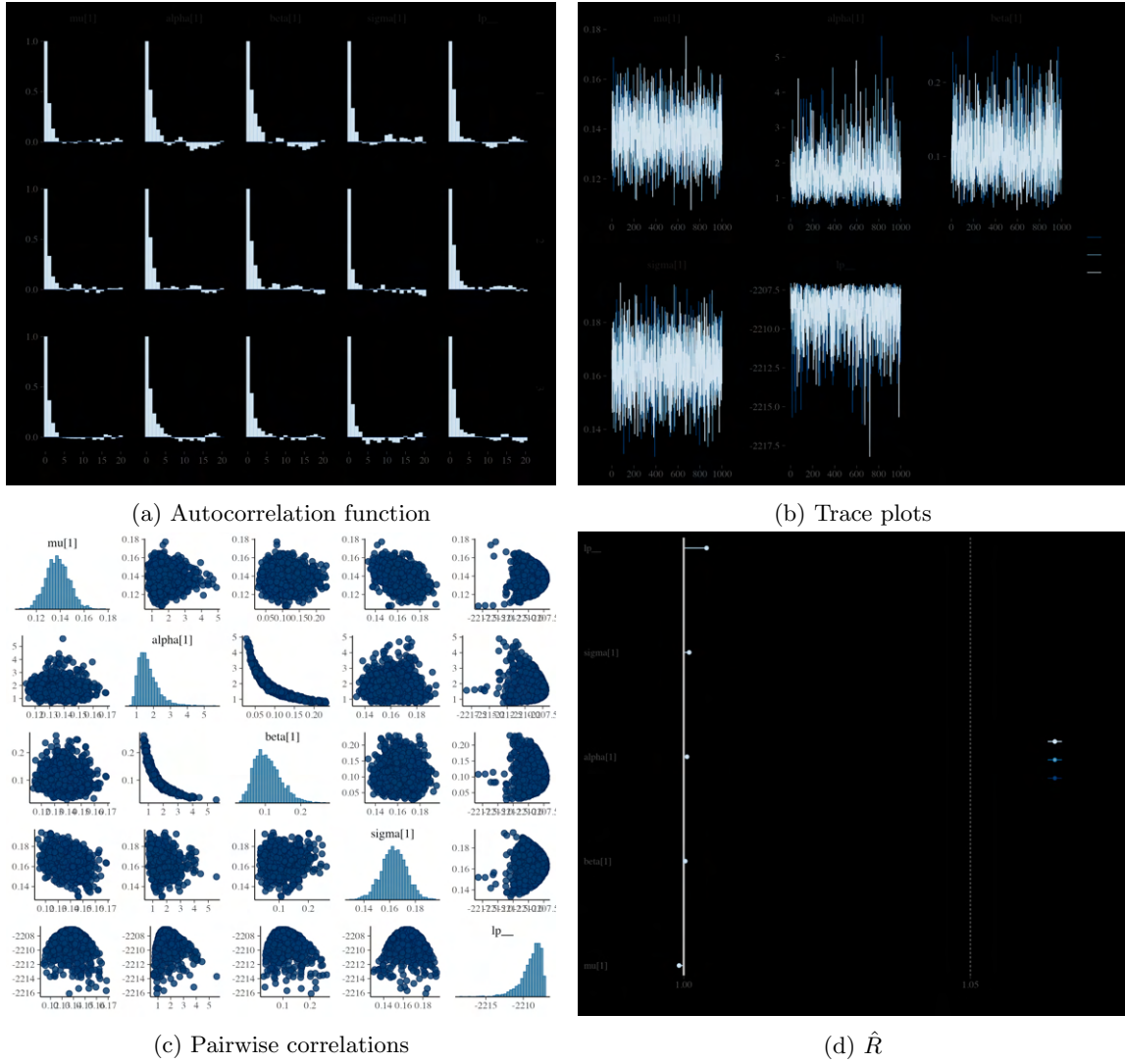
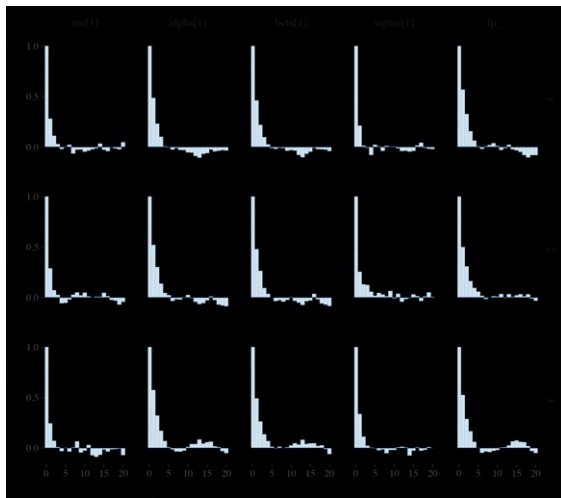
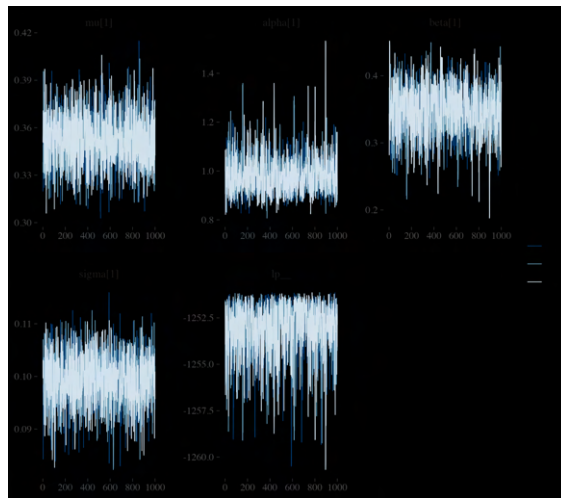


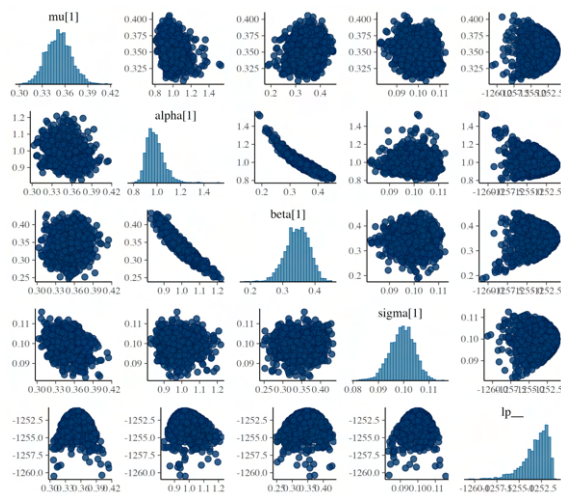
Figure 20: MCMC diagnostic plots for Battles in Bangladesh.



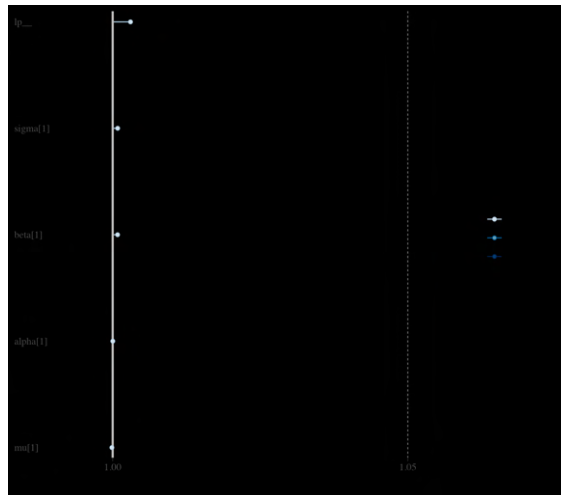
(a) Autocorrelation function



(b) Trace plots

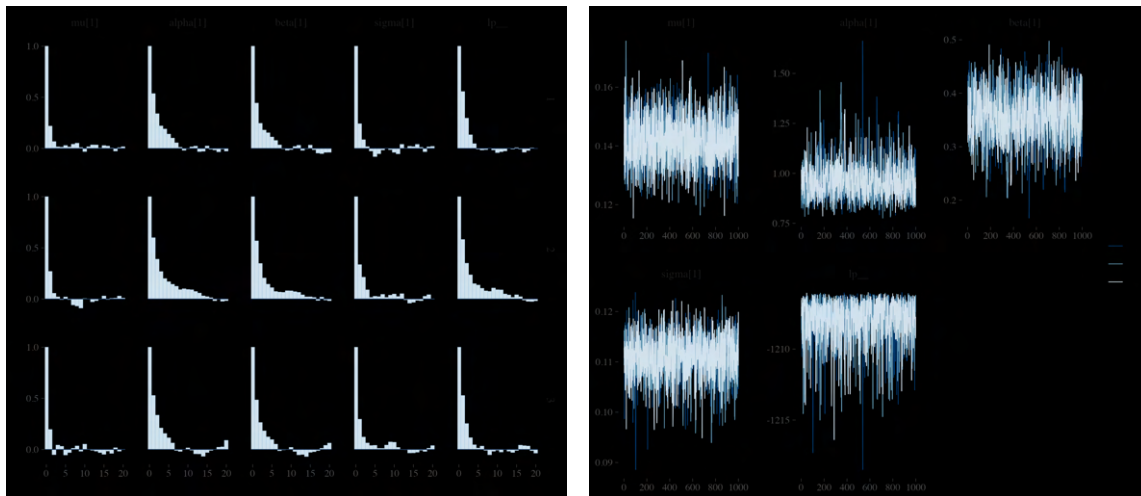


(c) Pairwise correlations



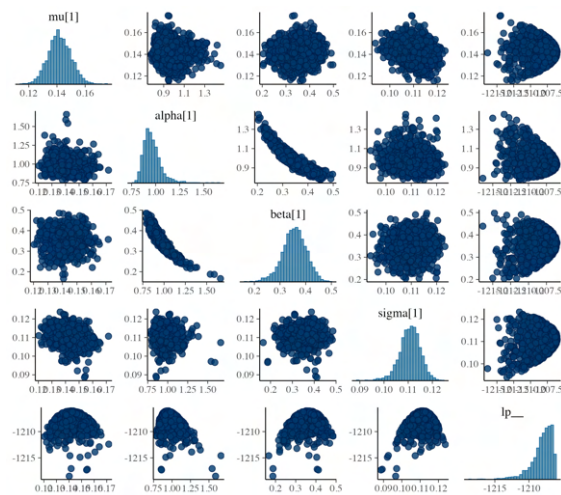
(d) \hat{R}

Figure 21: MCMC diagnostic plots for Riots in Bangladesh.

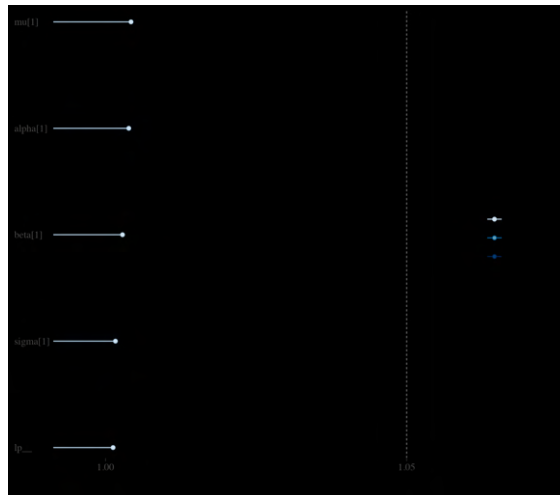


(a) Autocorrelation function

(b) Trace plots

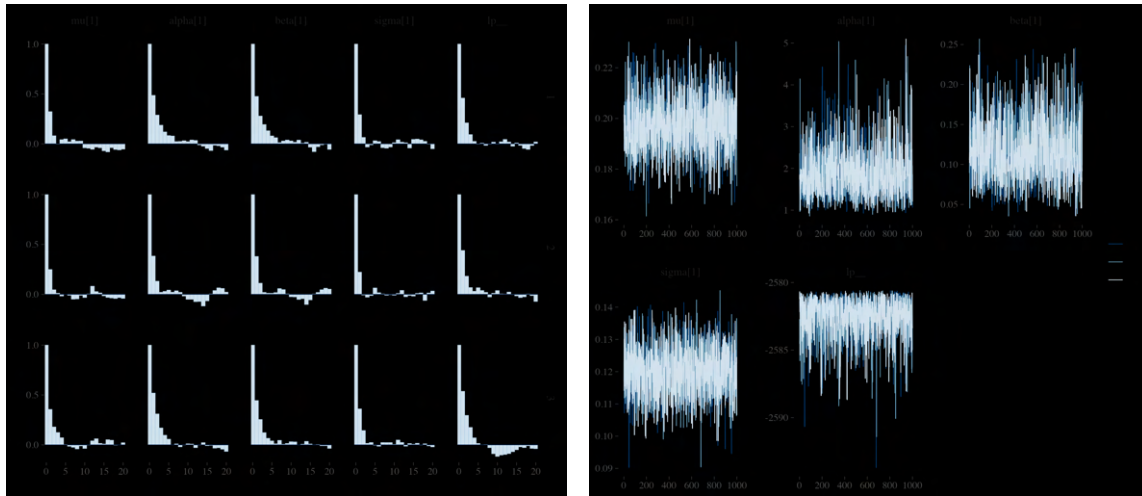


(c) Pairwise correlations



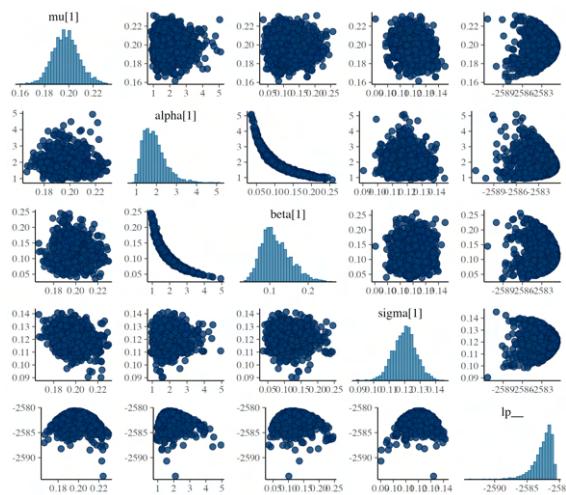
(d) \hat{R}

Figure 22: MCMC diagnostic plots for Protests in Bangladesh.

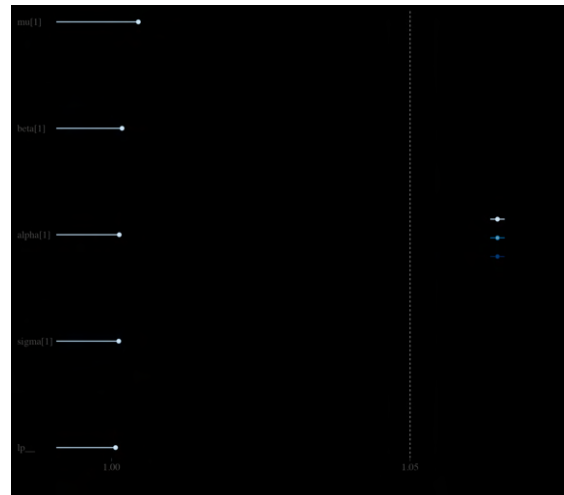


(a) Autocorrelation function

(b) Trace plots

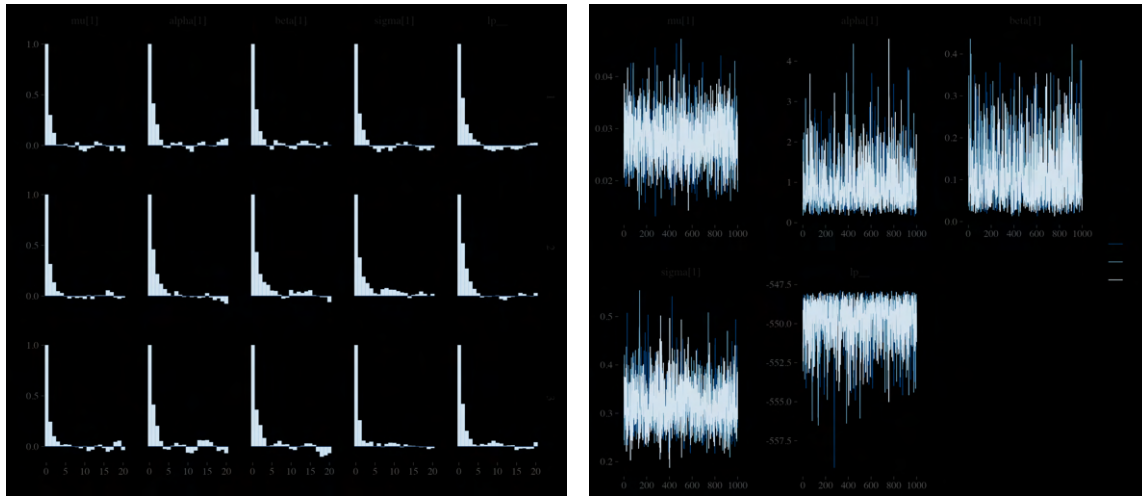


(c) Pairwise correlations



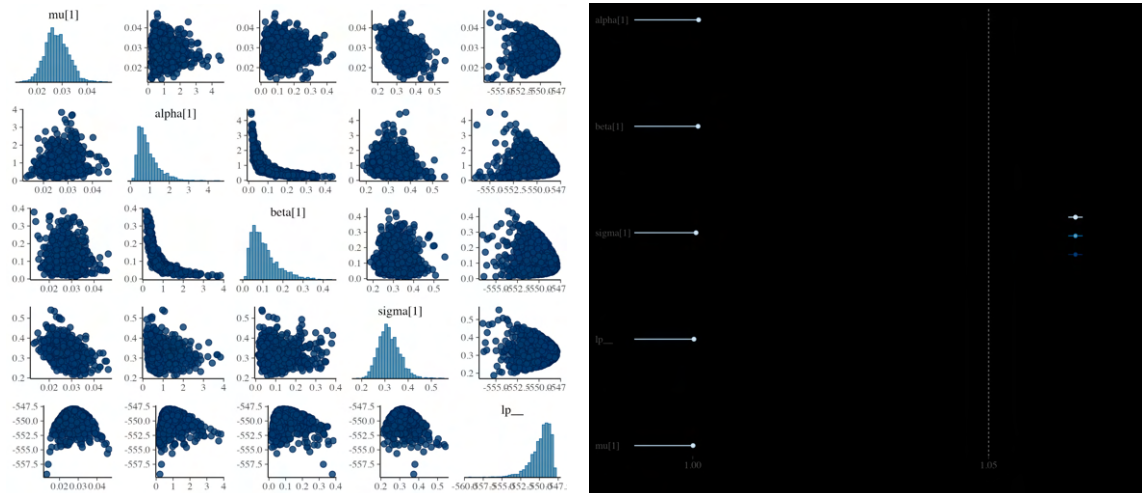
(d) \hat{R}

Figure 23: MCMC diagnostic plots for Violence against civilians in Bangladesh.



(a) Autocorrelation function

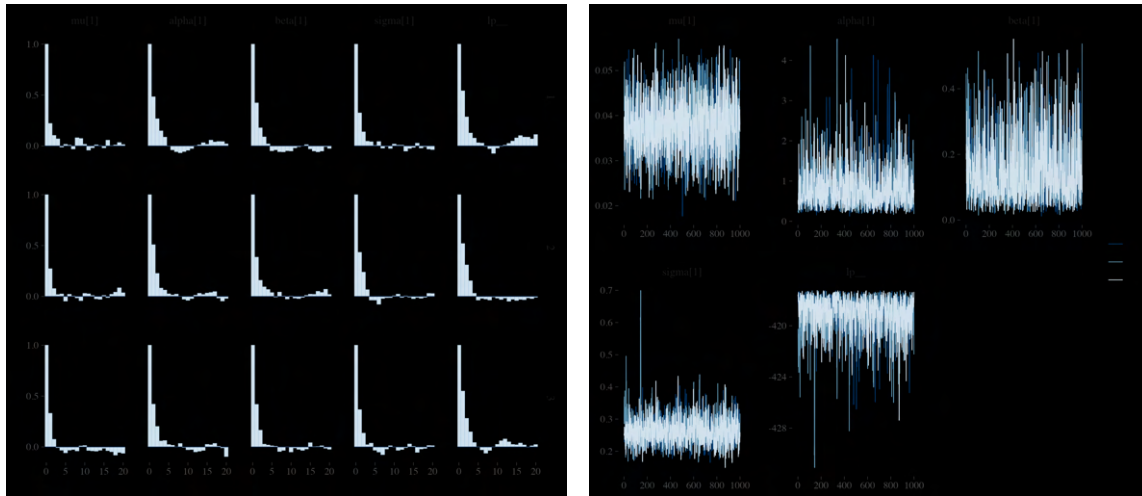
(b) Trace plots



(c) Pairwise correlations

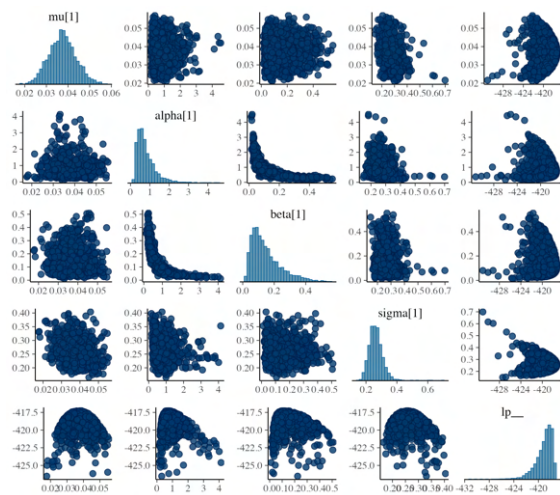
(d) \hat{R}

Figure 24: MCMC diagnostic plots for Strategic developments in Bangladesh.

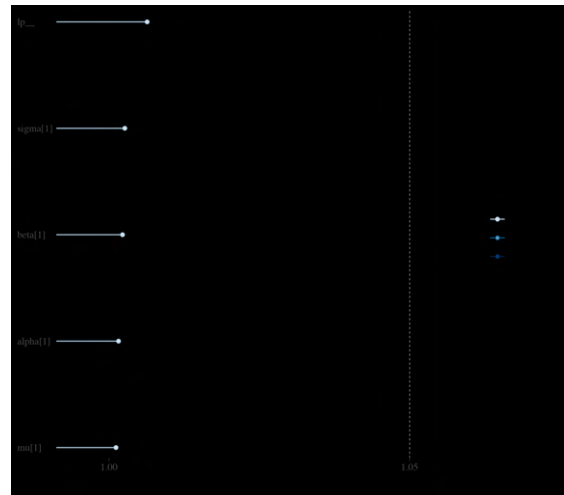


(a) Autocorrelation function

(b) Trace plots

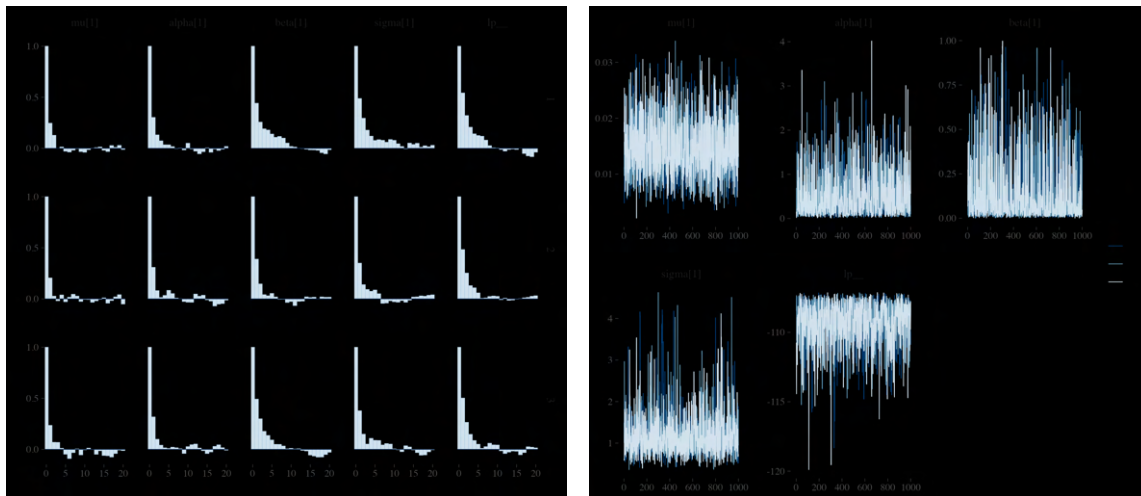


(c) Pairwise correlations



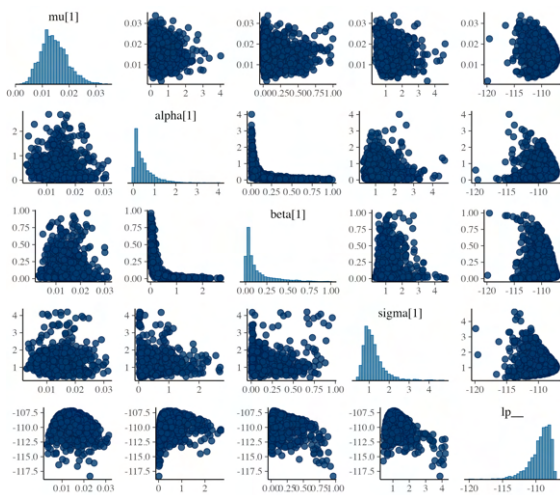
(d) \hat{R}

Figure 25: MCMC diagnostic plots for Explosions/remote violence in Bangladesh.

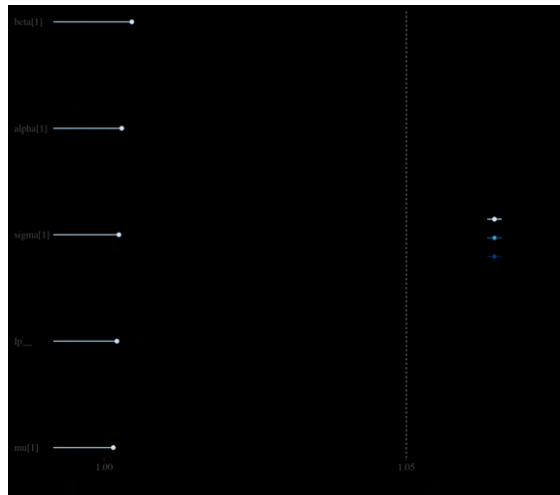


(a) Autocorrelation function

(b) Trace plots

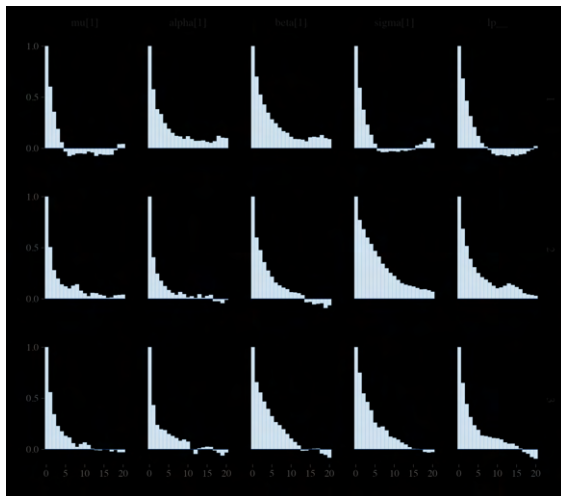


(c) Pairwise correlations

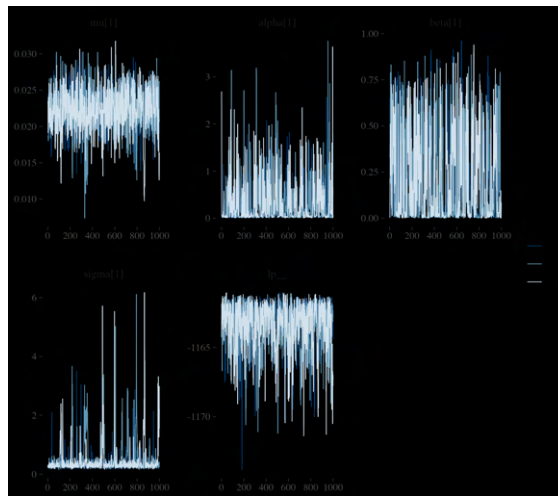


(d) \hat{R}

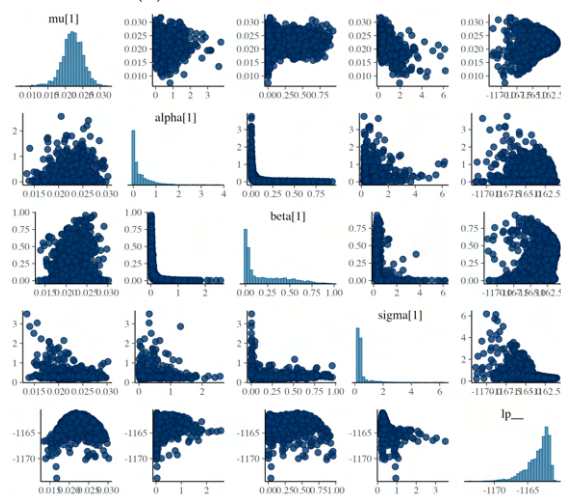
Figure 26: MCMC diagnostic plots for Battles in Sri Lanka.



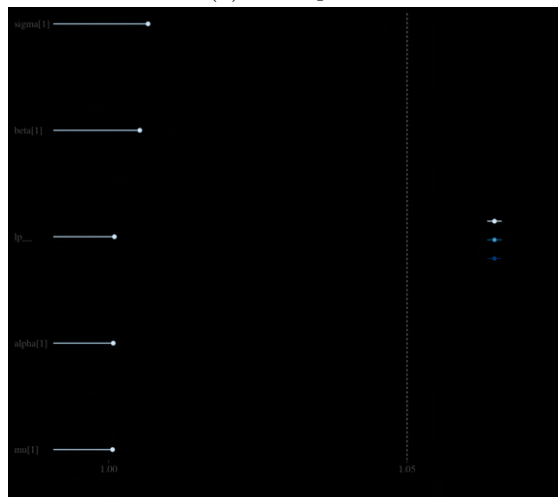
(a) Autocorrelation function



(b) Trace plots



(c) Pairwise correlations



(d) \hat{R}

Figure 27: MCMC diagnostic plots for Riots in Sri Lanka.

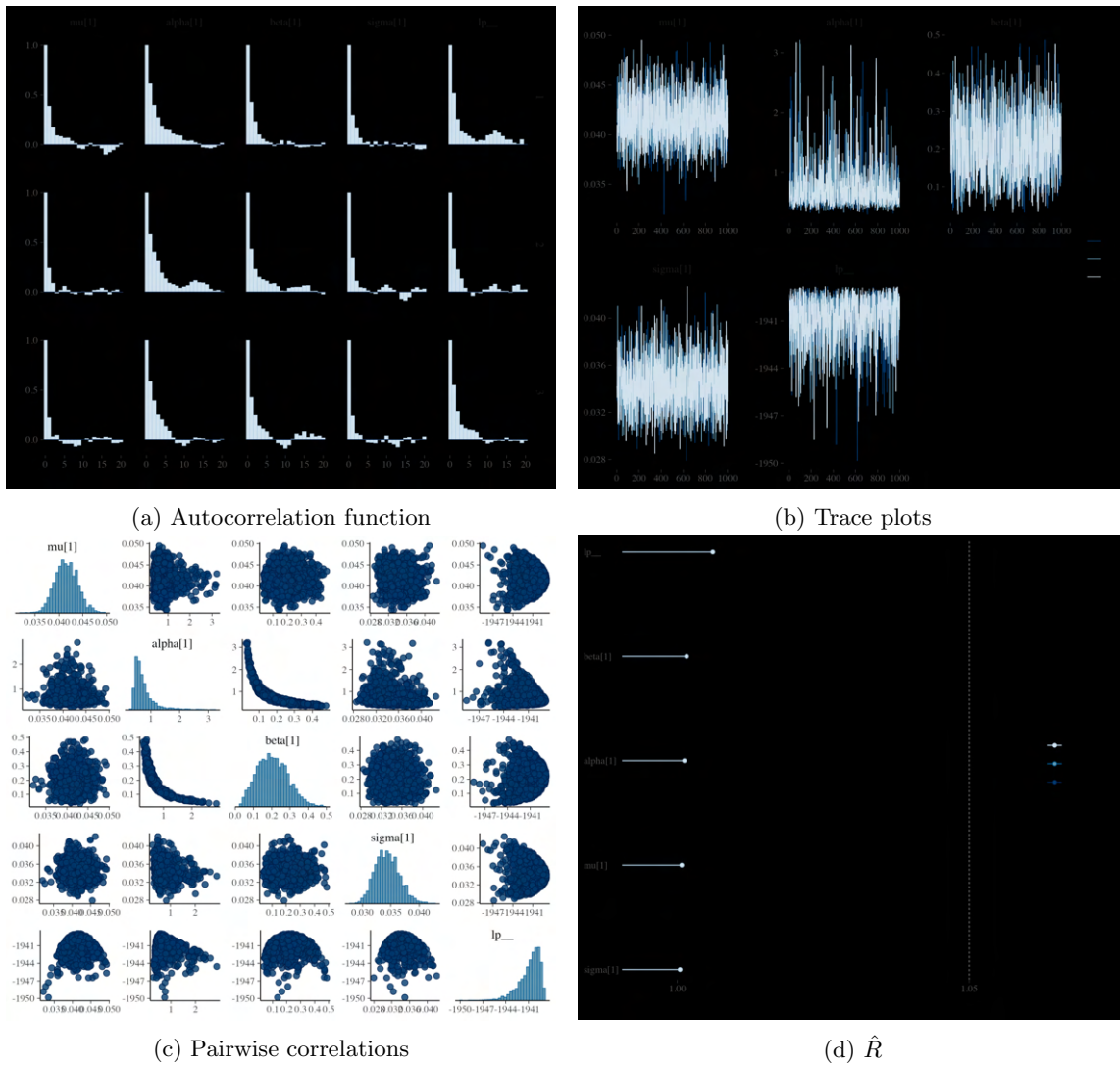
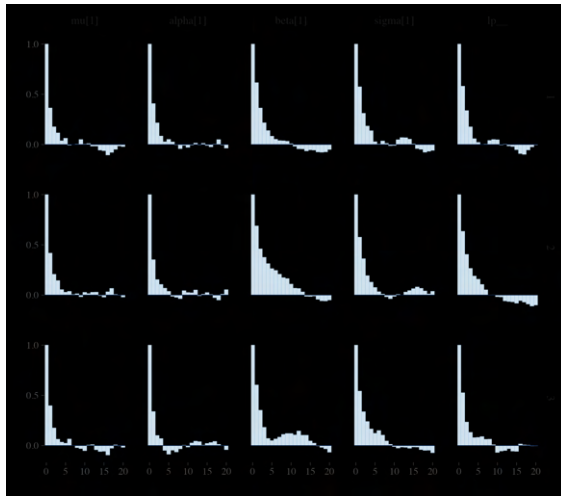
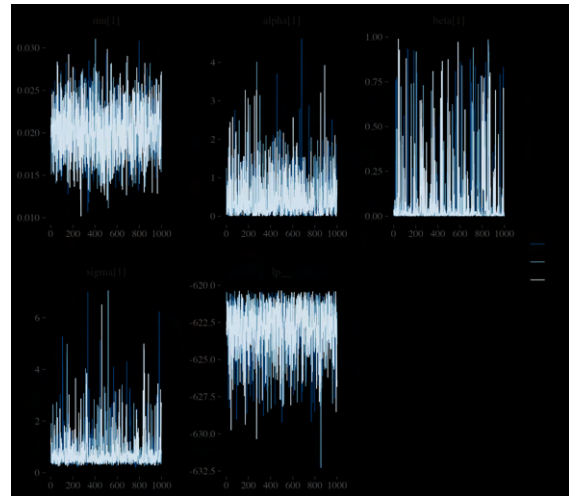


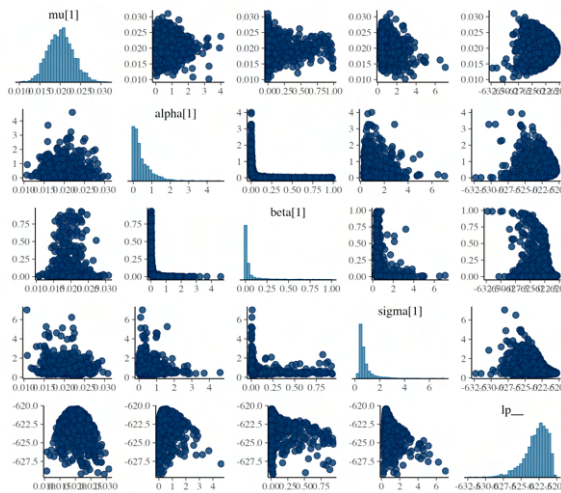
Figure 28: MCMC diagnostic plots for Protests in Sri Lanka.



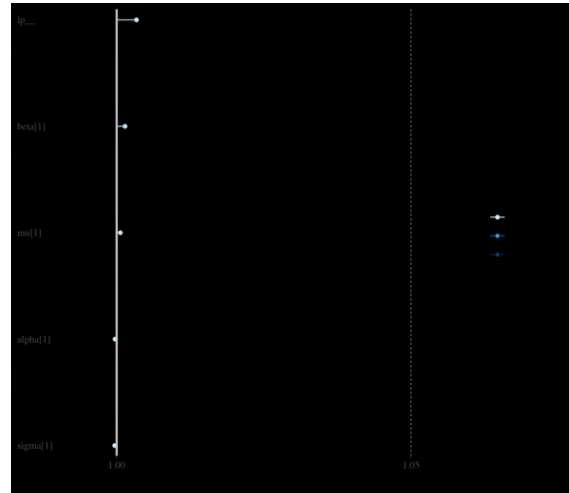
(a) Autocorrelation function



(b) Trace plots

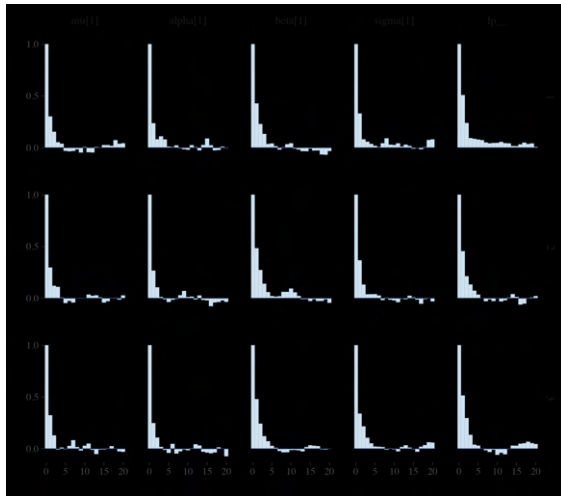


(c) Pairwise correlations

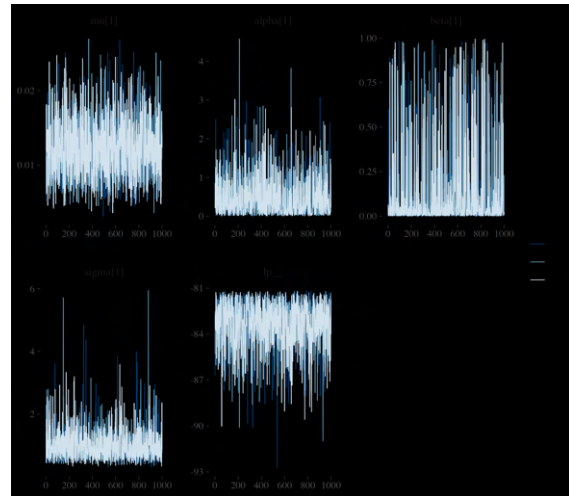


(d) \hat{R}

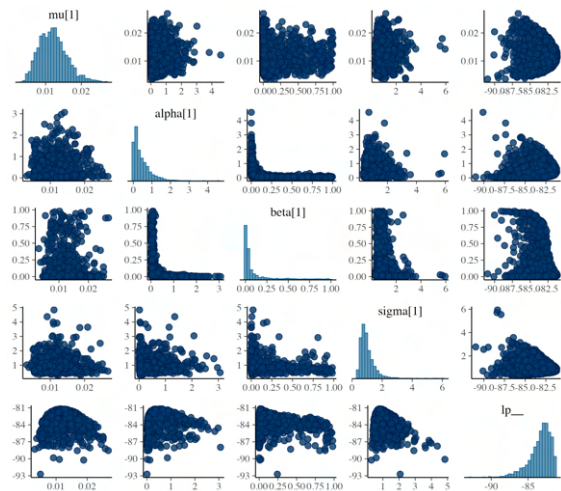
Figure 29: MCMC diagnostic plots for Violence against civilians in Sri Lanka.



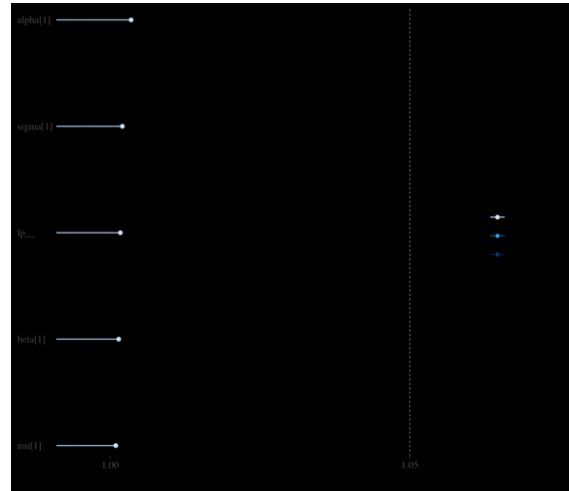
(a) Autocorrelation function



(b) Trace plots

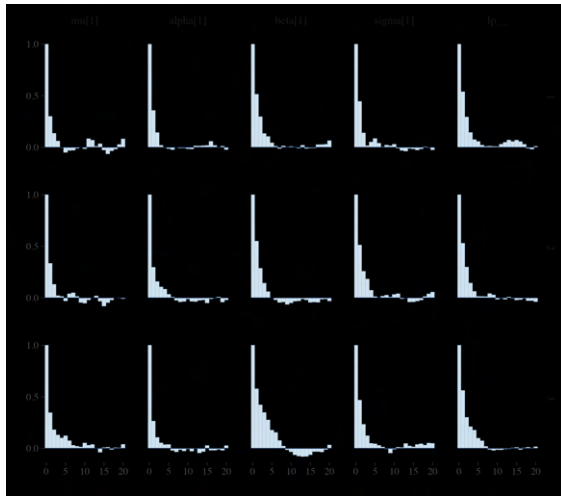


(c) Pairwise correlations

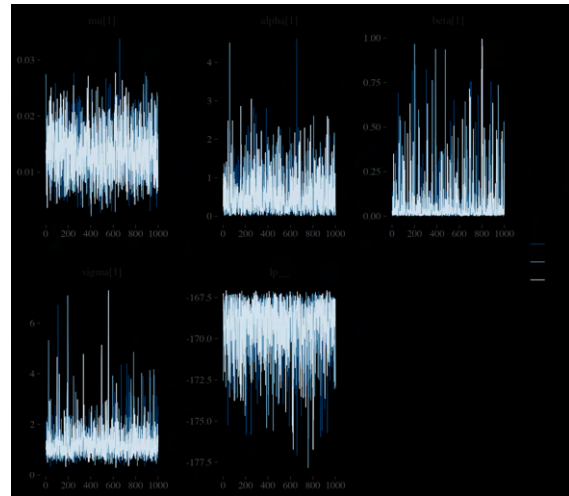


(d) \hat{R}

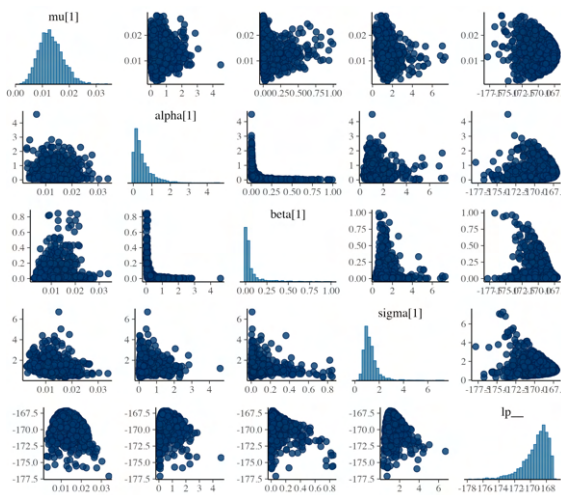
Figure 30: MCMC diagnostic plots for Strategic developments in Sri Lanka.



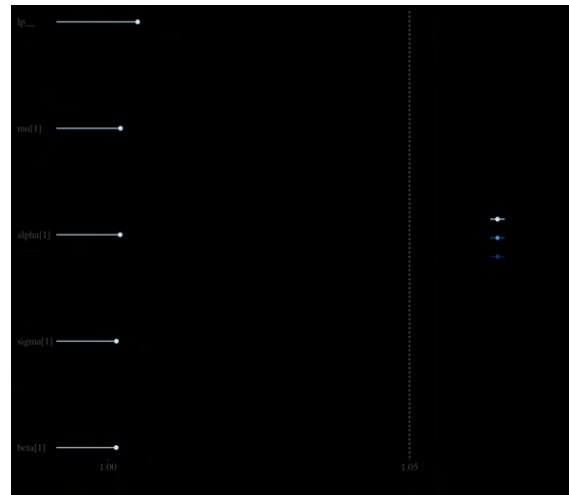
(a) Autocorrelation function



(b) Trace plots

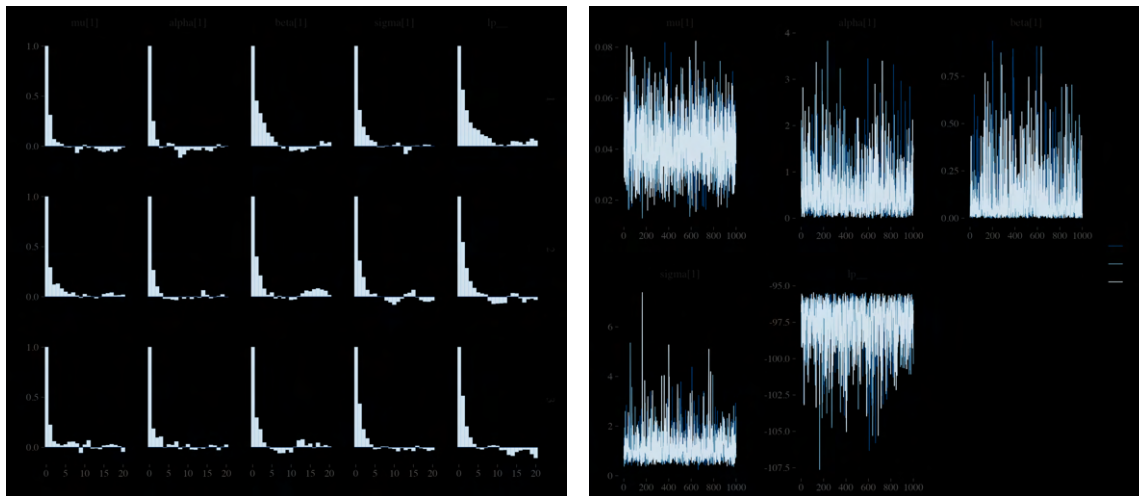


(c) Pairwise correlations



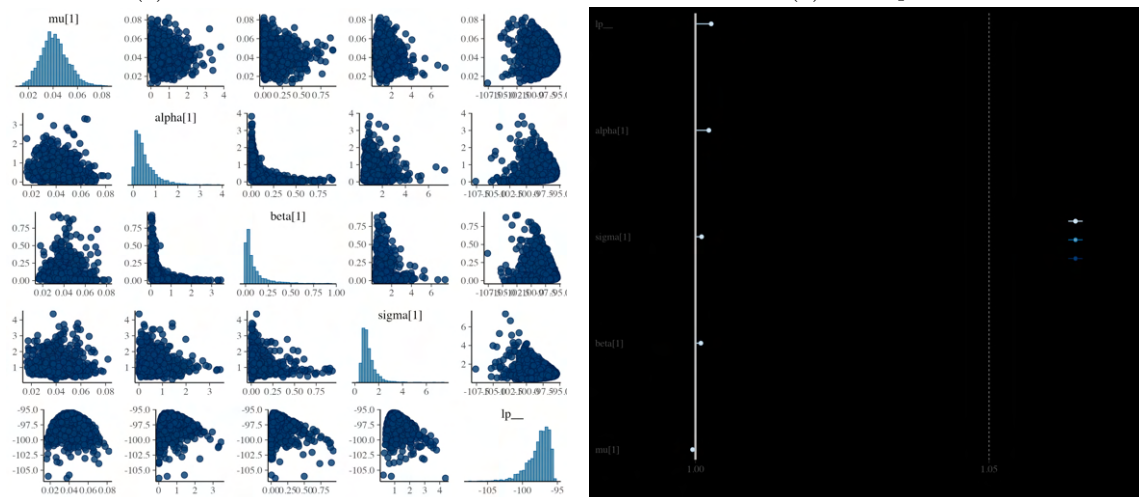
(d) \hat{R}

Figure 31: MCMC diagnostic plots for Explosions/remote violence in Sri Lanka.



(a) Autocorrelation function

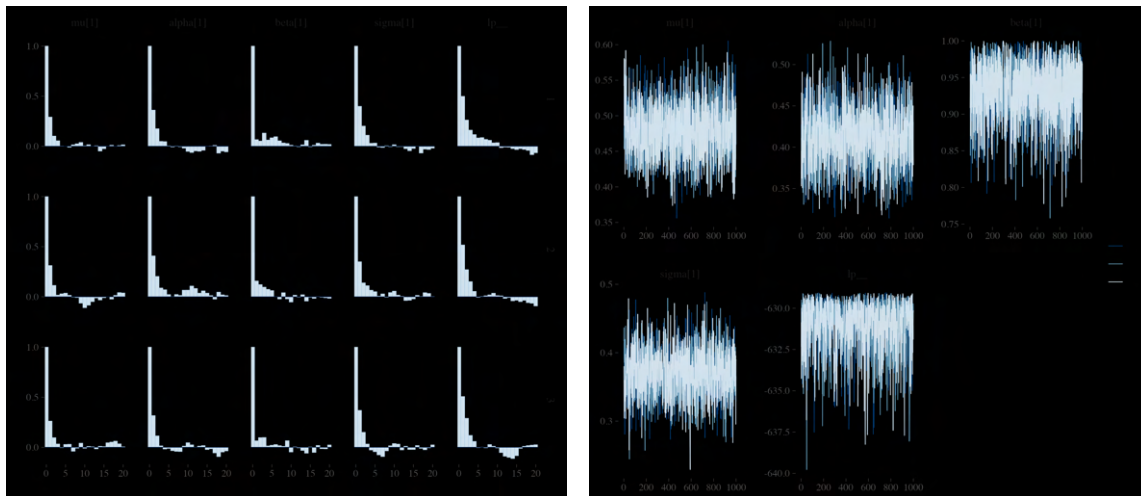
(b) Trace plots



(c) Pairwise correlations

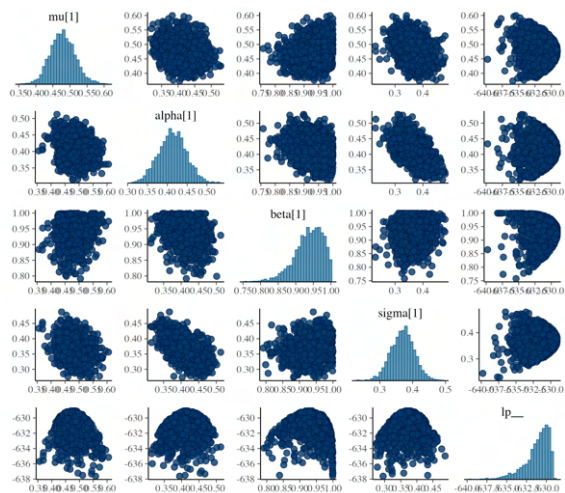
(d) \hat{R}

Figure 32: MCMC diagnostic plots for Battles in Nepal.

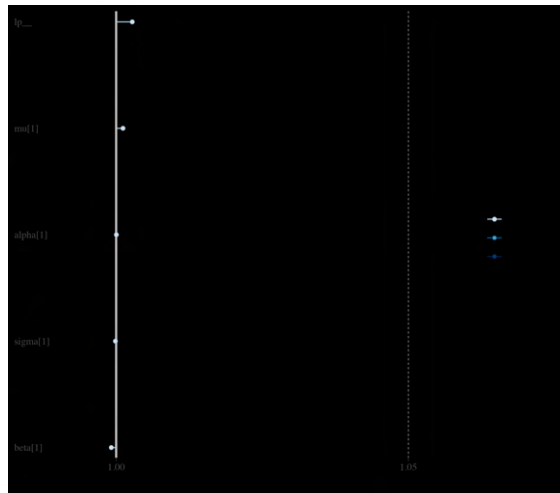


(a) Autocorrelation function

(b) Trace plots

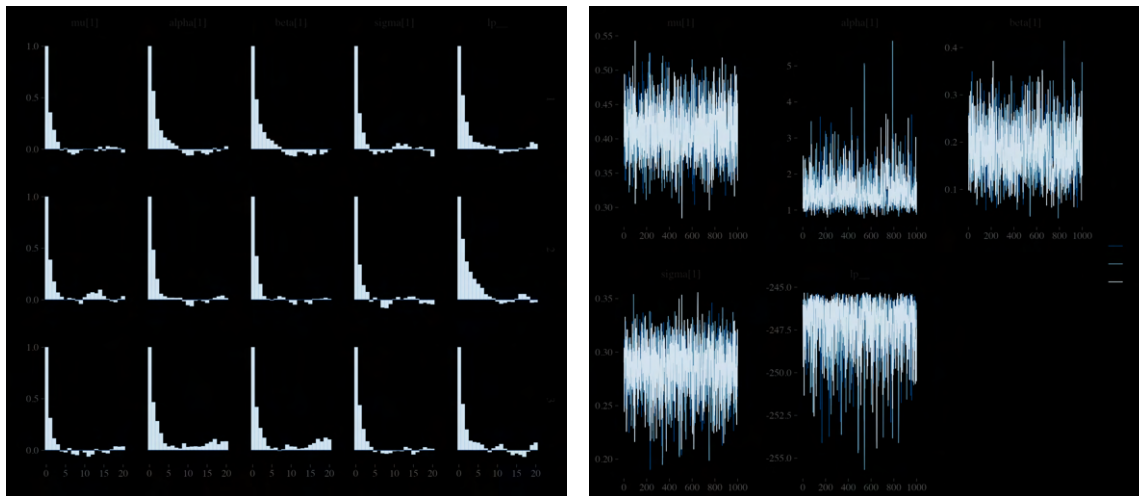


(c) Pairwise correlations



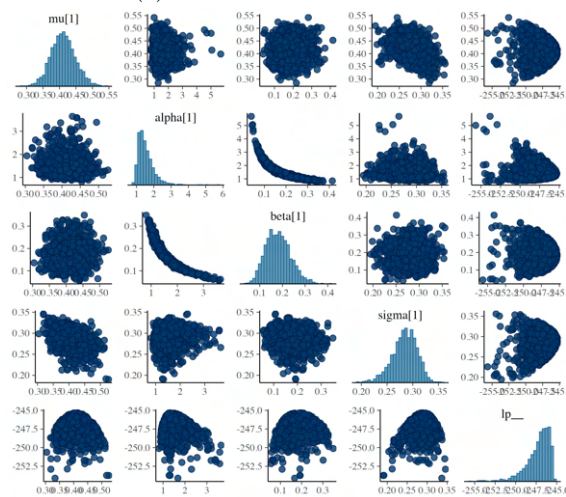
(d) \hat{R}

Figure 33: MCMC diagnostic plots for Riots in Nepal.

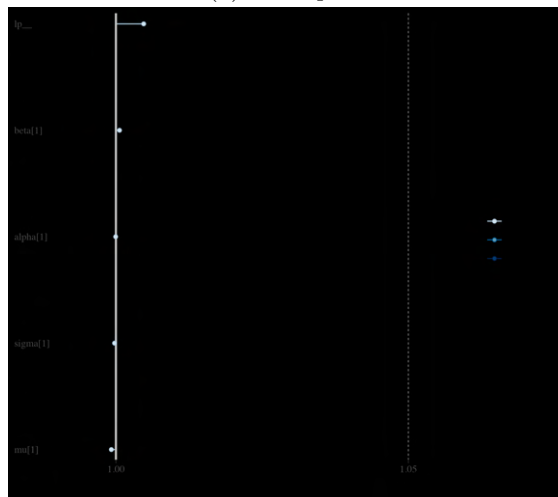


(a) Autocorrelation function

(b) Trace plots

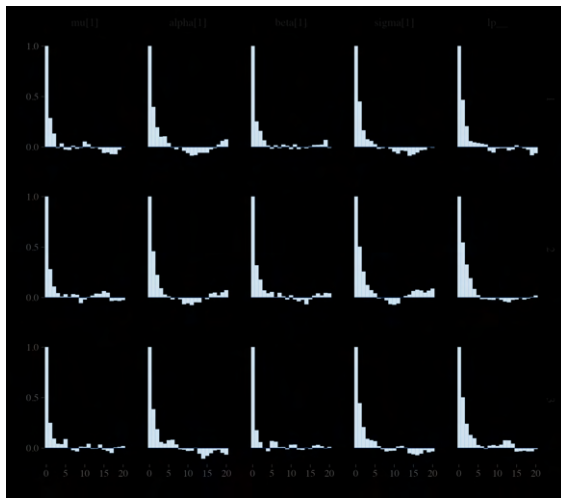


(c) Pairwise correlations

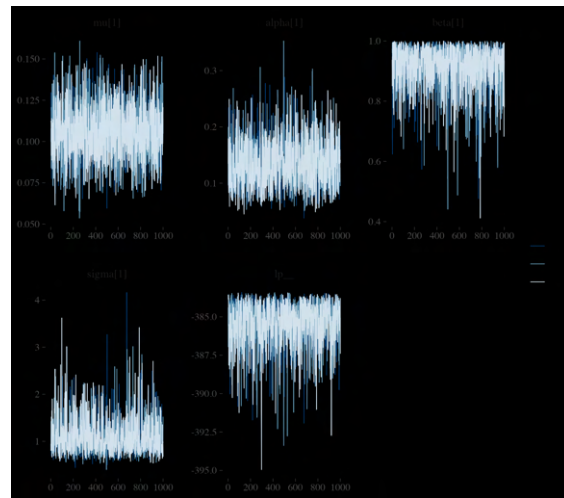


(d) \hat{R}

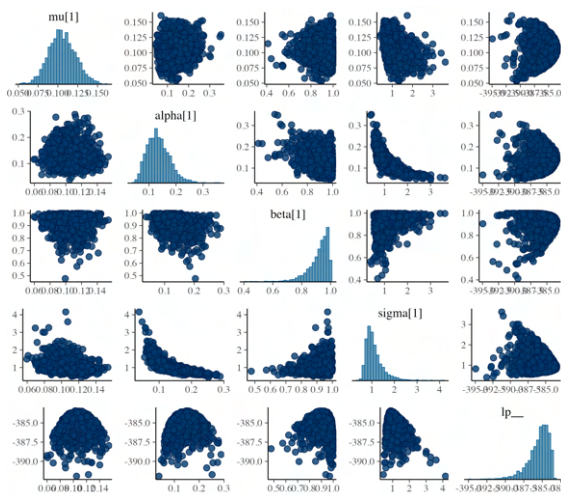
Figure 34: MCMC diagnostic plots for Protests in Nepal.



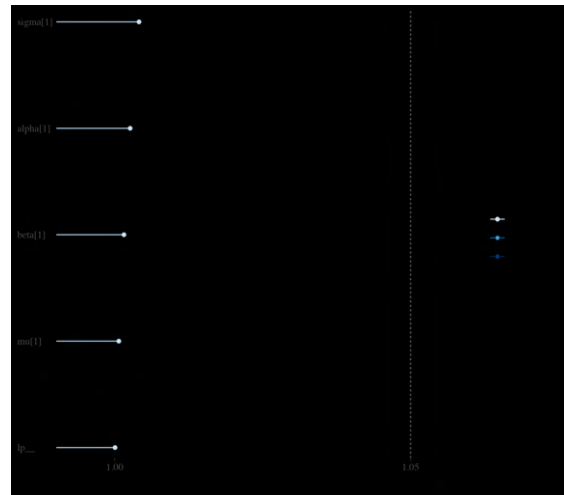
(a) Autocorrelation function



(b) Trace plots

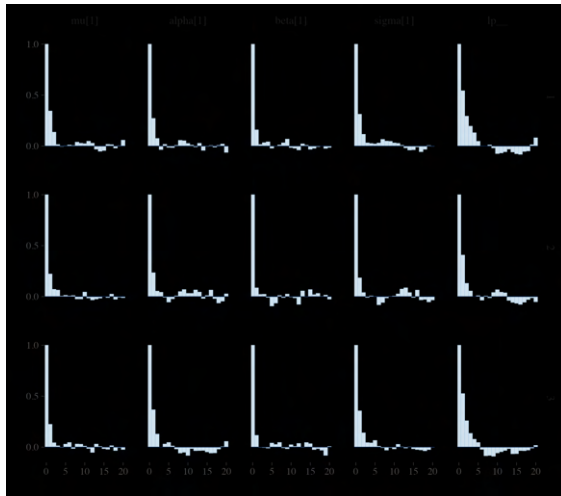


(c) Pairwise correlations

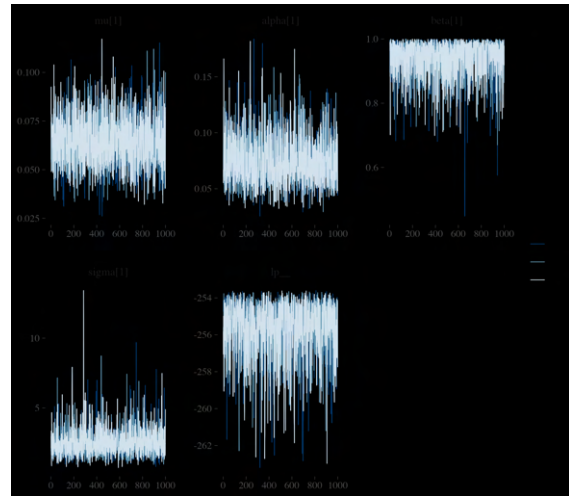


(d) \hat{R}

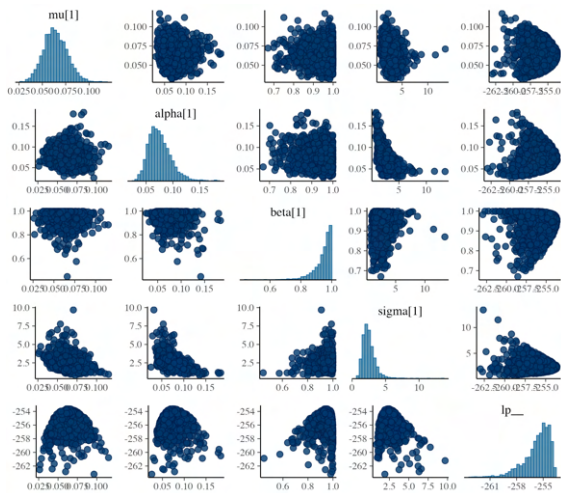
Figure 35: MCMC diagnostic plots for Violence against civilians in Nepal.



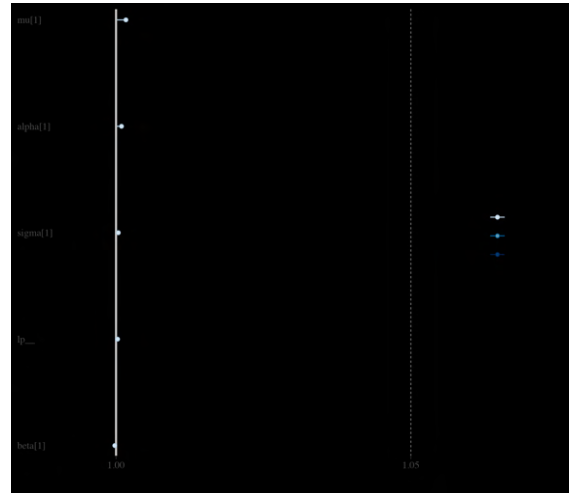
(a) Autocorrelation function



(b) Trace plots

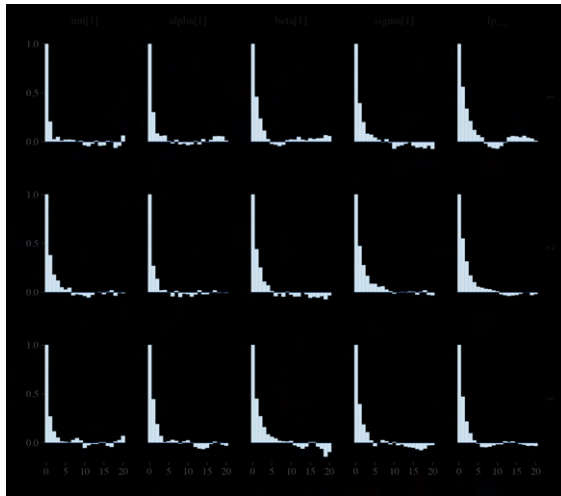


(c) Pairwise correlations

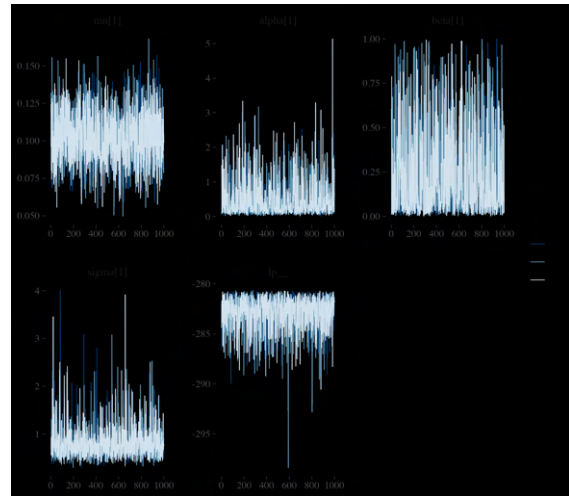


(d) \hat{R}

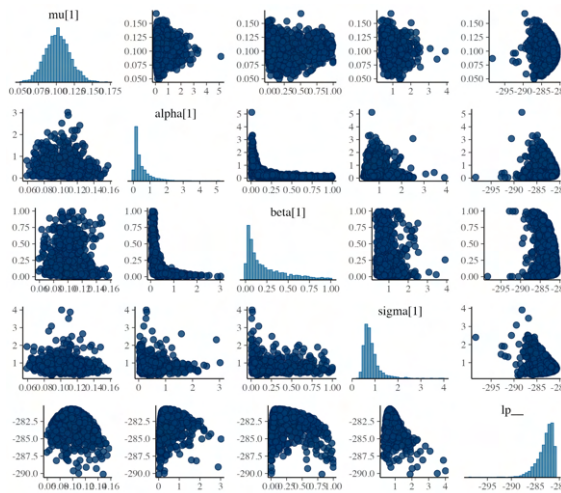
Figure 36: MCMC diagnostic plots for Strategic developments in Nepal.



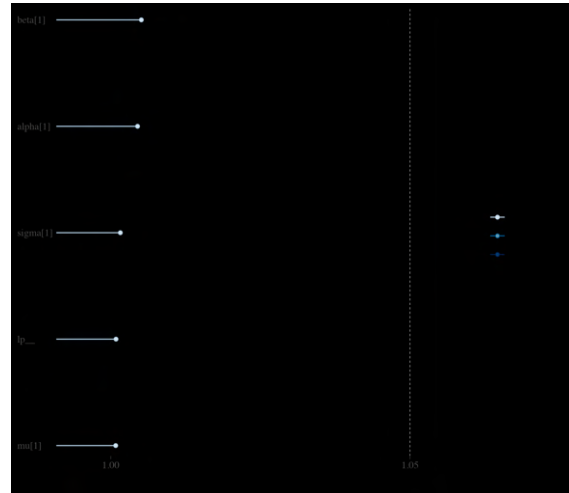
(a) Autocorrelation function



(b) Trace plots

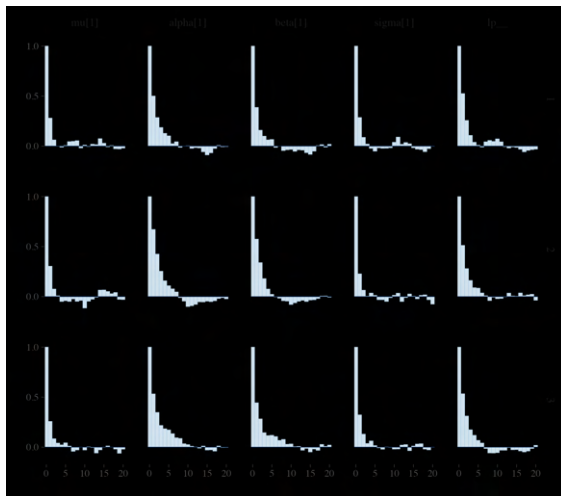


(c) Pairwise correlations

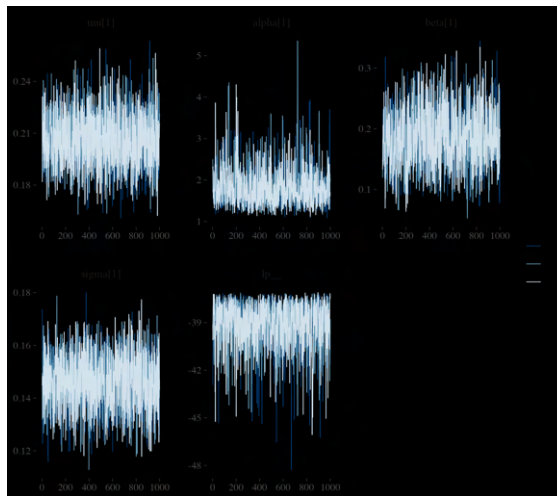


(d) \hat{R}

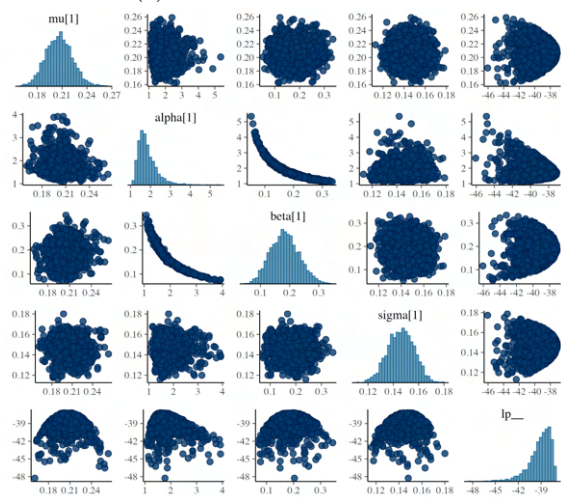
Figure 37: MCMC diagnostic plots for Explosions/remote violence in Nepal.



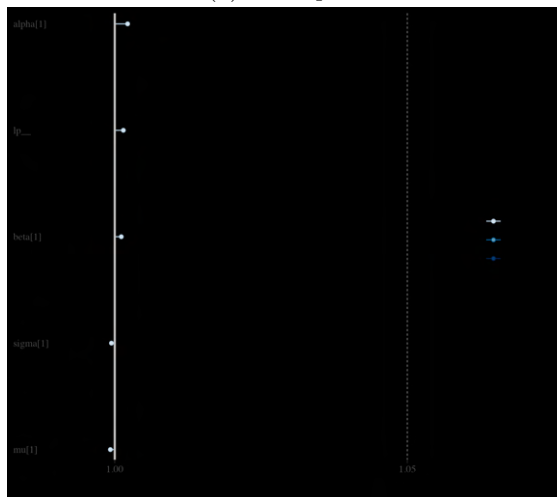
(a) Autocorrelation function



(b) Trace plots

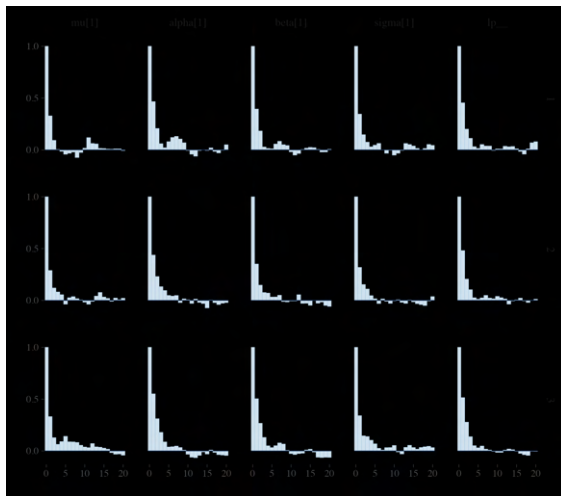


(c) Pairwise correlations

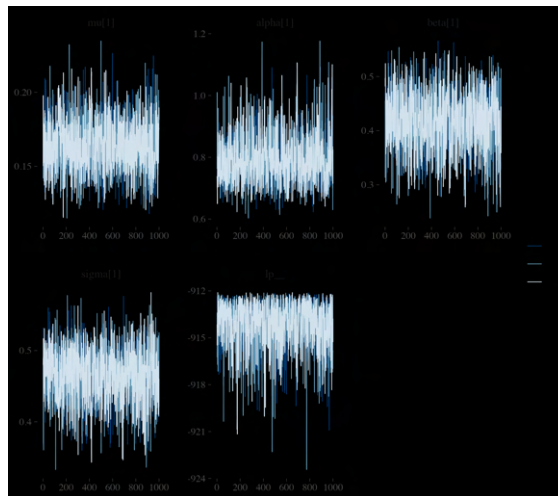


(d) \hat{R}

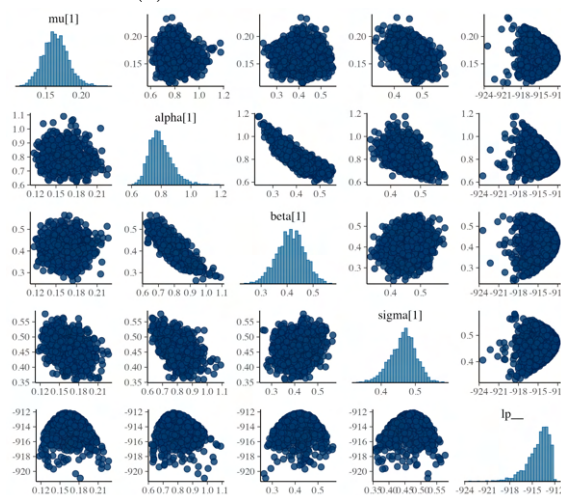
Figure 38: MCMC diagnostic plots for Battles in Pakistan.



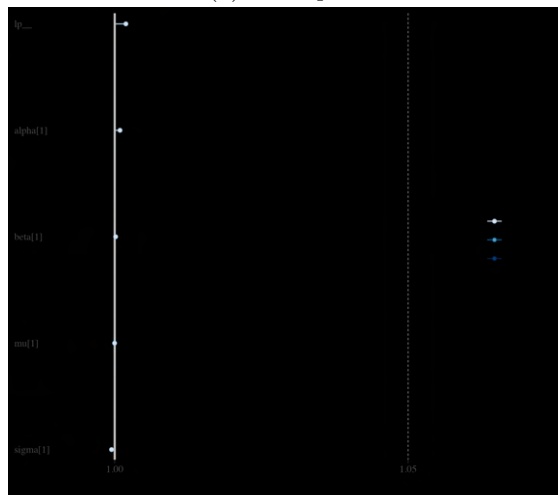
(a) Autocorrelation function



(b) Trace plots

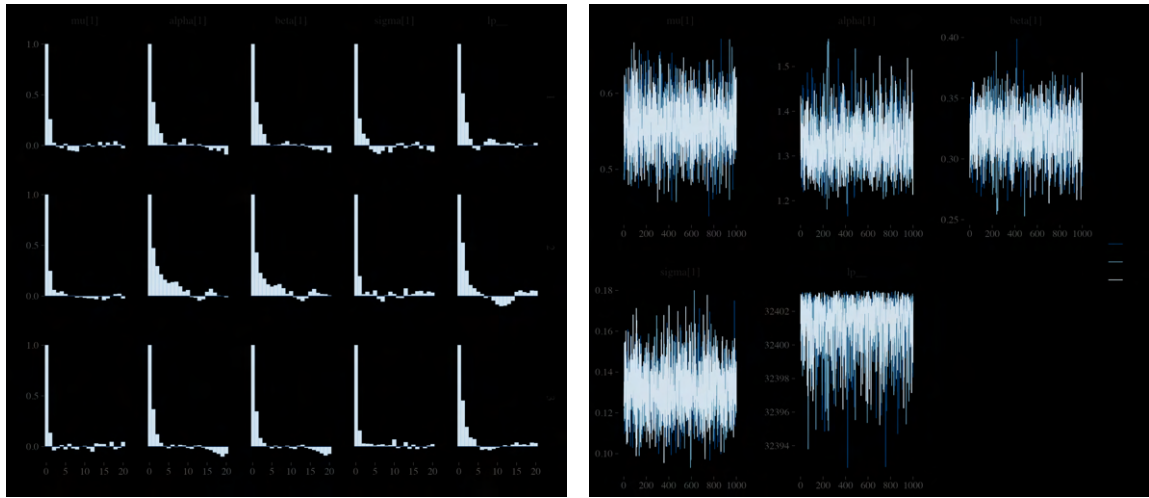


(c) Pairwise correlations



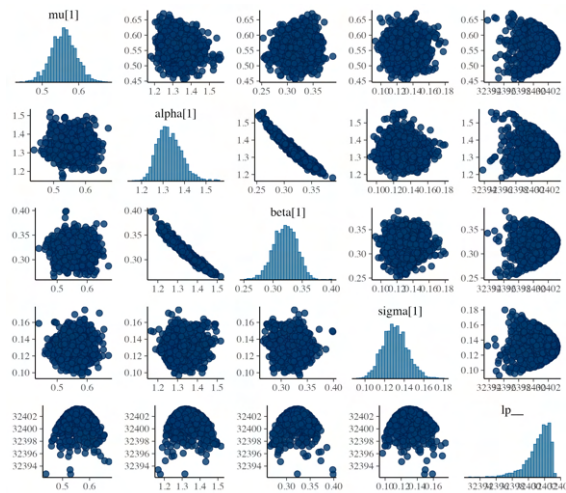
(d) \hat{R}

Figure 39: MCMC diagnostic plots for Riots in Pakistan.

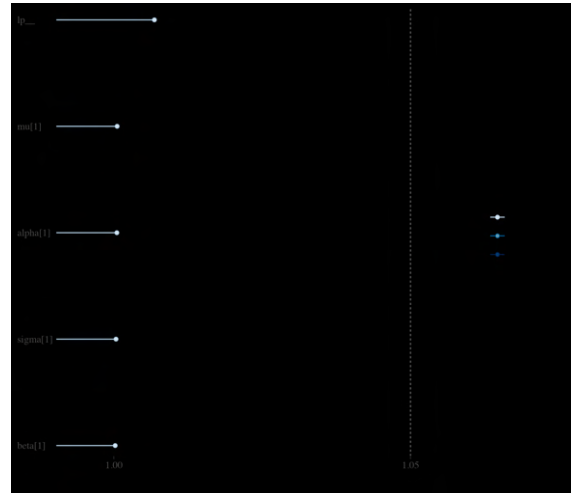


(a) Autocorrelation function

(b) Trace plots

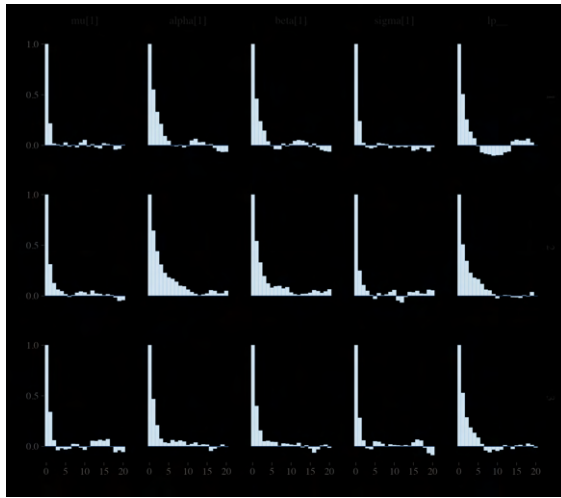


(c) Pairwise correlations

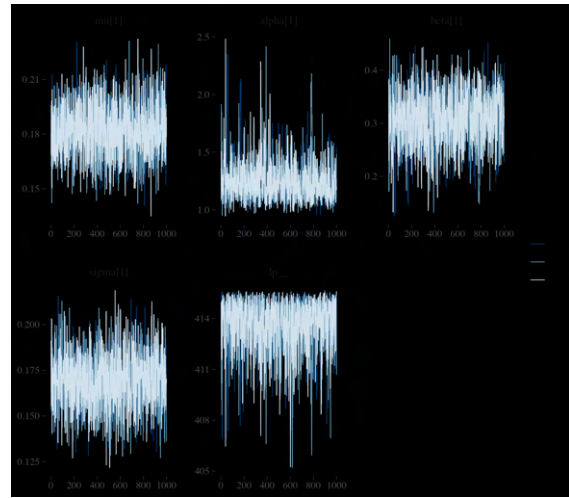


(d) \hat{R}

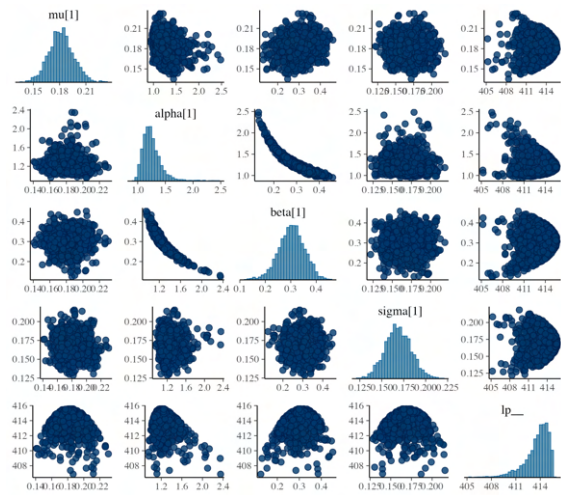
Figure 40: MCMC diagnostic plots for Protests in Pakistan.



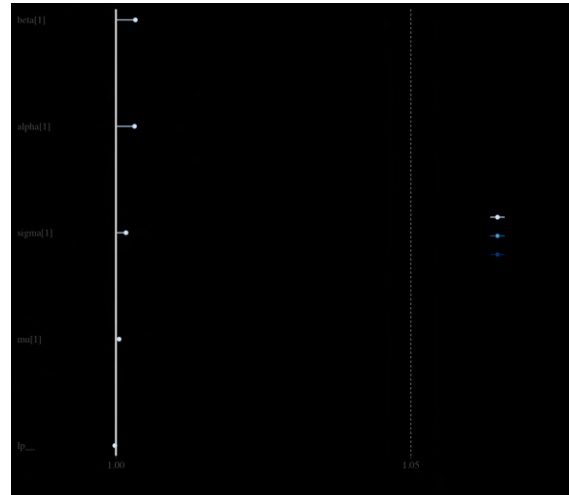
(a) Autocorrelation function



(b) Trace plots

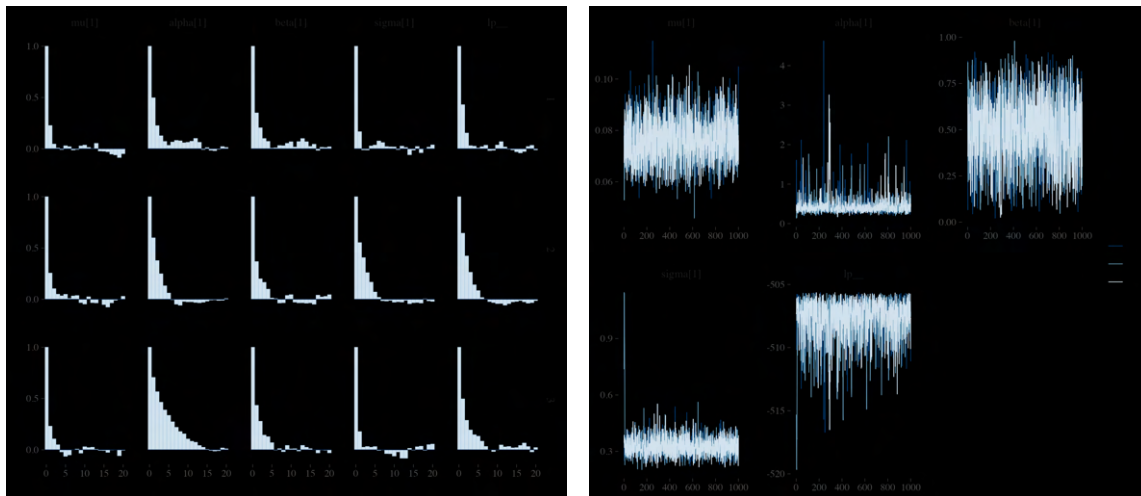


(c) Pairwise correlations



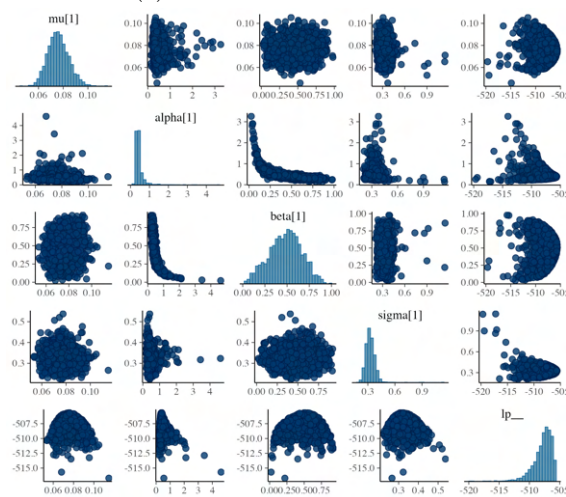
(d) \hat{R}

Figure 41: MCMC diagnostic plots for Violence against civilians in Pakistan.

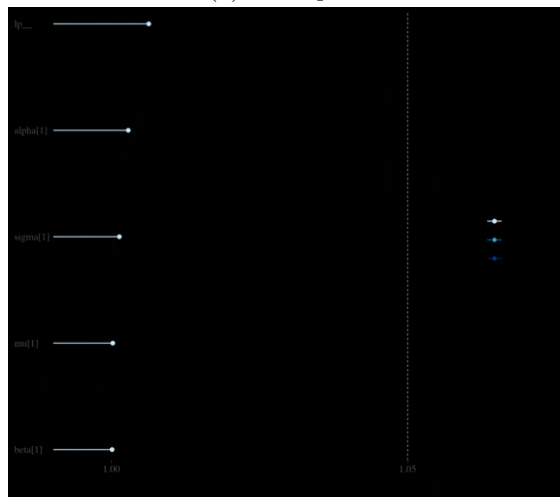


(a) Autocorrelation function

(b) Trace plots

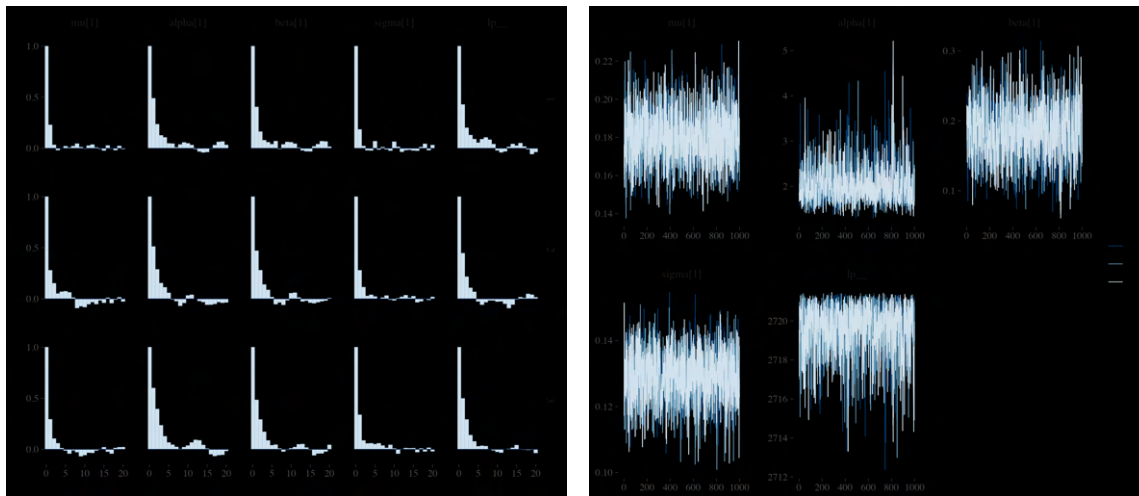


(c) Pairwise correlations



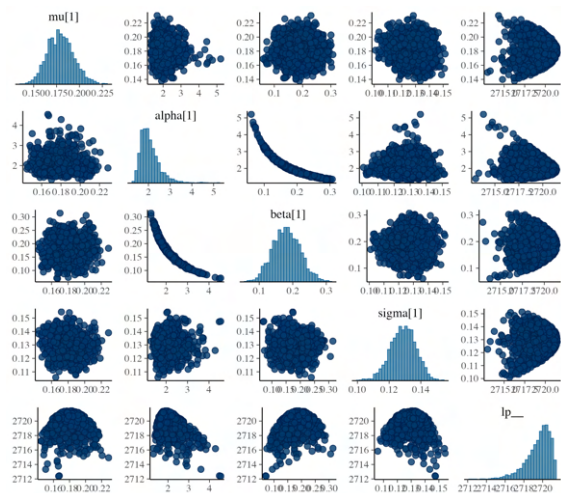
(d) \hat{R}

Figure 42: MCMC diagnostic plots for Strategic developments in Pakistan.

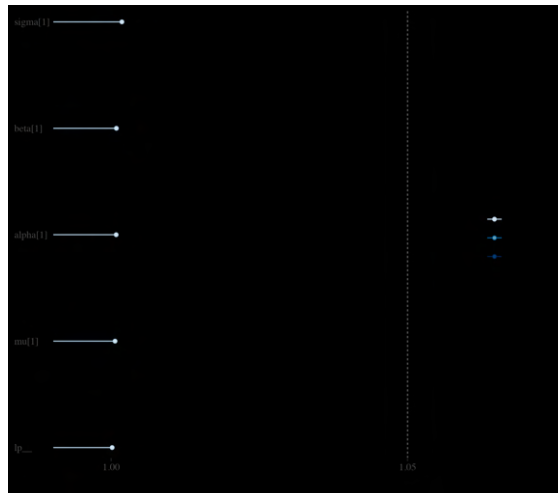


(a) Autocorrelation function

(b) Trace plots



(c) Pairwise correlations



(d) \hat{R}

Figure 43: MCMC diagnostic plots for Explosions/remote violence in Pakistan.

F Residual maps

Maps of the absolute value of the corresponding residuals for each country can be found in the supplementary materials. The residual number of events over this 5 year period was determined by calculating the absolute value of the difference between the total number of observed events and the median of the estimated expected number of events.

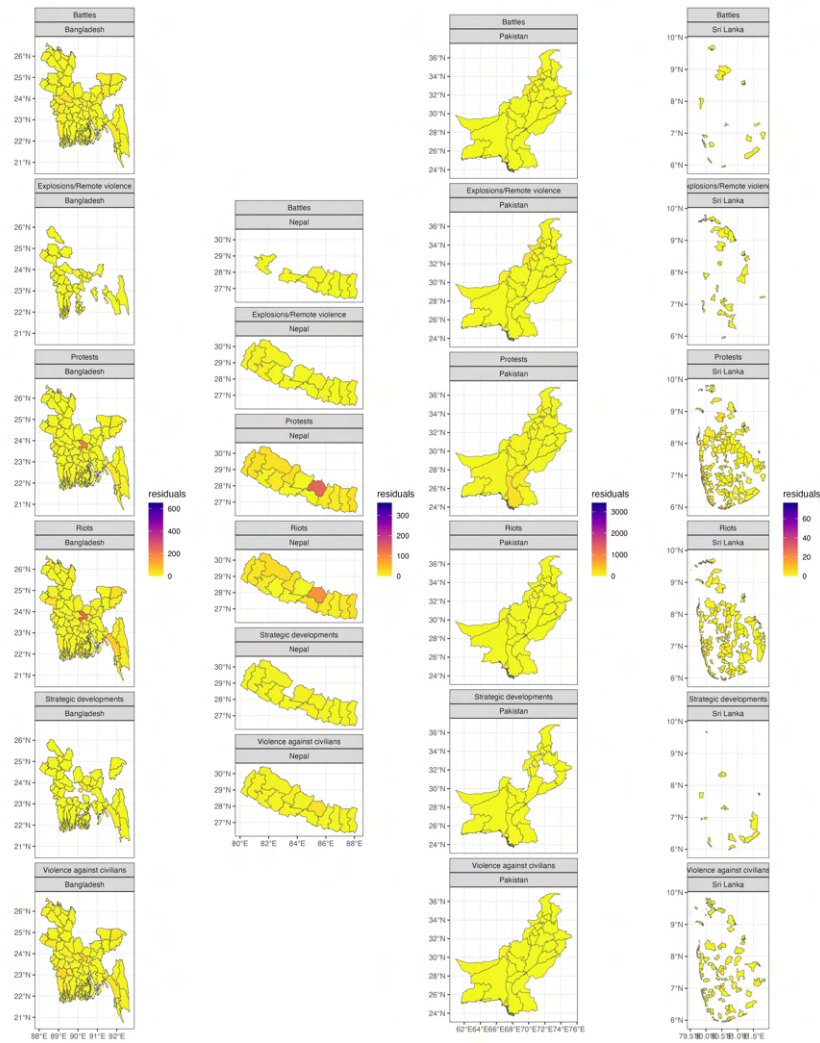


Figure 44: Residuals over 5 year observation window (absolute value of the sum of observed events minus the sum of median expected number of events)

G Maximum likelihood results for spatiotemporal DTHP

Table 4 presents the MLEs for the spatiotemporal DTHP model for each country and conflict type.

Country	Conflict type	μ	α	β	σ
Bangladesh	Battles	0.14	0.45	0.02	0.14
	Riots	0.37	0.68	0.41	0.00
	Protests	0.15	0.70	0.34	0.00
	Violence against civilians	0.20	0.55	0.04	0.02
	Strategic developments	0.03	0.25	0.02	0.23
	Explosions/Remote violence	0.04	0.34	0.02	0.15
Sri Lanka	Battles	0.01	0.06	0.11	1.28
	Riots	0.03	0.12	0.37	0.05
	Protests	0.04	0.45	0.46	0.00
	Violence against civilians	0.02	0.04	0.52	0.14
	Strategic developments	0.01	0.00	0.00	0.03
	Explosions/Remote violence	0.01	0.02	0.08	2.02
Nepal	Battles	0.04	0.04	0.00	1.18
	Riots	0.49	0.42	0.95	0.35
	Protests	0.46	0.65	0.22	0.00
	Violence against civilians	0.10	0.08	1.00	1.90
	Strategic developments	0.06	0.05	1.00	4.30
	Explosions/Remote violence	0.10	0.12	0.33	0.60
Pakistan	Battles	0.21	0.79	0.15	0.03
	Riots	0.16	0.63	0.42	0.46
	Protests	0.55	0.91	0.39	0.00
	Violence against civilians	0.18	0.82	0.30	0.05
	Strategic developments	0.07	0.35	0.53	0.00
	Explosions/Remote violence	0.18	0.89	0.15	0.01

Table 4: MLEs for spatiotemporal DTHP

Figure 45 shows the observed event counts for each month compared to the expected number of events $\lambda(t, x, y)$, estimated via maximum likelihood estimation. Using this approach, it is apparent that the performance is similar to the Bayesian approach, whereby the estimated mean number of events on a given month closely aligns with the observed data and the model is able to react quickly to recent events. However, while the MLE approach struggles to capture the self-excitation present for scenarios with low event counts, for example strategic developments in Sri Lanka, the Bayesian model can capture some self-excitation.

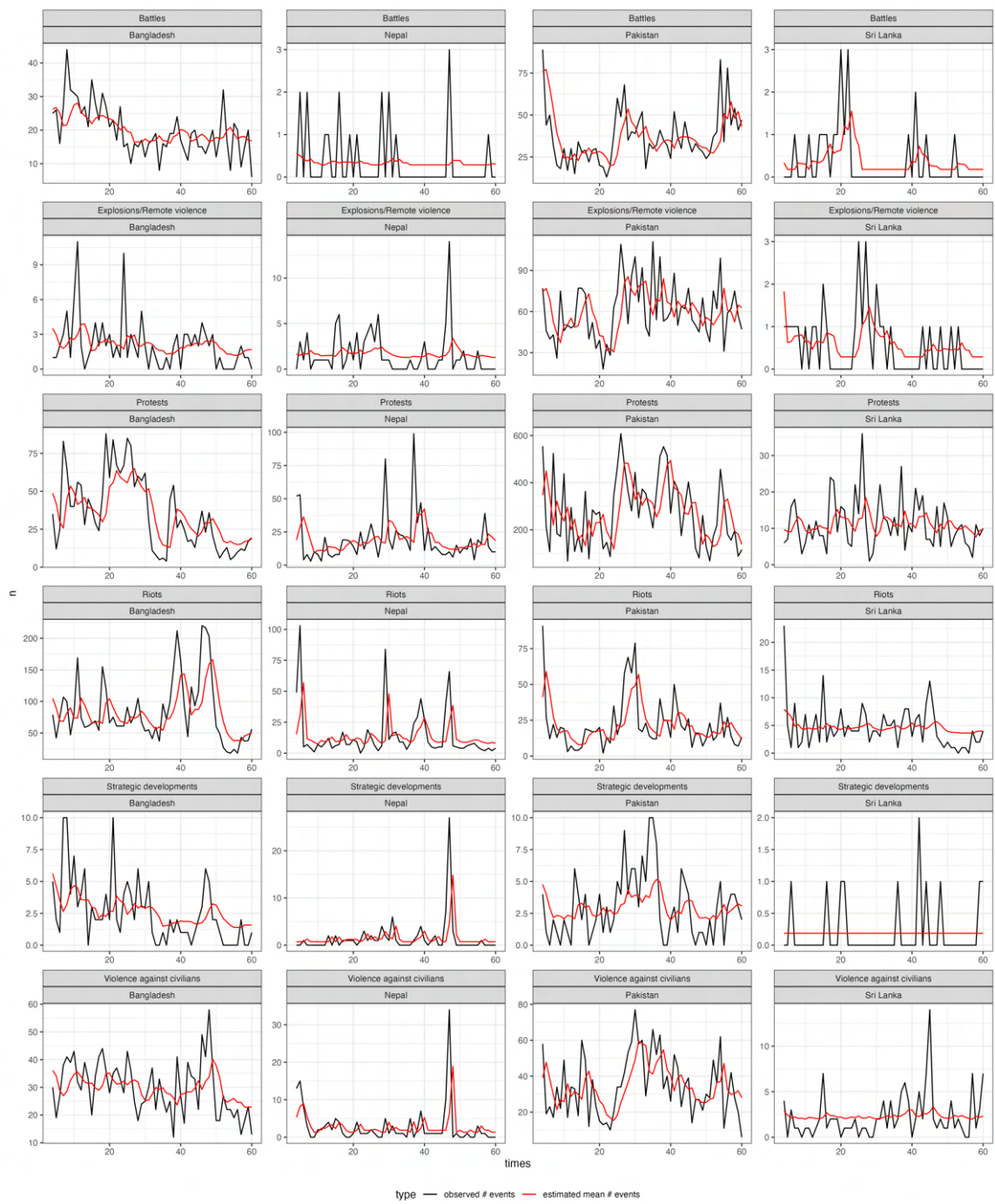


Figure 45: Observed data on month t (black line) versus estimated $\lambda(t)$ (red line). Model estimated via maximum likelihood.

H Summary of counts in data

Figure 46 presents a temporal summary of the data used in this study and Table 5 summarises the total event counts.

Country	Conflict type	Total event count	3 month rolling average
Bangladesh	Battles	1223.00	20.43
	Explosions/Remote violence	136.00	2.22
	Protests	2170.00	36.16
	Riots	5115.00	85.14
	Strategic developments	176.00	2.83
	Violence against civilians	1822.00	30.40
Nepal	Battles	25.00	0.40
	Explosions/Remote violence	93.00	1.59
	Protests	1138.00	19.23
	Riots	827.00	14.09
	Strategic developments	83.00	1.41
	Violence against civilians	176.00	2.93
Pakistan	Battles	2348.00	38.33
	Explosions/Remote violence	3661.00	61.16
	Protests	16738.00	282.24
	Riots	1372.00	23.06
	Strategic developments	190.00	3.16
	Violence against civilians	2081.00	35.28
Sri Lanka	Battles	20.00	0.33
	Explosions/Remote violence	39.00	0.57
	Protests	666.00	11.16
	Riots	327.00	5.27
	Strategic developments	18.00	0.24
	Violence against civilians	158.00	2.36

Table 5: Counts for each country and conflict type

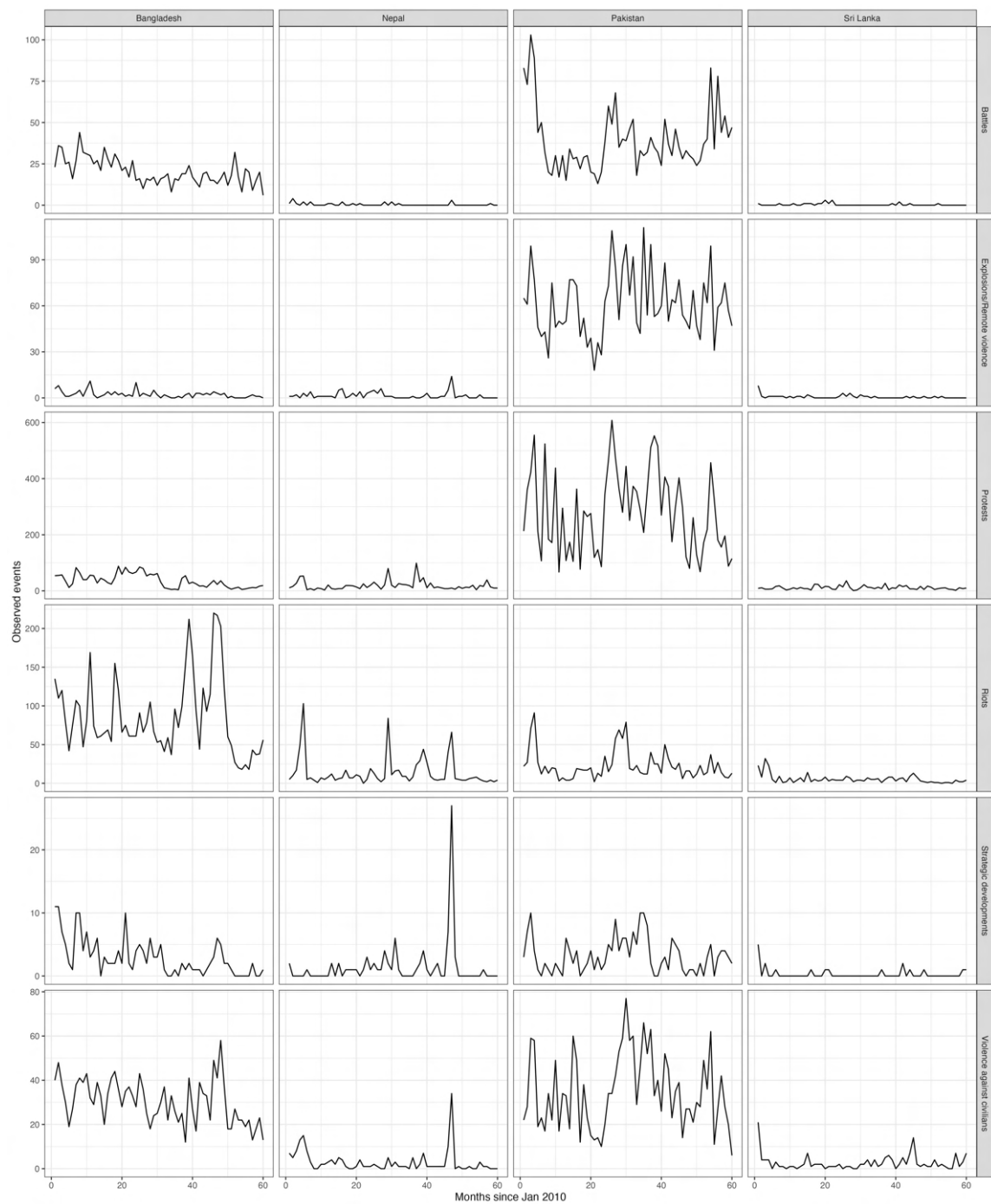


Figure 46: Observed conflict events from 2010 – 2014 by country and conflict type. Horizontal panels: conflict type. Vertical panels: country.